Supporting Information

Kinetic-Thermodynamic Correlation of Conformational Changes in Ammonium Complexes of a Flexible Naphthocage

Shan He,[a,b] Mao Quan,[b,c] Liu-Pan Yang,[b] Ho Yu Au-Yeung,[a]* and Wei Jiang[b]

[a] State Key Laboratory of Synthetic Chemistry and Department of Chemistry, the University of Hong Kong, Hong Kong, China

[b] Shenzhen Grubbs Institute, Guangdong Provincial Key Laboratory of Catalysis, and Department of Chemistry, Southern University of Science and Technology, Shenzhen 518055, China

[c] Shenzhen Key Laboratory of New Information Display and Storage Materials, College of Materials Science and Engineering, Shenzhen University, Shenzhen 518055, China

Email:hoyuay@hku.hk.

1. Synthesis

General. All reagents used were obtained from commercial sources and used without further purification. Solvents were either used as received or dried prior to use by standard laboratory procedures. Thin-layer chromatography (TLC) was carried out on 0.25 mm Yantai silica gel plates (60F-254). Column chromatography was performed on silica gel 60 (Tsingdao 40-63 nm, 200-300 mesh). ^{1}H NMR spectra were recorded on Bruker Avance 400 or 500 spectrometers. All chemical shifts are reported in *ppm* with residual solvents or tetramethylsilane as the internal standards. The following abbreviations are used for signal multiplicities: s, singlet; d, doublet; t triplet; m, multiplet. Host-guest complexes were prepared by mixing the host and excess guest in CD_2Cl_2/CD_3CN (*v*/*v* = 1:1). Counterions of the guests are PF_6^-.

Synthesis of G2-G8, G17 G20, G21, G23 and G24

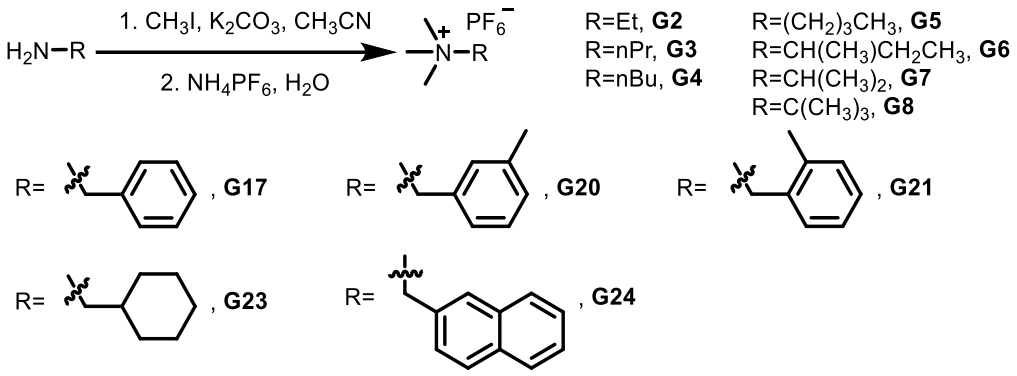

In a typical experiment, a mixture of the starting primary amine (~500 mg), CH_3I (5.0 eq.) and K_2CO_3 (5.0 eq.) in CH_3CN (20 mL) was stirred at room temperature for 8 h. The solid suspension was filtered and the solution was dried over vacuum to yield the corresponding iodide salt of the quaternary ammoniums. The obtained iodide salt was then dissolved in deionized water to give a saturated solution of the ammonium salts, which was then added dropwisely into a saturated aqueous NH_4PF_6 solution. The resulting mixture was stirred for 1 h at room temperature, and the precipitate formed was collected by filtration, washed several times with deionized water and dried under vacuum to give the hexafluorophosphate salt of the ammonium guests.

G2: White solid obtained in a total yield of 71%. ^{1}H NMR (500 MHz, CD_3CN) δ 3.29 (q, *J* = 7.3 Hz, 2H), 2.98 (s, 9H), 1.34–1.27 (m, 3H).

G3: White solid obtained in a total yield of 75%. ^{1}H NMR (500 MHz, CD_3CN) δ 3.20–3.12 (m, 2H), 2.99 (s, 9H), 1.74 (dq, *J* = 15.2, 7.5 Hz, 2H), 0.95 (t, *J* = 7.3 Hz, 3H).

G4: White solid obtained in a total yield of 70%. ^{1}H NMR (500 MHz, CD_3CN) δ 3.25–3.18 (m, 2H), 3.02 (s, 9H), 1.77–1.67 (m, 2H), 1.39 (h, *J* = 7.4 Hz, 2H), 0.99 (t, *J* = 7.4 Hz, 3H).

G5: White solid obtained in a total yield of 68%. ^{1}H NMR (500 MHz, CD_3CN) δ 3.22–3.14 (m, 2H), 2.99 (s, 9H), 1.77–1.66 (m, 2H), 1.42–1.25 (m, 4H), 0.93 (t, *J* = 7.2 Hz, 3H).

G6: light-yellow solid obtained in a total yield of 68%. ^{1}H NMR (400 MHz, CD_3CN) δ 3.28-3.17 (m, 1H), 2.95 (s, 9H), 1.52–1.36 (m, 1H), 1.36-1.31 (m, 3H), 1.00 (t, *J* = 7.4 Hz, 3H).

G7: yellow solid obtained in a total yield of 72%. ^{1}H NMR (500 MHz, CD_3CN) δ 3.12 (d, *J* = 5.1 Hz, 2H), 3.02 (s, 9H), 1.08 (d, *J* = 6.8 Hz, 6H).

G8: light-yellow solid obtained in a total yield of 63%. ^{1}H NMR (500 MHz, CD_3CN) δ 3.20 (s, 2H), 3.10 (s, 9H), 1.16 (s, 9H).

G17: white solid obtained in a total yield of 66%. ^{1}H NMR (500 MHz, CD_3CN) δ 7.61–7.47 (m, 5H), 4.37 (s, 2H), 2.99 (s, 9H).

G20: light-yellow solid obtained in a total yield of 67%. ^{1}H NMR (400 MHz, CD_3CN) δ 7.50–7.29 (m, 4H), 4.43 (s, 2H), 3.01 (s, 9H), 2.44 (s, 3H).

G21: yellow solid obtained in a total yield of 73%. ^{1}H NMR (500 MHz, CD_3CN) δ 7.47–7.39 (m, 2H), 7.33 (s, 1H), 7.32-7.28 (m, 1H), 4.35 (s, 2H), 3.01 (s, 9H), 2.42 (s, 3H).

G23: light-yellow solid obtained in a total yield of 75%. ^{1}H NMR (500 MHz, CD_3CN) δ 3.11 (d, *J* = 4.1 Hz, 2H), 3.03 (s, 9H), 1.90–1.80 (m, 3H), 1.78–1.71 (m, 2H), 1.70-1.62 (m, 1H), 1.44-1.33 (m, 2H), 1.27–1.12 (m, 3H).

G24: white solid obtained in a total yield of 72%. ^{1}H NMR (500 MHz, CD_3CN) δ 8.07–8.02 (m, 2H), 8.02–7.98 (m, 2H), 7.67–7.61 (m, 2H), 7.56 (dd, *J* = 8.4, 1.9 Hz, 1H), 4.54 (s, 2H), 3.05 (s, 9H).

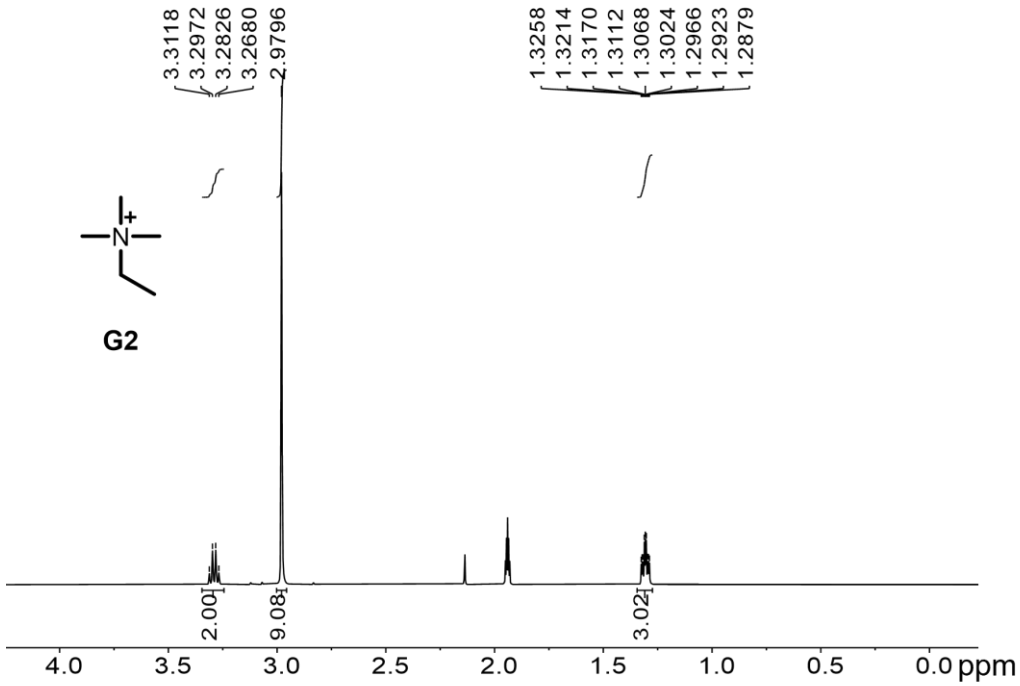

Figure S1. ^{1}H NMR spectrum (500 MHz, CD_3CN, 298 K) of PF_6^- salt of **G2**.

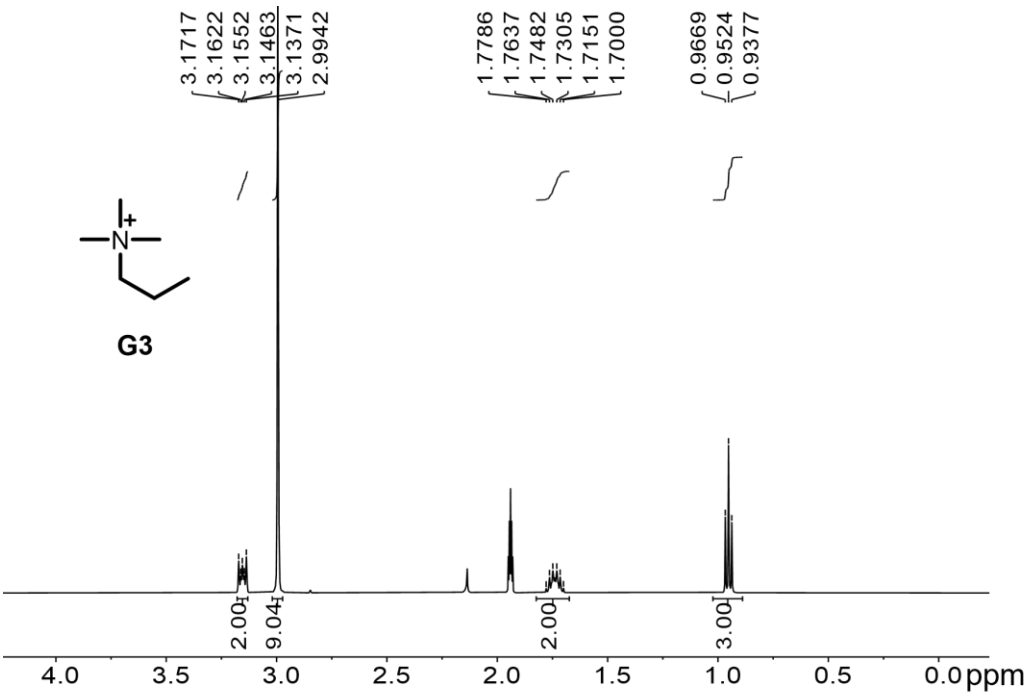

Figure S2. ^{1}H NMR spectrum (500 MHz, CD_3CN, 298 K) of PF_6^- salt of **G3**.

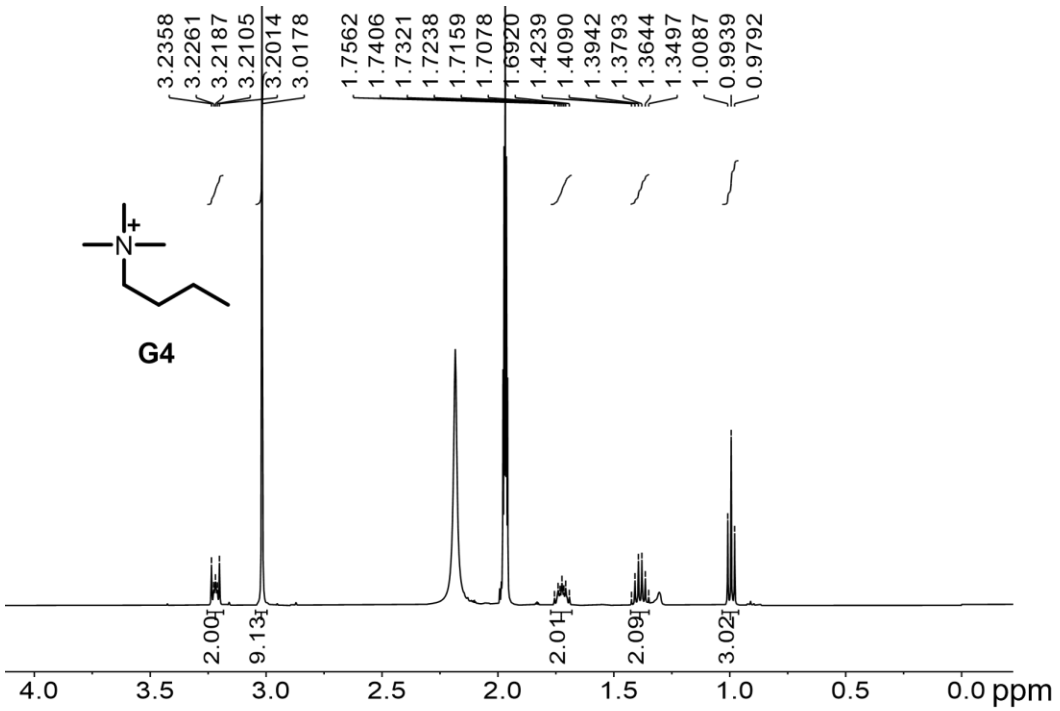

Figure S3. ^{1}H NMR spectrum (500 MHz, CD_3CN, 298 K) of PF_6^- salt of **G4**.

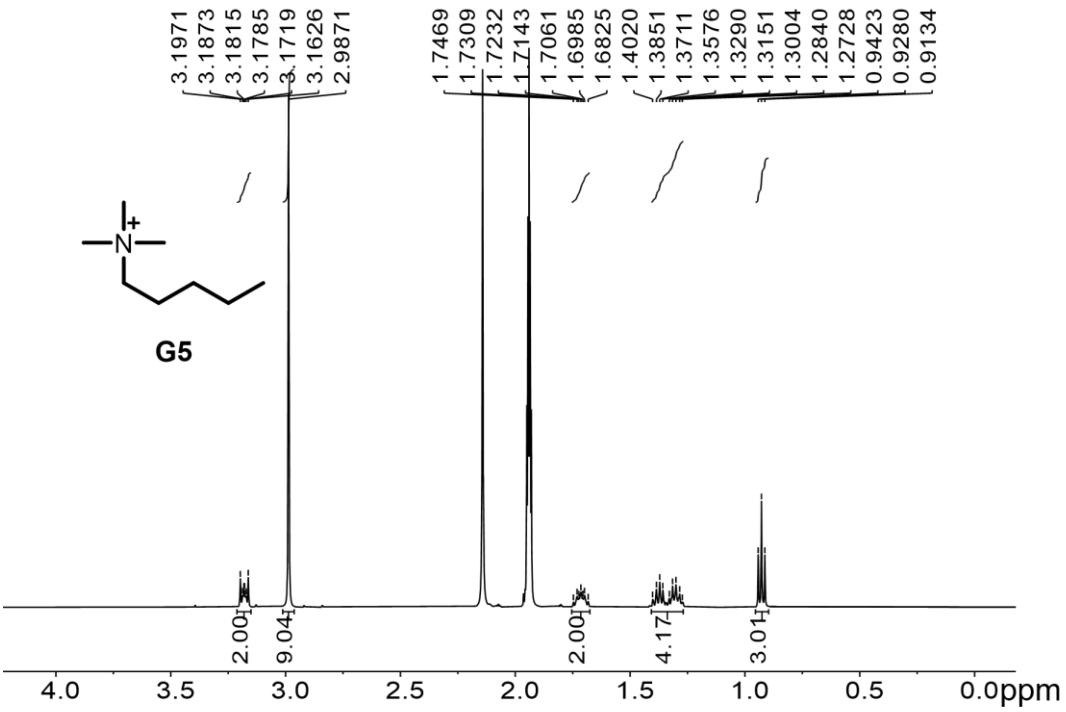

Figure S4. ^{1}H NMR spectrum (500 MHz, CD_3CN, 298 K) of PF_6^- salt of **G5**.

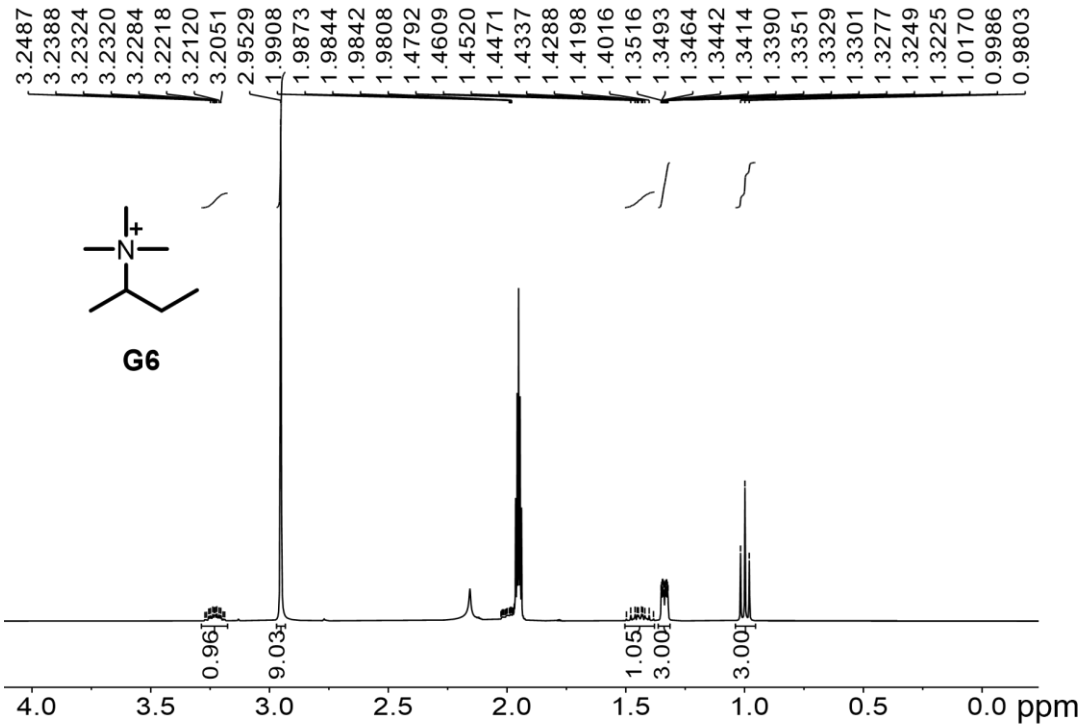

Figure S5. ^{1}H NMR spectrum (400 MHz, CD_3CN, 298 K) of PF_6^- salt of **G6**.

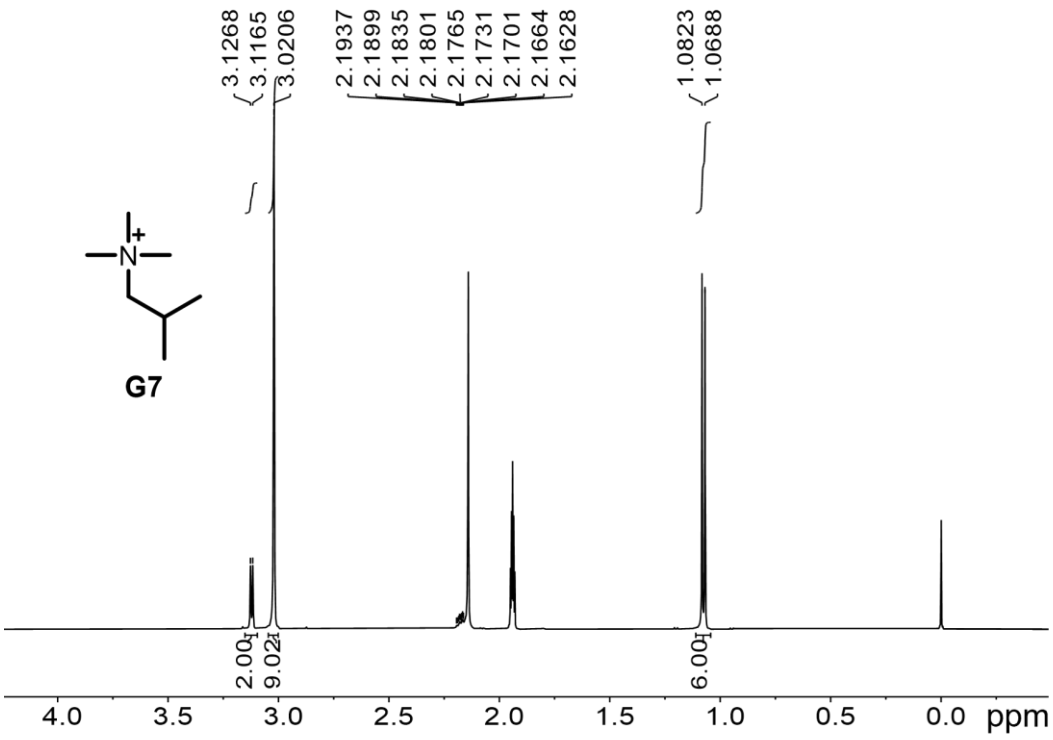

Figure S6. ^{1}H NMR spectrum (500 MHz, CD_3CN, 298 K) of PF_6^- salt of **G7**.

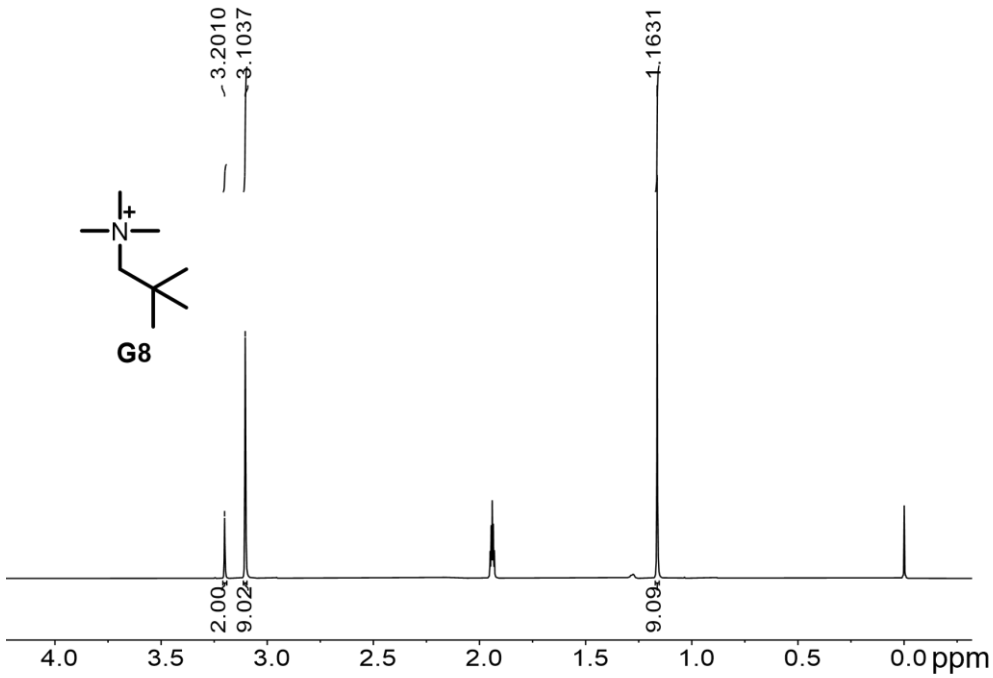

Figure S7. ^{1}H NMR spectrum (500 MHz, CD_3CN, 298 K) of PF_6^- salt of **G8**.

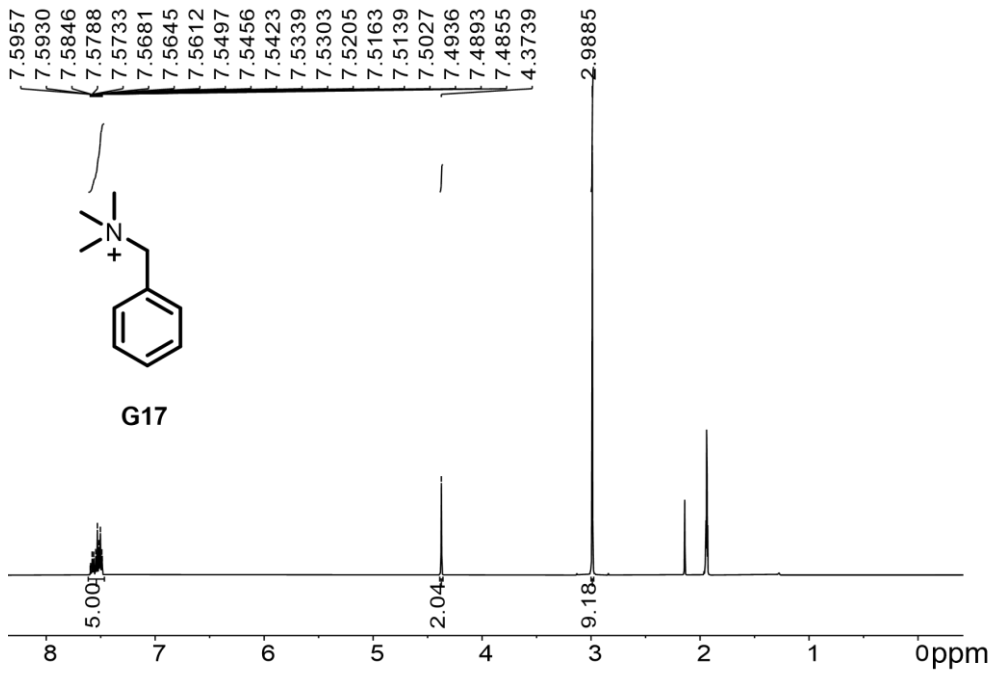

Figure S8. ^{1}H NMR spectrum (500 MHz, CD_3CN, 298 K) of PF_6^- salt of **G17**.

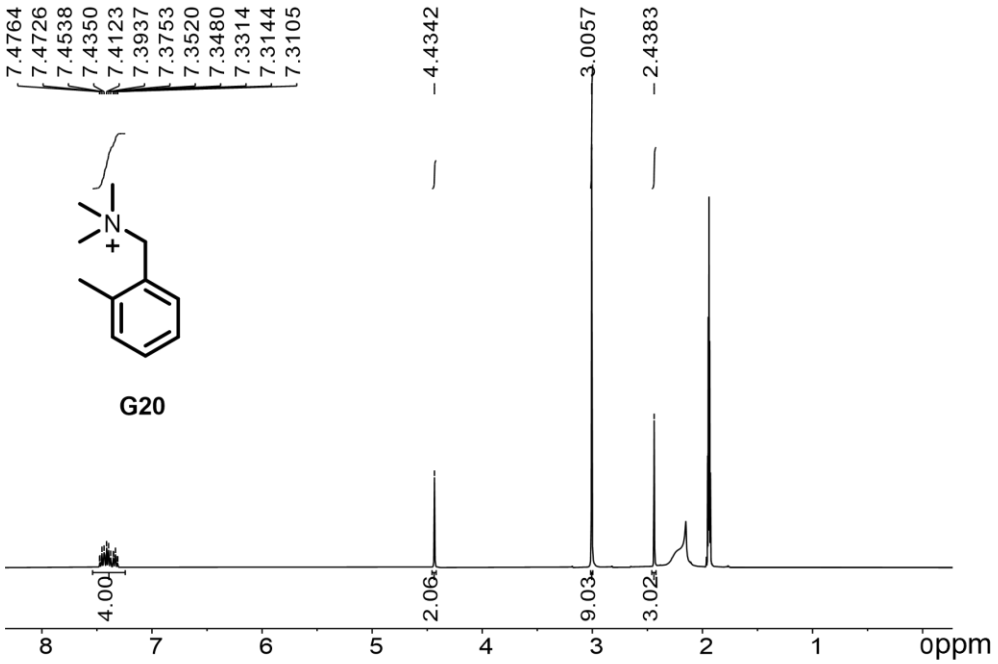

Figure S9. ^{1}H NMR spectrum (400 MHz, CD_3CN, 298 K) of PF_6^- salt of **G20**.

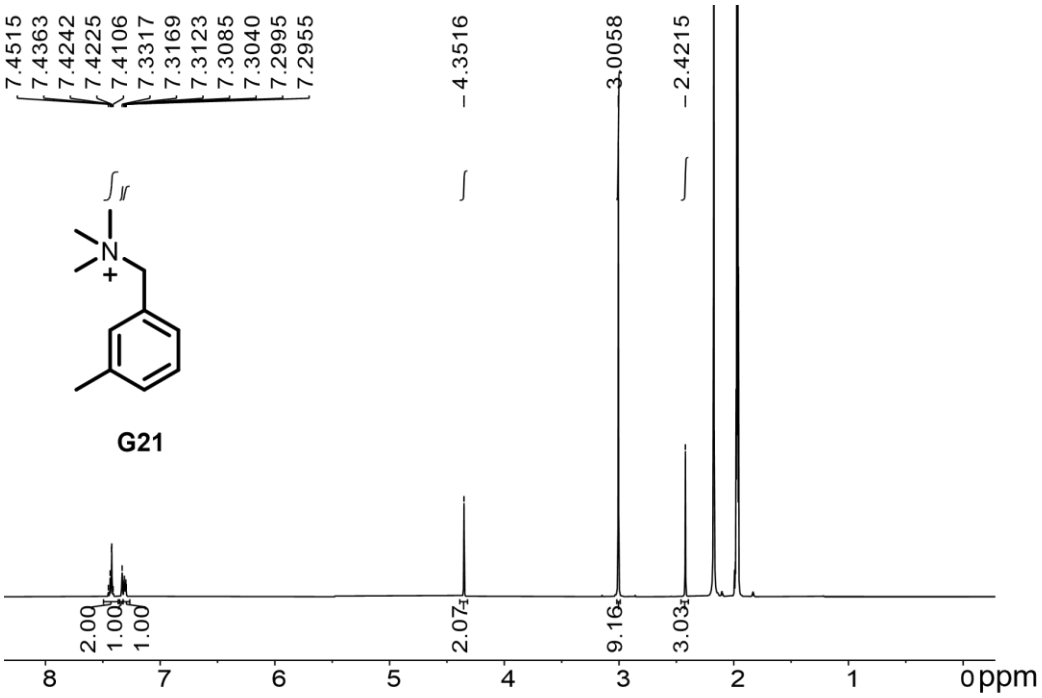

Figure S10. ^{1}H NMR spectrum (500 MHz, CD_3CN, 298 K) of PF_6^- salt of **G21**.

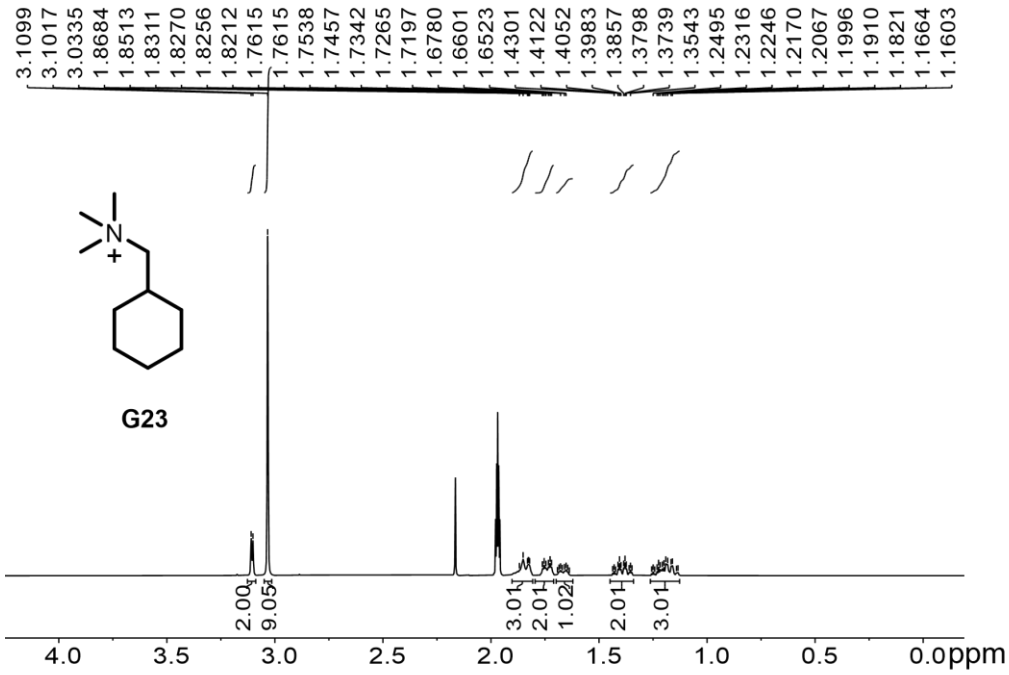

Figure S11. ^{1}H NMR spectrum (500 MHz, CD_3CN, 298 K) of PF_6^- salt of **G23**.

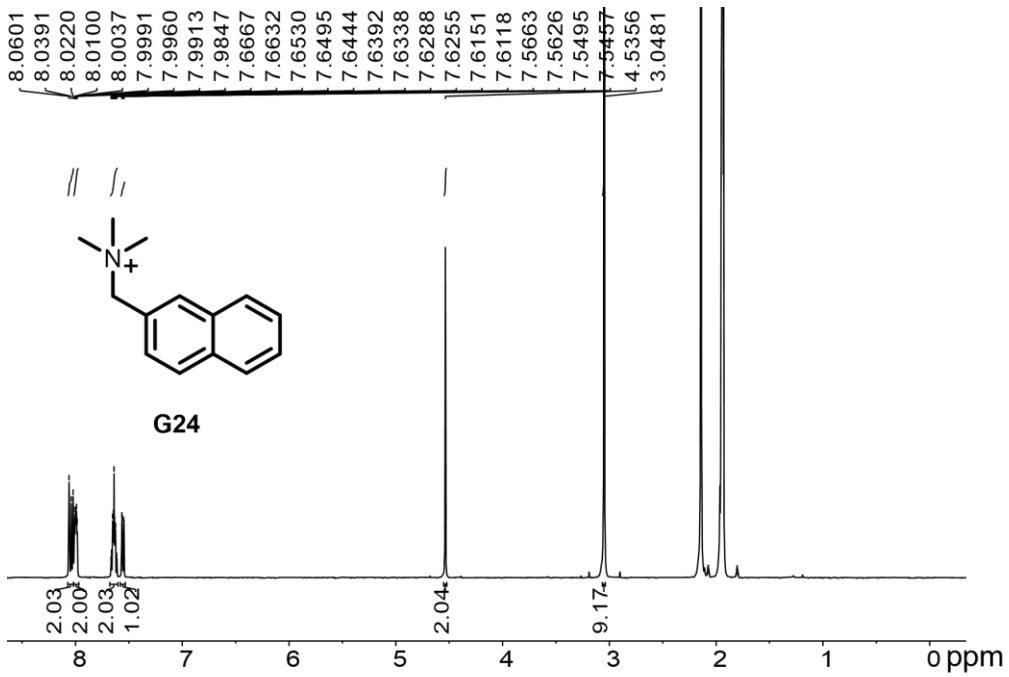

Figure S12. ^{1}H NMR spectrum (500 MHz, CD_3CN, 298 K) of PF_6^- salt of **G24**.

Synthesis of G9

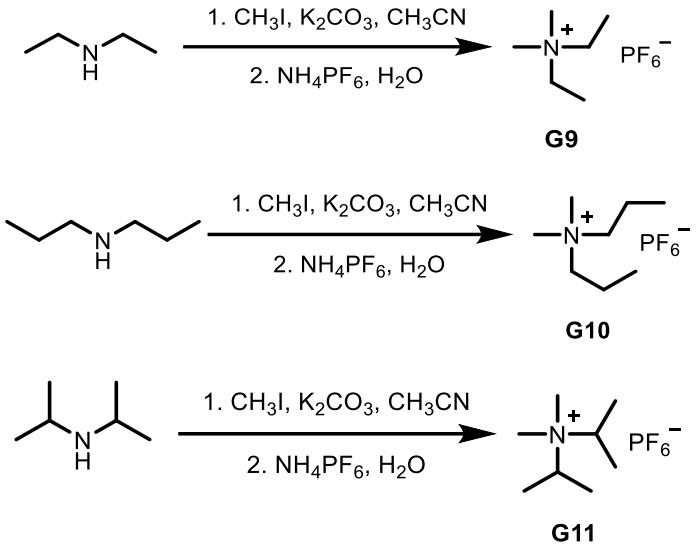

A mixture of the corresponding secondary amine (1 eq.), CH_3I (5.0 eq.) and K_2CO_3 (5.0 eq.) in CH_3CN (30 mL) was stirred at room temperature for 8 h. The solid suspension was filtered and the solution was dried over vacuum to yield **G9** as the iodide salt. The obtained iodide salt was then dissolved in deionized water to give a saturated solution of the ammonium salts, which was then added dropwisely into a saturated aqueous NH_4PF_6 solution. The resulting mixture was stirred for 1 h at room temperature, and the precipitate formed was collected by filtration, washed several times with deionized water and dried under vacuum to give the hexafluorophosphate salt.

G9: Yellow solid obtained in a total yield of 79%. ^{1}H NMR (500 MHz, CD_3CN) δ 3.25 (q, *J* = 7.3 Hz, 2H), 2.90 (s, 3H), 1.31–1.24 (m, 3H).

G10: Yellow solid obtained in a total yield of 77%. ^{1}H NMR (400 MHz, CD_3CN) δ 3.16 – 3.07 (m, 4H), 2.93 (s, 6H), 1.78 – 1.64 (m, 4H), 0.95 (t, *J* = 7.3 Hz, 6H).

G11: White solid obtained in a total yield of 65%. ^{1}H NMR (400 MHz, CD_3CN) δ 3.77 (p, *J* = 6.5 Hz, 2H), 2.73 (s, 6H), 1.32 (dt, *J* = 6.5, 1.7 Hz, 12H).

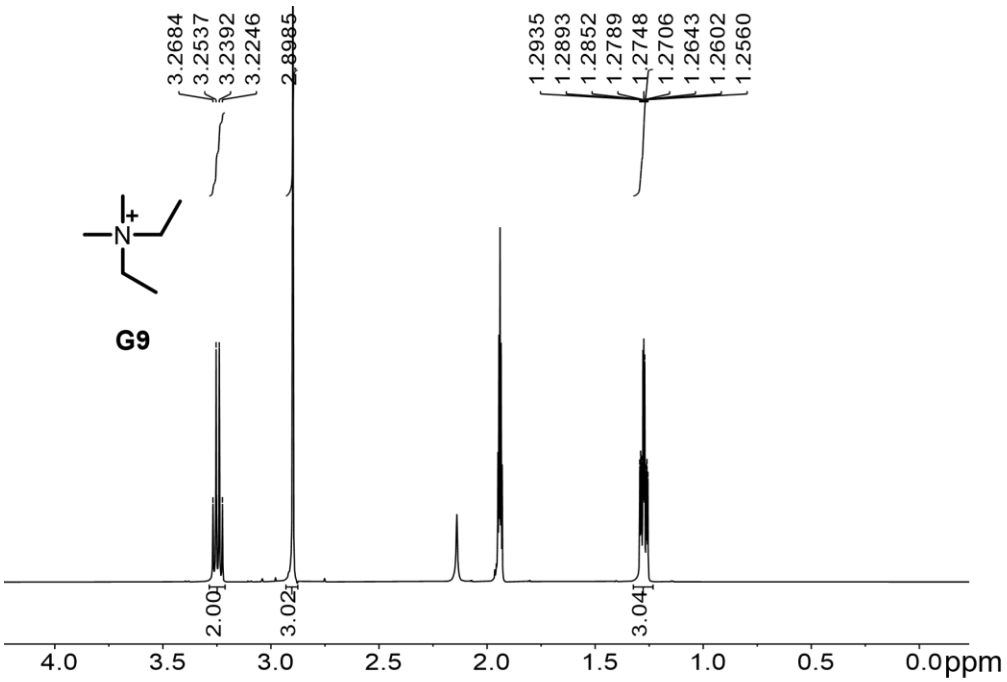

Figure S13. ^{1}H NMR spectrum (500 MHz, CD_3CN, 298 K) of PF_6^- salt of **G9**.

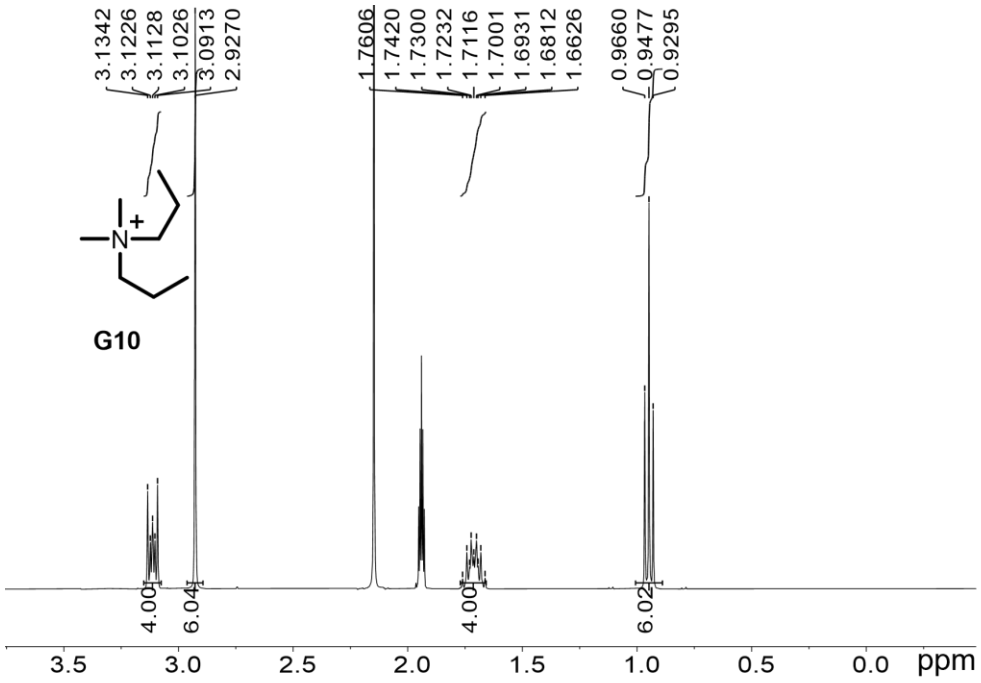

Figure S14. ^{1}H NMR spectrum (400 MHz, CD_3CN, 298 K) of PF_6^- salt of **G10**.

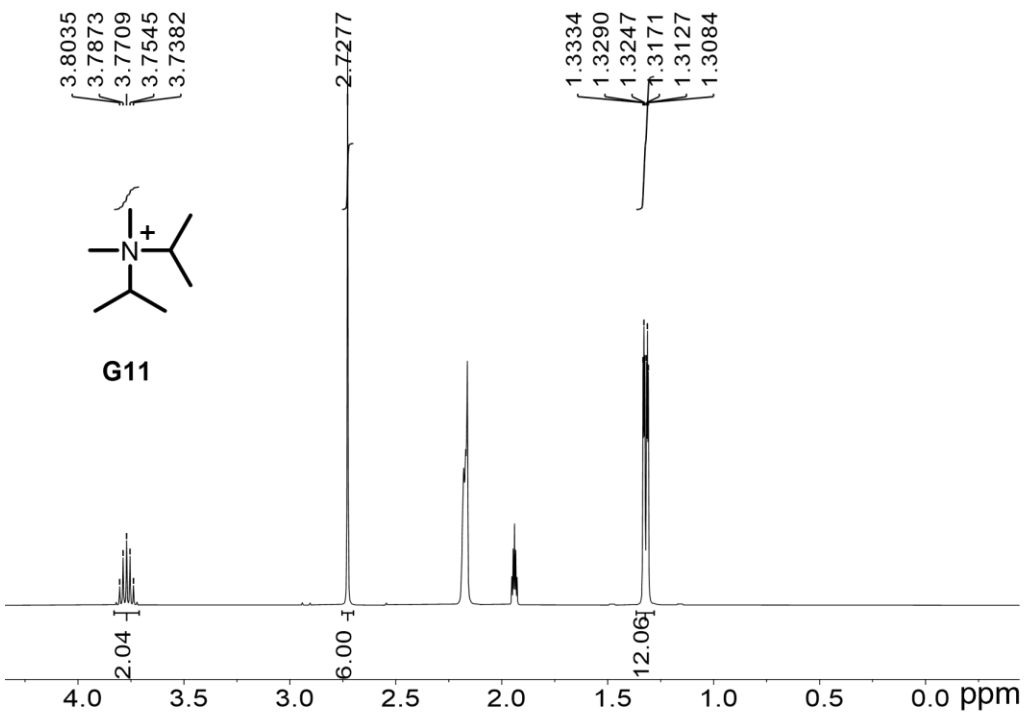

Figure S15. ^{1}H NMR spectrum (400 MHz, CD_3CN, 298 K) of PF_6^- salt of **G11**.

Synthesis of G12

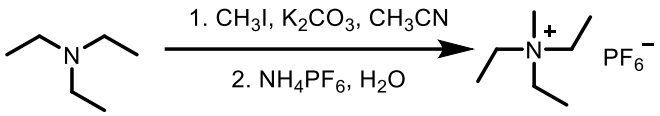

G12

A mixture of the triethylamine (1 g), CH_3I (5.0 eq.) and K_2CO_3 (5.0 eq.) in CH_3CN (30 mL) was stirred at room temperature for 8 h. The solid suspension was filtered and the solution was dried over vacuum to yield **G12** as the iodide salt. The obtained iodide salt was then dissolved in deionized water to give a saturated solution of the ammonium salts, which was then added dropwisely into a saturated aqueous NH_4PF_6 solution. The resulting mixture was stirred for 1 h at room temperature, and the precipitate formed was collected by filtration, washed several times with deionized water and dried under vacuum to give the hexafluorophosphate salt of **G12** as a white solid. Yield = 85%. ^{1}H NMR (400 MHz, CD_3CN) δ 3.21 (q, *J* = 7.3 Hz, 6H), 2.82 (s, 3H), 1.29 – 1.20 (m, 9H).

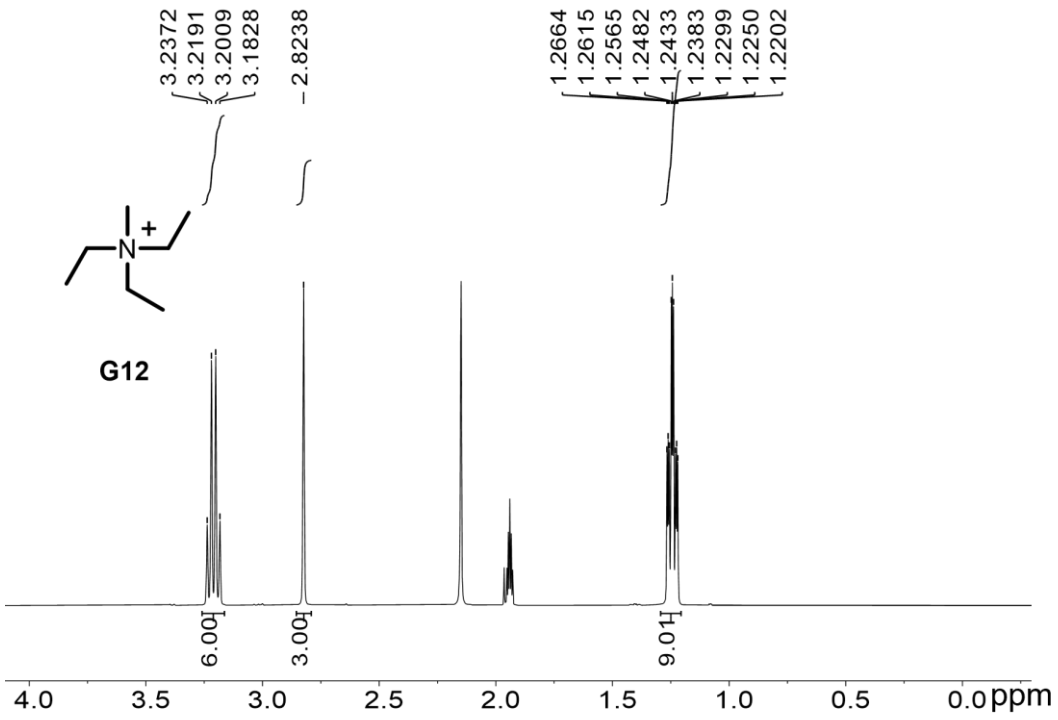

Figure S16. ^{1}H NMR spectrum (400 MHz, CD_3CN, 298 K) of PF_6^- salt of **G12**.

Synthesis of G14

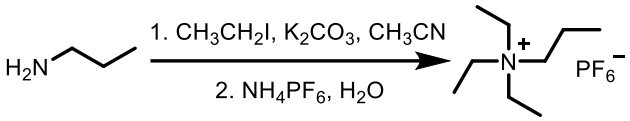

G14

A mixture of the propylamine (1 eq.), C_2H_5I (5.0 eq.) and K_2CO_3 (5.0 eq.) in CH_3CN (30 mL) was stirred at room temperature for 8 h. The solid suspension was filtered and the solution was dried over vacuum to yield **G14** as the iodide salt. The obtained iodide salt was then dissolved in deionized water to give a saturated solution of the ammonium salts, which was then added dropwisely into a saturated aqueous NH_4PF_6 solution. The resulting mixture was stirred for 1 h at room temperature, and the precipitate formed was collected by filtration, washed several times with deionized water and dried under vacuum to give the hexafluorophosphate salt of **G14** as a white solid. Yield = 70%. ^{1}H NMR (400 MHz, CD_3CN) δ 3.17 (q, *J* = 7.3 Hz, 6H), 3.05 – 2.96 (m, 2H), 1.63 (dq, *J* = 15.0, 7.5 Hz, 2H), 1.25 – 1.16 (m, 9H), 0.96 (t, *J* = 7.3 Hz, 3H).

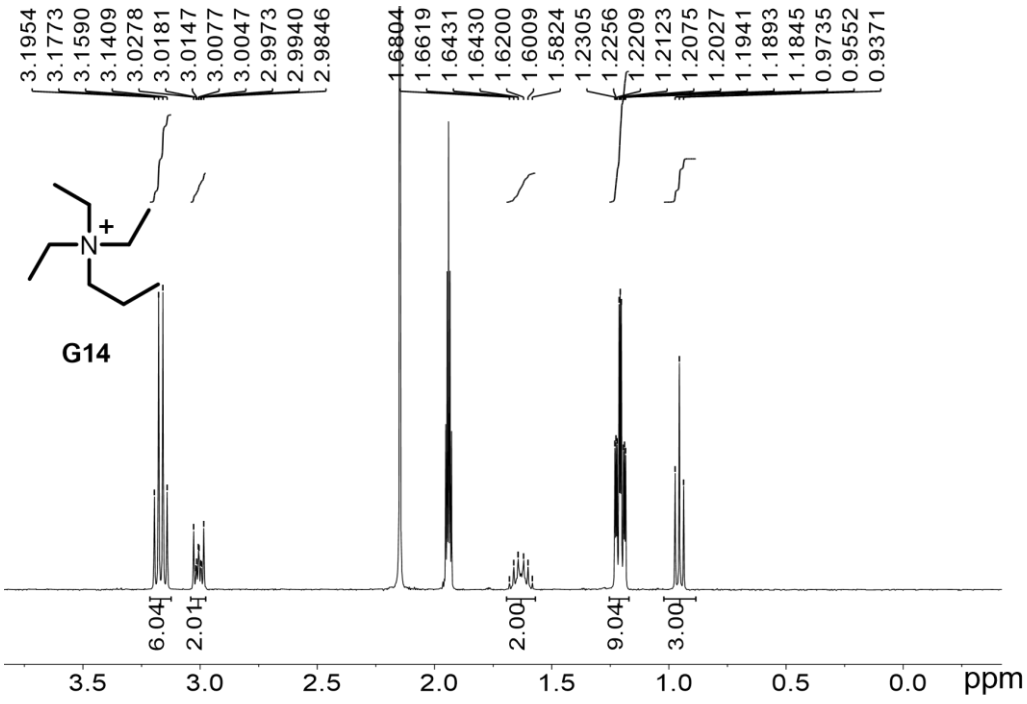

Figure S17. ^{1}H NMR spectrum (400 MHz, CD_3CN, 298 K) of PF_6^- salt of **G14**.

Synthesis of G15 and G16

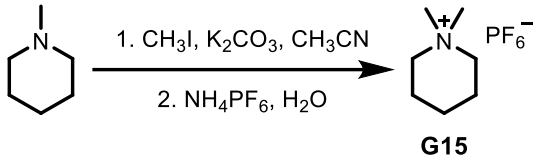

G15

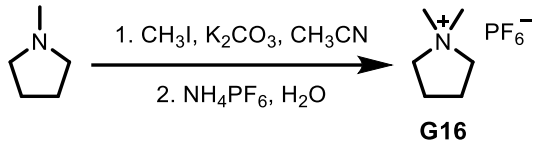

G16

A mixture of the 1-methylpiperidine (1 g) or 1-methylpyrrolidine (1 g), CH_3I (5.0 eq.) and K_2CO_3 (5.0 eq.) in CH_3CN (30 mL) was stirred at room temperature for 8 h. The solid suspension was filtered and the solution was dried over vacuum to yield **G15** or **G16** as the iodide salt. The obtained iodide salt was then dissolved in deionized water to give a saturated solution of the ammonium salts, which was then added dropwisely into a saturated aqueous NH_4PF_6 solution. The resulting mixture was stirred for 1 h at room temperature, and the precipitate formed was collected by filtration, washed several times with deionized water and dried under vacuum to give the hexafluorophosphate salt of **G15** and **G16** as white solids. Yield = 77% (for **G15**) and 88% (for **G16**). ^{1}H NMR for [**G15**][PF_6] (500 MHz, CD_3CN) δ 3.27 – 3.21 (m, 4H), 3.00 (s, 6H), 1.88–1.79 (m, 4H), 1.61 (p, *J* = 6.1 Hz, 2H). ^{1}H NMR for [**G16**][PF_6] (500 MHz, CD_3CN) δ 3.41 (t, *J* = 7.3 Hz, 4H), 3.04 (s, 6H), 2.20–2.15 (m, 4H).

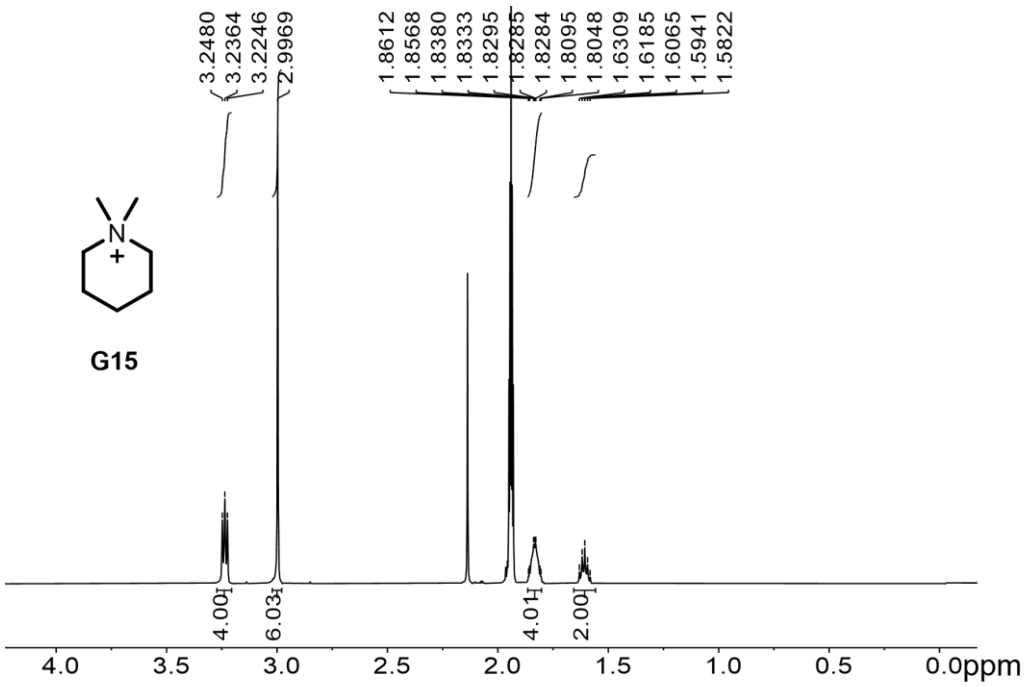

Figure S18. ^{1}H NMR spectrum (500 MHz, CD_3CN, 298 K) of PF_6^- salt of **G15**.

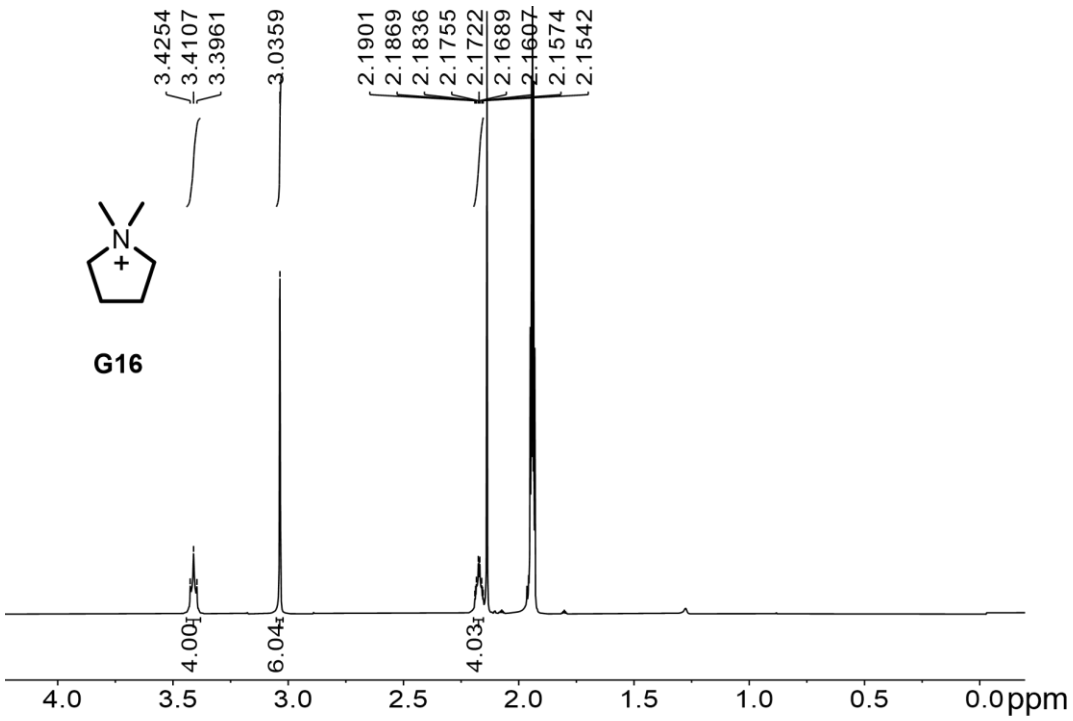

Figure S19. ^{1}H NMR spectrum (500 MHz, CD_3CN, 298 K) of PF_6^- salt of **G16**.

Synthesis of G18

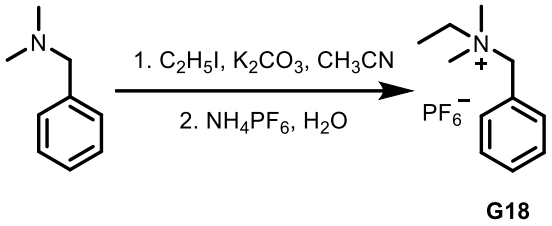

A mixture of the N,N'-dimethylbenzylamine (500 mg), CH_3CH_2I (5.0 eq.) and K_2CO_3 (5.0 eq.) in CH_3CN (20 mL) was stirred at room temperature for 8 h. The solid suspension was filtered and the solution was dried over vacuum to yield **G18** as the iodide salt. The obtained iodide salt was then dissolved in deionized water to give a saturated solution of the ammonium salts, which was then added dropwisely into a saturated aqueous NH_4PF_6 solution. The resulting mixture was stirred for 1 h at room temperature, and the precipitate formed was collected by filtration, washed several times with deionized water and dried under vacuum to give the hexafluorophosphate salt of **G18** as white solids. Yield = 70%. ^{1}H NMR for [**G18**][PF_6] (500 MHz, CD_3CN) δ 7.60 – 7.46 (m, 5H), 4.35 (s, 2H), 3.30 (q, *J* = 7.3 Hz, 2H), 2.88 (s, 6H), 1.38 (tt, *J* = 7.3, 2.0 Hz, 3H).

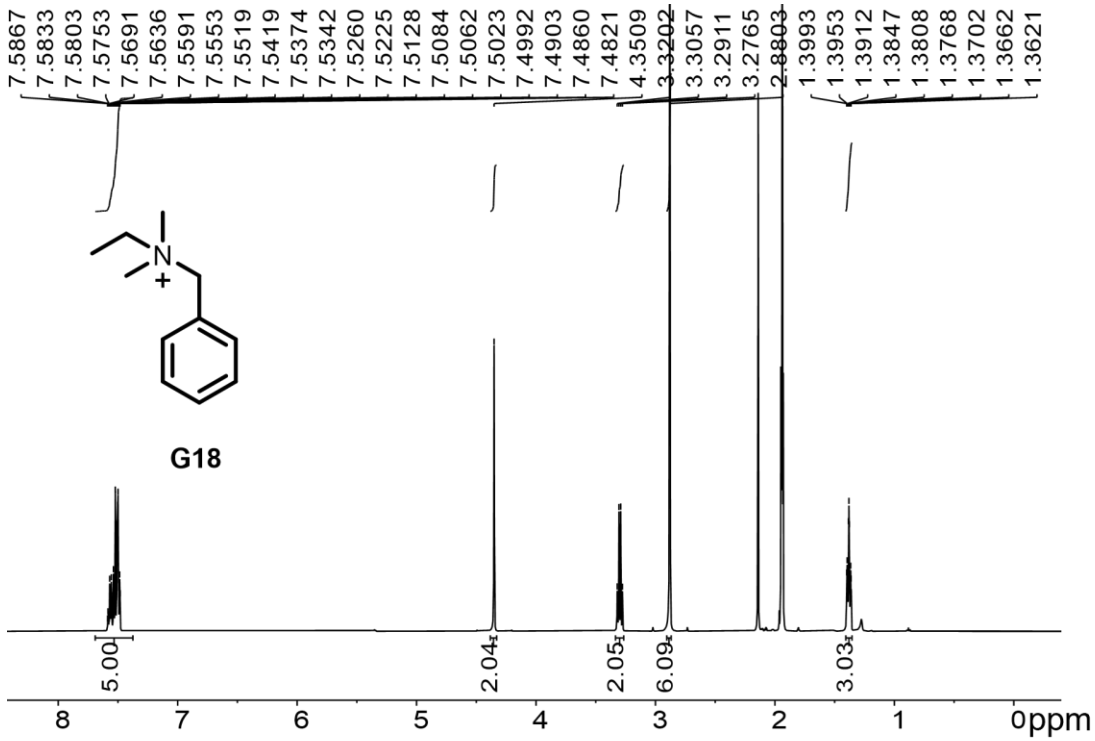

Figure S20. ^{1}H NMR spectrum (500 MHz, CD_3CN, 298 K) of PF_6^- salt of **G18**.

Synthesis of G19 and G22

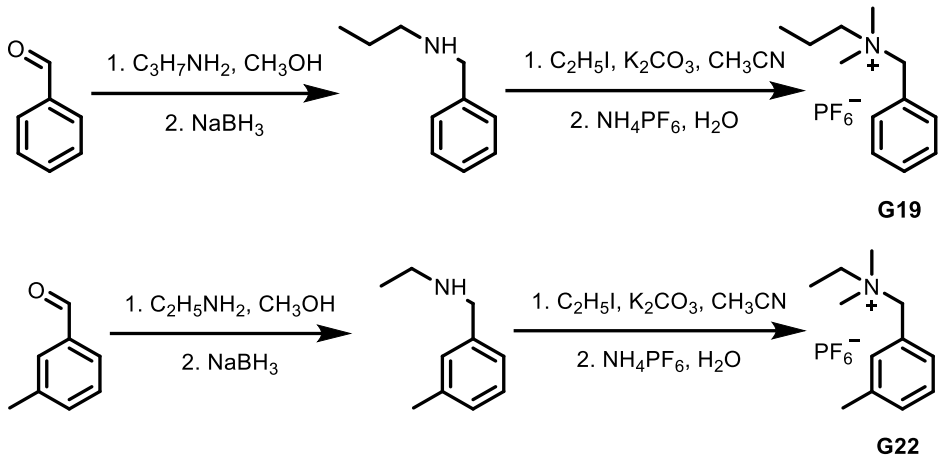

Corresponding benzaldehyde (1 eq.) was added into the solution of $C_3H_7NH_2$ or $C_2H_5NH_2$ (1.5 eq.) in CH_3OH. The resulting solution was stirred at room temperature for 8 h. After the reaction has been completed, the reaction mixture was slowly cooled to 0^{o}C in an ice bath and $NaBH_4$ (3 e.q.) was added. Evaporated the solvent to get the secondary amine.

Corresponding secondary amine was added into the solution of CH_3I (5.0 eq.) in CH_3CN. The resulting solution was stirred at room temperature for 8 h. The suspended solid was removed by filtration and the solution was dried over vacuum to yield the iodide salts. The saturated solution of corresponding iodide salt (1.0 eq.) in deionized water was added dropwise into saturated aqueous NH_4PF_6 (20 eq.) solution. After stirring for 1 h, the precipitate was filtered off and the filter cake was washed several times with deionized water and dried to give the hexafluorophosphate salts of **G19** and **G22** as yellow solids. Yield = 52% (for **G19**) and 44% (for **G22**). ^{1}H NMR for [**G19**][PF_6] (500 MHz, CD_3CN) δ 7.57 – 7.46 (m, 1H), 4.37 (s, 1H), 3.19 – 3.12 (m, 0H), 1.89 – 1.78 (m, 0H), 0.96 (t, *J* = 7.3 Hz, 1H). ^{1}H NMR for [**G22**][PF_6] (400 MHz, CD_3CN) δ 7.50 – 7.29 (m, 4H), 4.43 (s, 2H), 3.01 (s, 9H), 2.44 (s, 3H).

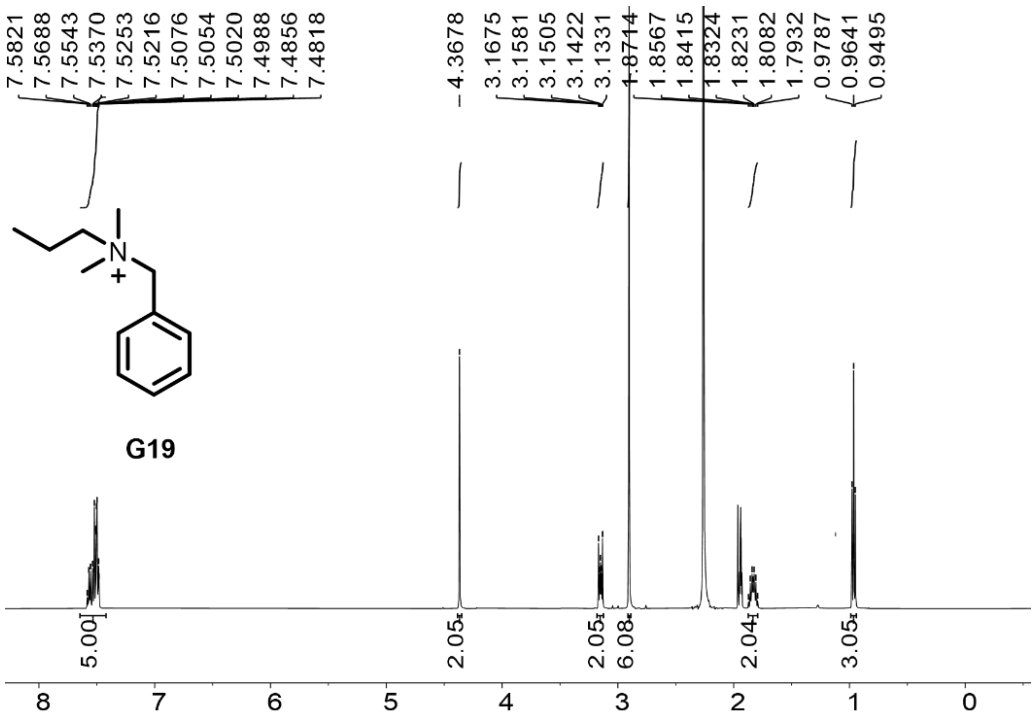

Figure S21. ^{1}H NMR spectrum (500 MHz, CD_3CN, 298 K) of PF_6^- salt of **G19**.

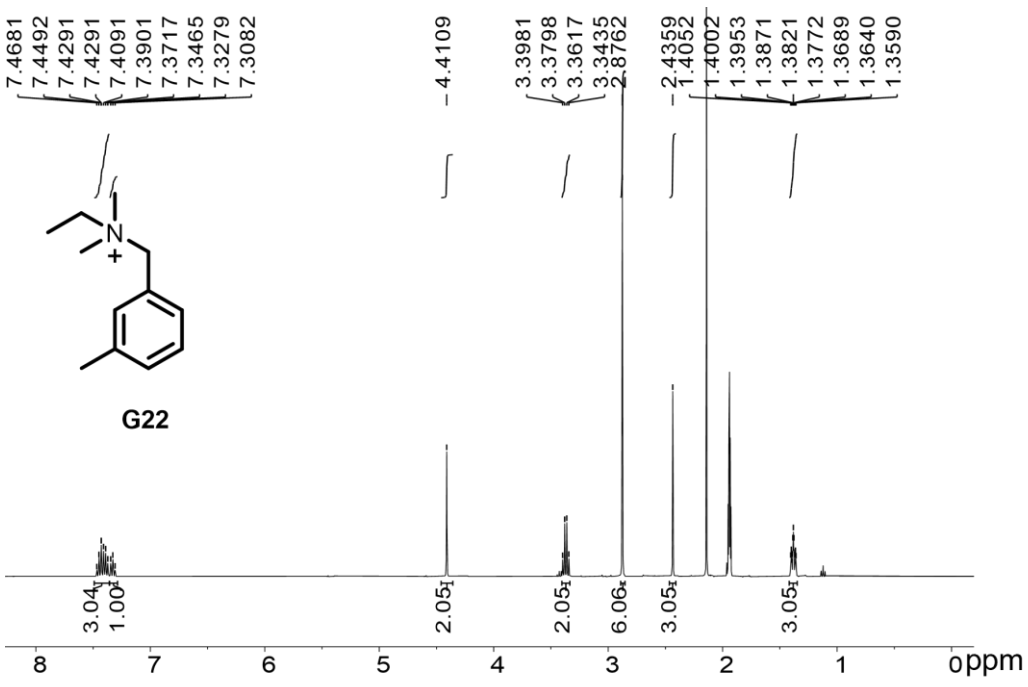

Figure S22. ^{1}H NMR spectrum (400 MHz, CD_3CN, 298 K) of PF_6^- salt of **G22**.

Synthesis of A1 and A2

A saturated solution of choline chloride (5 mL) or acetylcholine chloride (5 mL) in deionized water was added dropwise into saturated aqueous NH_4PF_6 solution (20 mL). After stirring for 1 h, the precipitate formed was collected by filtration and washed several times with deionized water and dried under vacuum to give the hexafluorophosphate salt of **A1** and **A2** as white solids. Yield = 90% (for **A1**) and 88% (for **A2**). ^{1}H NMR for [**A1**][PF_6] (500 MHz, CD_3CN) δ 3.96-3.88 (m, 2H), 3.40 (s, 1H), 3.37–3.34 (m, 2H), 3.09 (s, 9H). ^{1}H NMR for [**A2**][PF_6] (500 MHz, CD_3CN) δ 4.43–4.37 (m, 2H), 3.56–3.51 (m, 2H), 3.08 (s, 9H), 2.06 (s, 3H).

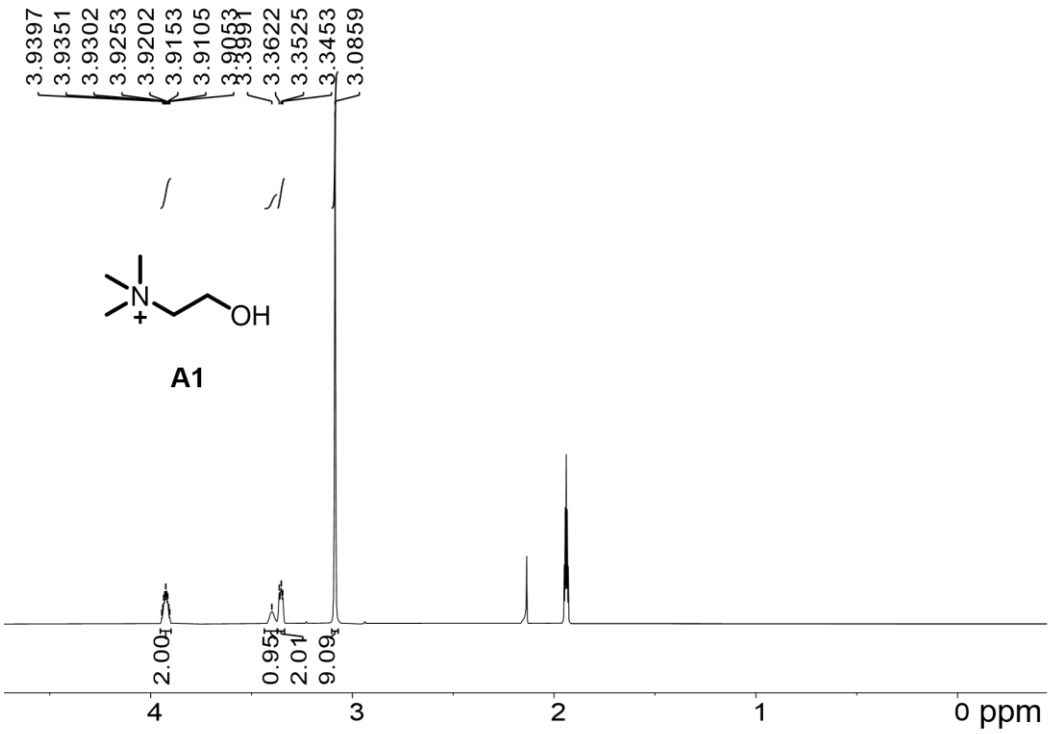

Figure S23. ^{1}H NMR spectrum (500 MHz, CD_3CN, 298 K) of PF_6^- salt of **A1**.

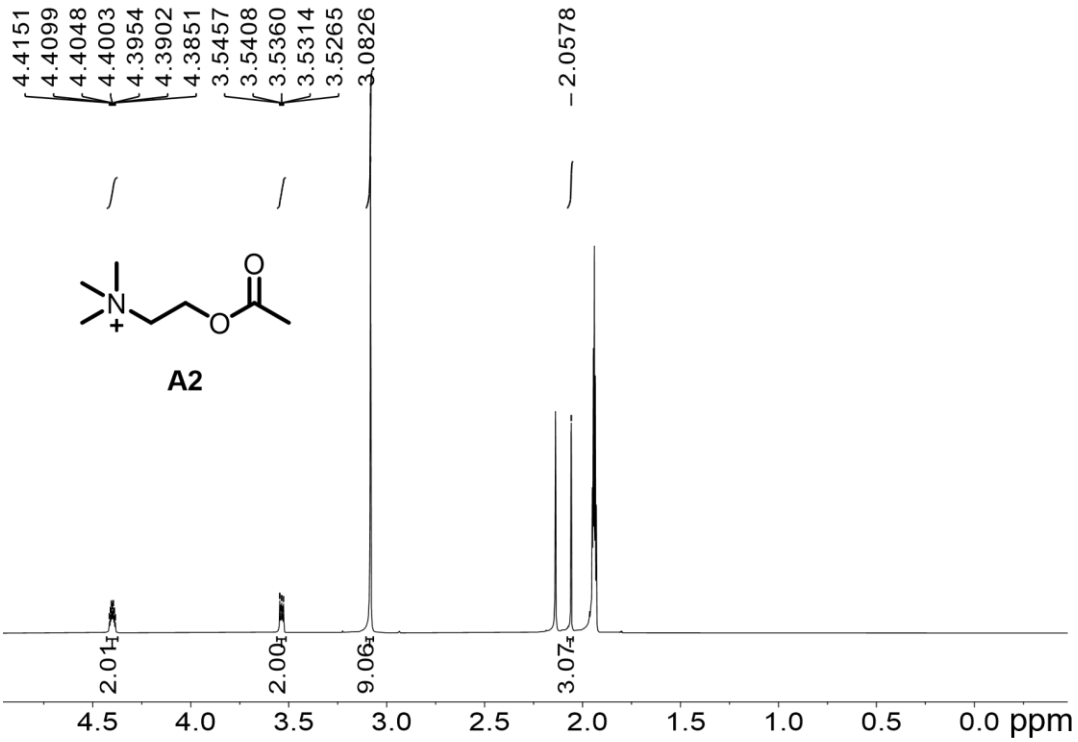

Figure S24. ^{1}H NMR spectrum (500 MHz, CD_3CN, 298 K) of PF_6^- salt of **A2**.

Synthesis of A3, A4 and A7

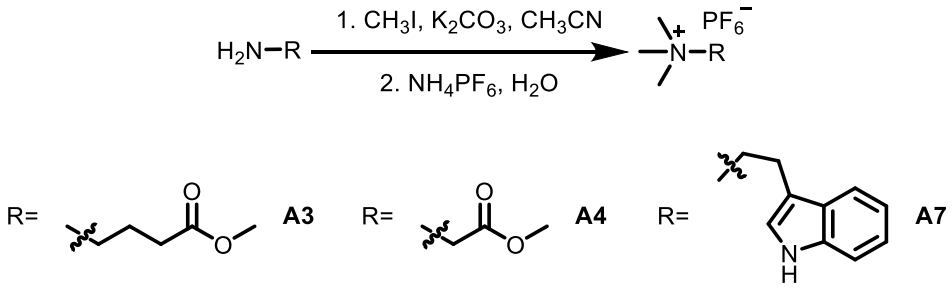

The corresponding amine (1.0 eq.) was added into the solution of CH_3I (5.0 eq.) and K_2CO_3 (5.0 eq.) in CH_3CN. The resulting solution was stirred at room temperature for 8 h. The suspended solid was removed by filtration and the solution was dried over vacuum to yield the iodide salts. The saturated solution of corresponding iodide salt (1.0 eq.) in deionized water was added dropwise into saturated aqueous NH_4PF_6 (20 eq.) solution. After stirring for 1 h, the precipitate was filtered off and the filter cake was washed several times with deionized water and dried to give the hexafluorophosphate salts.

A3: White solid obtained in a total yield of 83%. ^{1}H NMR (500 MHz, CD_3CN) δ 3.65 (s, 1H), 3.27 - 3.20 (m, 1H), 3.02 (s, 4H), 2.00 (dt, *J* = 15.3, 7.2 Hz, 1H).

A4: White solid obtained in a total yield of 73%. ^{1}H NMR (500 MHz, CD_3CN) δ 4.08 (s, 1H), 3.79 (s, 1H), 3.21 (s, 4H).

A7: Yellow solid obtained in a total yield of 68%. ^{1}H NMR (500 MHz, CD_3CN) δ 9.28 (s, 1H), 7.64 (d, *J* = 7.9 Hz, 1H), 7.47 (d, *J* = 8.1 Hz, 1H), 7.25-7.17 (m, 2H), 7.18-7.09 (m, 1H), 3.58-3.49 (m, 2H), 3.29-3.22 (m, 2H), 3.15 (s, 9H).

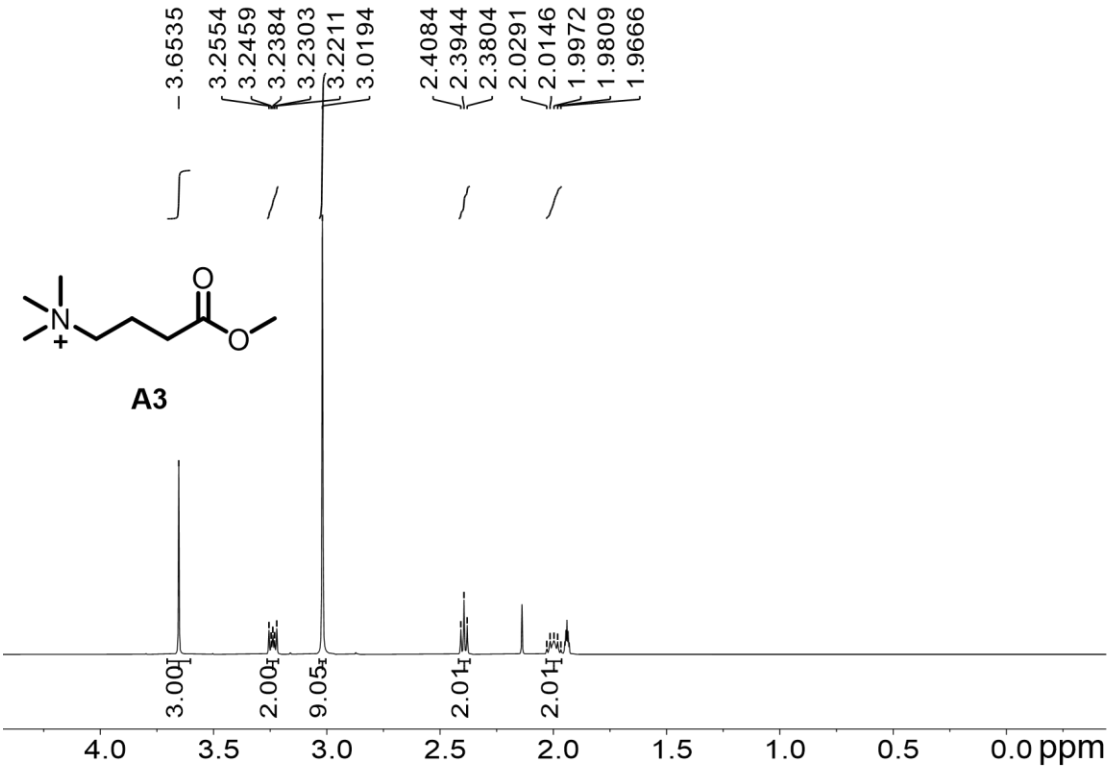

Figure S25. ^{1}H NMR spectrum (500 MHz, CD_3CN, 298 K) of PF_6^- salt of **A3**.

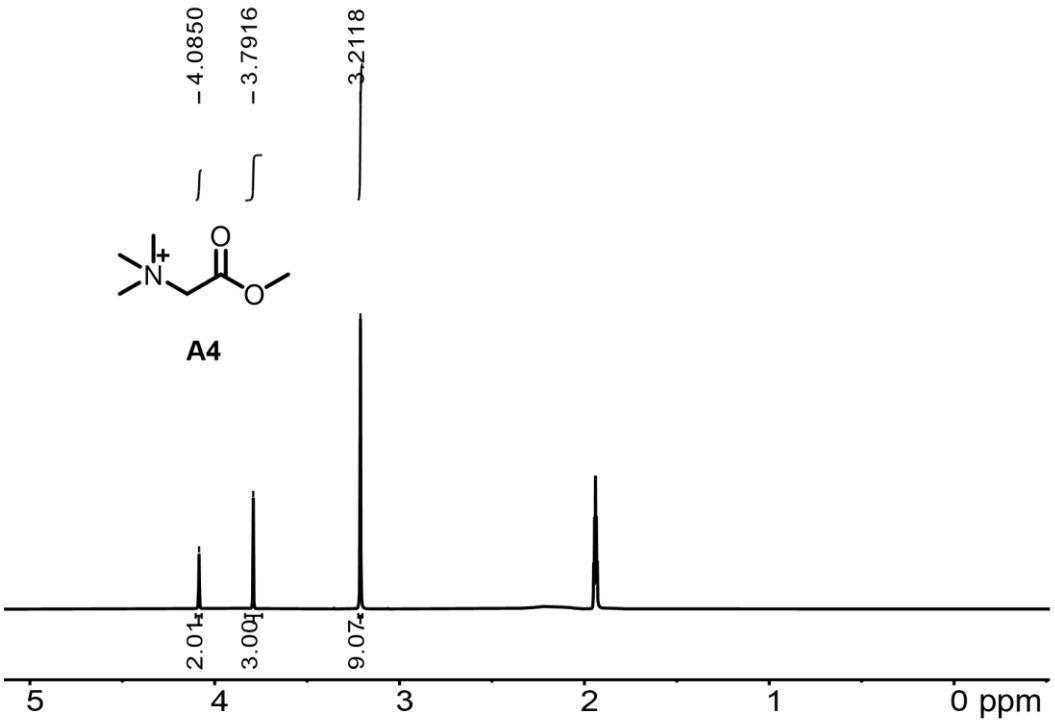

Figure S26. ^{1}H NMR spectrum (500 MHz, CD_3CN, 298 K) of PF_6^- salt of **A4**.

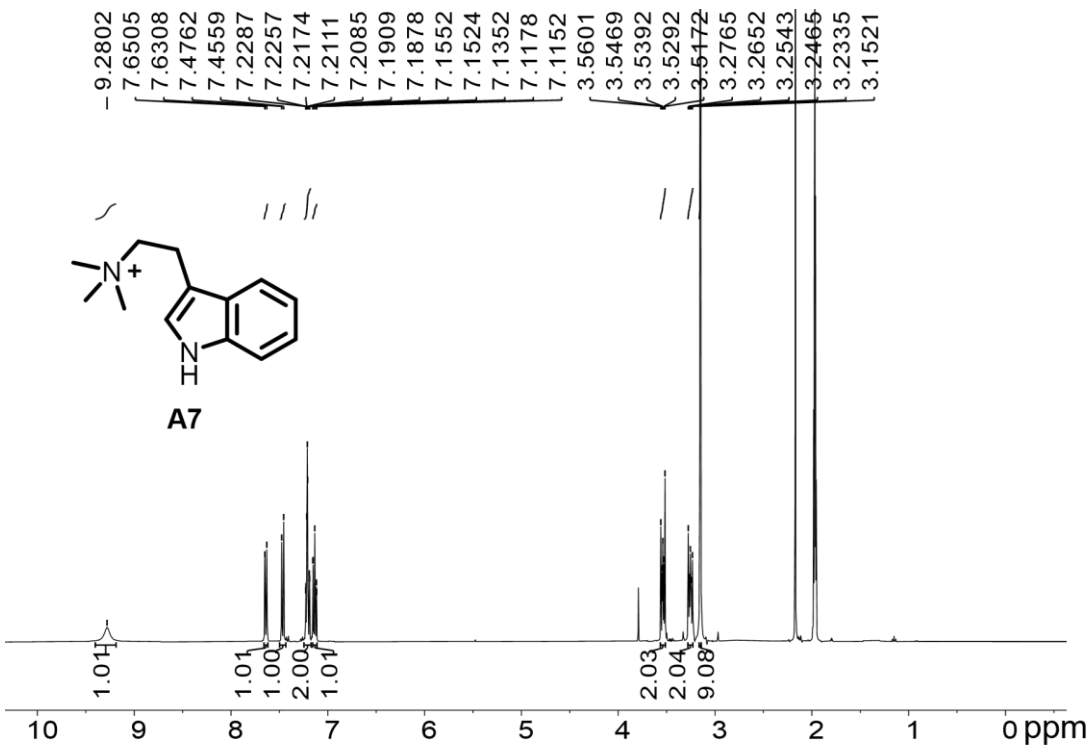

Figure S27. ^{1}H NMR spectrum (500 MHz, CD_3CN, 298 K) of PF_6^- salt of **A7**.

Synthetic procedure for A5 and A6

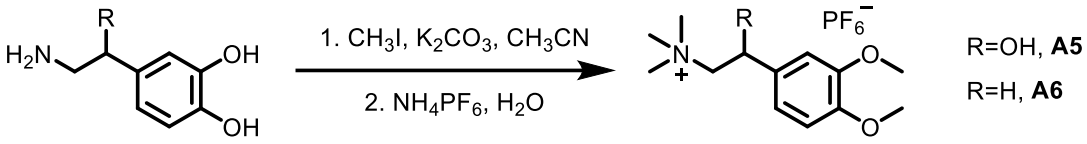

The corresponding amine (1.0 eq.) was added into the solution of CH_3I (5.0 eq.), K_2CO_3 (5.0 eq.) in CH_3CN. The resulting solution was stirred at room temperature for 8 h. The suspended solid was removed by filtration and the solution was dried over vacuum to yield the iodide salts. The saturated solution of corresponding iodide salt (1.0 eq.) in deionized water was added dropwise into saturated aqueous NH_4PF_6 (20 eq.) solution. After stirring for 1 h, the precipitate was filtered off and the filter cake was washed several times with deionized water and dried to give the hexafluorophosphate salt of **A5** and **A6** as white solids. Yield = 64% (for **A5**) and 75% (for **A6**). ^{1}H NMR for [**A5**][PF_6] (500 MHz, CD_3CN) δ 6.97 (s, 1H), 6.94 (s, 1H), 6.94 (s, 1H), 5.17 (dt, *J* = 10.5, 2.9 Hz, 1H), 4.00 (dd, *J* = 3.6, 1.7 Hz, 1H), 3.81 (d, *J* = 12.6 Hz, 6H), 3.48 (dd, *J* = 13.7, 10.5 Hz, 1H), 3.26 (dt, *J* = 13.7, 2.1 Hz, 1H), 3.18 (s, 9H). ^{1}H NMR for [**A6**][PF_6] (500 MHz, CD_3CN) δ 6.92 - 6.86 (m, 2H), 6.81 (d, *J* = 8.2 Hz, 1H), 3.79 (d, *J* = 14.1 Hz, 6H), 3.45-3.38 (m, 2H), 3.08 (s, 9H), 3.02-2.95 (m, 2H).

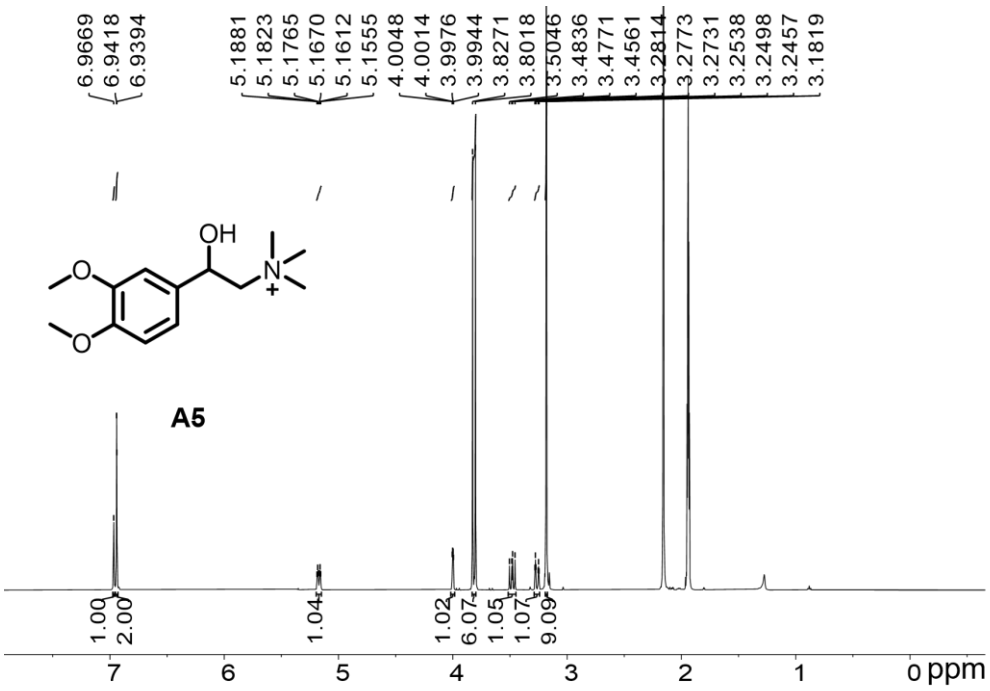

Figure S28. ^{1}H NMR spectrum (500 MHz, CD_3CN, 298 K) of PF_6^- salt of **A5**.

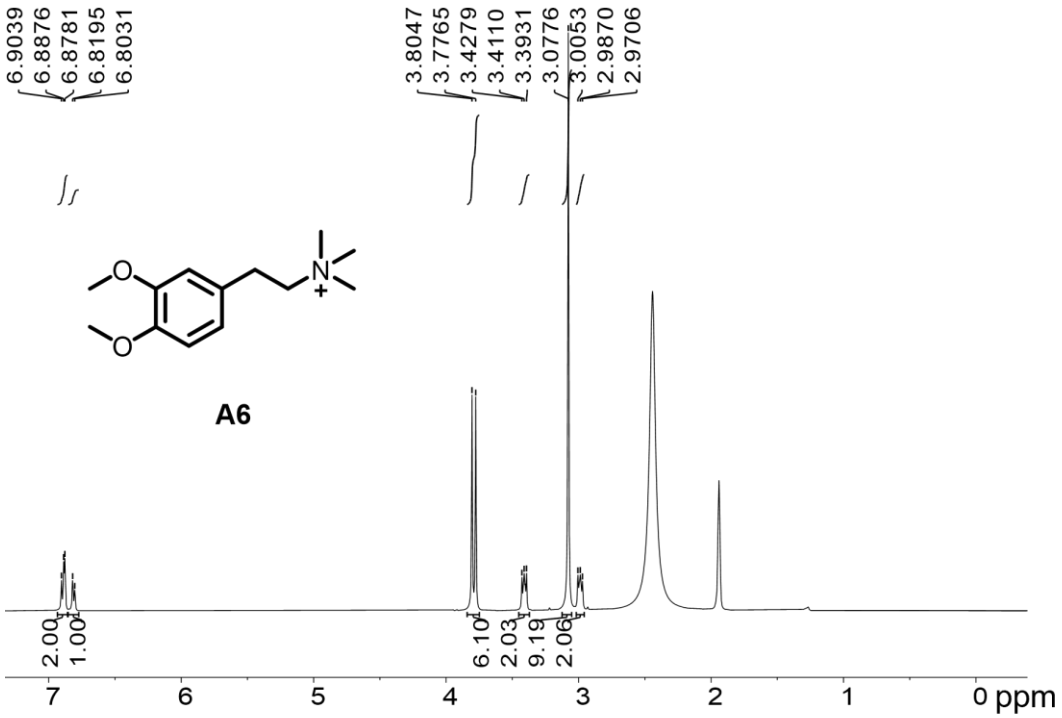

Figure S29. ^{1}H NMR spectrum (500 MHz, CD_3CN, 298 K) of PF_6^- salt of **A6**.

Synthetic procedure of A8.

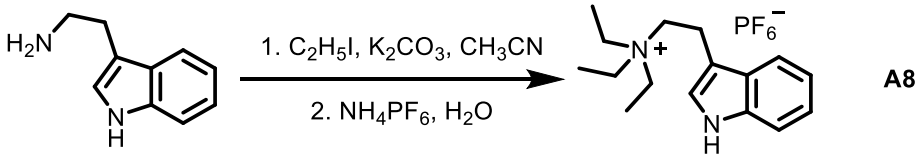

Tryptamine (1.0 eq.) was added into the solution of C_2H_5I (5.0 eq.), K_2CO_3 (5.0 eq.) in CH_3CN. The resulting solution was stirred at room temperature for 8 h. The suspended solid was removed by filtration and the solution was dried over vacuum to yield the iodide salts. The saturated solution of corresponding iodide salt (1.0 eq.) in deionized water was added dropwise into saturated aqueous NH_4PF_6 (20 eq.) solution. After stirring for 1 h, the precipitate was filtered off and the filter cake was washed several times with deionized water and dried to give the hexafluorophosphate salt of **A8** as white solids. Yield = 70%. ^{1}H NMR for [**A8**][PF_6] (500 MHz, CD_3CN) δ 9.29 (s, 1H), 7.61 (d, *J* = 8.0 Hz, 1H), 7.47 (dd, *J* = 8.1, 1.1 Hz, 1H), 7.28-7.19 (m, 2H), 7.24-7.09 (m, 1H), 3.43-3.29 (m, 8H), 3.20-3.11 (m, 2H), 1.31 (ddd, *J* = 9.1, 5.5, 1.9 Hz, 9H).

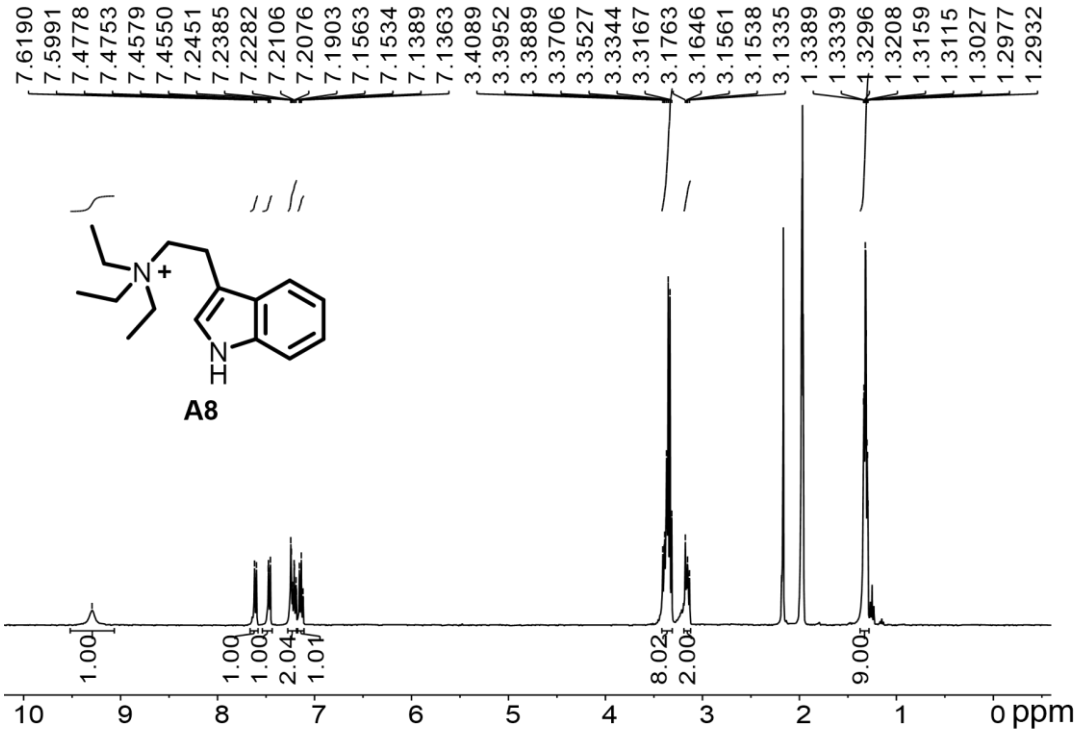

Figure S30. ^{1}H NMR spectrum (500 MHz, CD_3CN, 298 K) of PF_6^- salt of **A8**.

2. Thermodynamics of binding

General. ^{1}H NMR spectra were recorded on Bruker Avance 400 or 500 spectrometers. All chemical shifts are reported in *ppm* with residual solvents or tetramethylsilane as the internal standards. The following abbreviations are used for signal multiplicities: s, singlet; d, doublet; t triplet; m, multiplet. Host-guest complexes were prepared by mixing the host and excess guest in CD_2Cl_2/CD_3CN (*v*/*v* = 1:1). Counterions of the guests are PF_6^-.

For a typical kinetic experiment, binding constants of ammonium guests to **NC** to form **G@NC1** (K_{a1}) was studied by NMR competition as previously described.[1] **G0** ([^{n}Pr$_3$MeN][PF_6]) was used as the reference guest when binding constant for **G1** was determined, and **G1** was used as the reference guest when the binding constant of other ammonium guests was determined. Binding constant of **G0** to **NC** was determined by measuring the equilibrium concentration of **G0@NC**, free **G0** and **NC** of a solution containing an initial concentration of **NC** at 0.49 mM and **G0** at 0.64 mM, and was found to be 3.72 (±1.62) x 10^3 M^{-1} from three measurements.

In a typical competition experiment, solutions containing **NC** (*ca.* 0.5 mM), $\mathbf{G_{ref}}$ (*ca.* 50 mM when **G0** was used, and 0.6–7 mM when **G1** was used) and **G** in a total volume of 0.5 mL in CD_2Cl_2:CD_3CN (*v*/*v* = 1:1) was prepared. Different [$\mathbf{G_{ref}}$]:[**G**] ratios were tested such that the final concentration of the two complexes are comparable at equilibrium. A small excess of the tighter binding guest (to ensure there is no free **NC**) and a larger excess of the weaker binding guest were used. The systems were allowed to equilibrate for 3 days to 2 weeks (according to the time required to reach equilibrium from the kinetic experiments) before a ^{1}H NMR spectrum was obtained. Equilibrium concentrations of the two complexes $\mathbf{G_{ref}}$**@NC** and **G@NC** were determined from the integration of the corresponding ^{1}H NMR signals, and the equilibrium concentration of free $\mathbf{G_{ref}}$ and **G** were calculated by subtracting the equilibrium concentration of the corresponding complexes from the initial concentration of the guests. The relative binding constant K_{rel} is given by equation S18, and binding constant of the target guest is given by equation S23. Each measurement was repeated for three times and the results are summarized in Table S2.

For the competition between **G_{ref}** and **G** for **NC** binding:

$$\mathbf{G_{ref}@NC + G} \rightleftharpoons \mathbf{G@NC + G_{ref}}$$

$$K_{rel} = \frac{[\boldsymbol{G@NC}][\boldsymbol{G_{ref}}]}{[\boldsymbol{G_{ref}@NC}][\boldsymbol{G}]} \quad (S1)$$

binding constant of **G_{ref}** and **G** to **NC**:

$$K_{a,G_{ref}} = \frac{[\boldsymbol{G_{ref}@NC}]}{[\boldsymbol{NC}][\boldsymbol{G_{ref}}]} \quad (S2)$$

$$K_{a,G} = \frac{[\boldsymbol{G@NC}]}{[\boldsymbol{NC}][\boldsymbol{G}]} \quad (S3)$$

therefore,

$$K_{rel} = \frac{K_{a,G}}{K_{a,G_{ref}}} \quad (S4)$$

Binding constants of **G@NC2** are calculated from the equilibrium concentration of the two complex conformers in the kinetic experiment according to equation S31, and the results are summarized in Table S3.

$$K_{a2} = \frac{[\boldsymbol{G@NC2}]}{[\boldsymbol{G@NC1}]} K_{a1} \quad (S5)$$

Table S1. Binding constants of **G@NC1** (K_{a1}) for **G1**-**G24** and **A1**–**A8**.

	K_{a1}/M^{-1}		K_{a1}/M^{-1}
G1	$(1.91\pm1.34) \times 10^6$	**A1**	$(3.0\pm0.2)\times10^6$
G2	$(1.87\pm0.36) \times 10^7$	**A2**	$(1.3\pm0.2)\times10^6$
G3	$(6.22\pm3.57) \times 10^6$	**A3**	$(8.4\pm3.6)\times10^5$
G4	$(2.48\pm0.50) \times 10^6$	**A4**	$(3.0\pm1.0)\times10^4$
G5	$(1.64\pm0.39) \times 10^6$	**A5**	$(3.6\pm1.3)\times10^5$
G6	$(4.16\pm1.24) \times 10^6$	**A6**	$(7.1\pm2.5)\times10^5$
G7	$(8.58\pm4.53) \times 10^5$	**A7**	$(1.3\pm0.0)\times10^5$
G8	$(2.40\pm1.20) \times 10^3$	**A8**	$(2.0\pm0.5)\times10^4$
G9	$(2.38\pm2.14) \times 10^7$		
G10	$(1.21\pm0.71) \times 10^6$		
G11	$(5.86\pm2.08) \times 10^5$		
G12	$(3.35\pm1.19) \times 10^6$		
G13	$(5.59\pm2.16) \times 10^5$		
G14	$(1.11\pm0.44) \times 10^5$		
G15	$(1.02\pm0.33) \times 10^7$		
G16	$(1.43\pm0.37) \times 10^7$		
G17	$(1.41\pm0.80) \times 10^5$		
G18	$(2.14\pm0.70) \times 10^5$		
G19	$(6.18\pm2.14) \times 10^4$		
G20	$(3.04\pm0.97) \times 10^3$		
G21	$(3.77\pm0.68) \times 10^4$		
G22	$(1.89\pm1.08) \times 10^4$		
G23	$(1.10\pm0.62) \times 10^5$		
G24	$(1.65\pm0.34) \times 10^5$		

Table S2. Binding constants of **G@NC2** (K_{a2}) for **G1**-**G24** and **A1**–**A8**.

	K_{a2}		K_{a2}
G1	3.89×10^{4}	**A1**	$(1.7\pm0.1)\times10^{5}$
G2	8.32×10^{5}	**A2**	$(1.1\pm0.3)\times10^{5}$
G3	6.91×10^{5}	**A3**	$(1.6\pm0.8)\times10^{5}$
G4	1.58×10^{5}	**A4**	$(4.0\pm1.4)\times10^{3}$
G5	7.46×10^{4}	**A5**	$(3.1\pm0.9)\times10^{4}$
G6	4.11×10^{5}	**A6**	$(7.6\pm2.4)\times10^{4}$
G7	1.62×10^{5}	**A7**	$(6.0\pm0.1)\times10^{3}$
G8	3.37×10^{2}	**A8**	$(4.5\pm0.9)\times10^{3}$
G9	1.25×10^{6}		
G10	4.56×10^{5}		
G11	2.69×10^{5}		
G12	7.46×10^{4}		
G13	9.10×10^{4}		
G14	5.28×10^{4}		
G15	7.70×10^{5}		
G16	2.92×10^{5}		
G17	2.10×10^{4}		
G18	2.91×10^{4}		
G19	5.49×10^{3}		
G20	2.96×10^{2}		
G21	4.19×10^{3}		
G22	1.45×10^{3}		
G23	7.03×10^{3}		
G24	6.87×10^{3}		

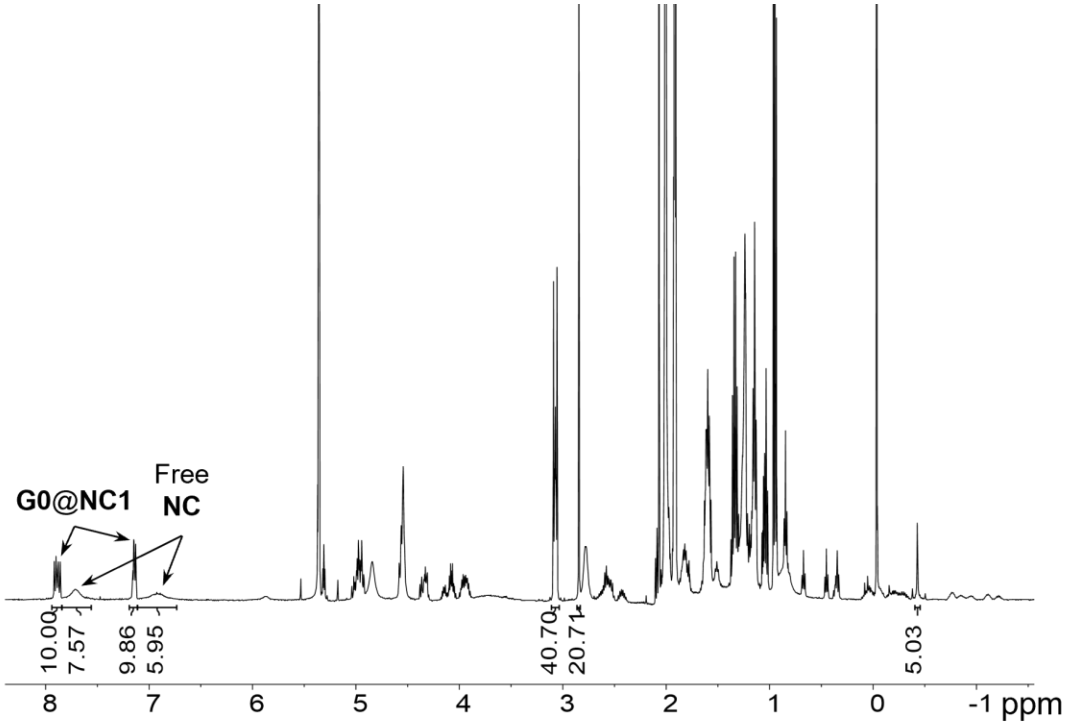

Figure S31. A representative ^{1}H NMR spectrum (500 MHz, CD_2Cl_2:CD_3CN (*v*/*v* = 1:1), 298 K) of an equilibrium mixture containing **NC** (0.49 mM) and **G0** (0.64 mM) for determining K_{a1} for **G0**.

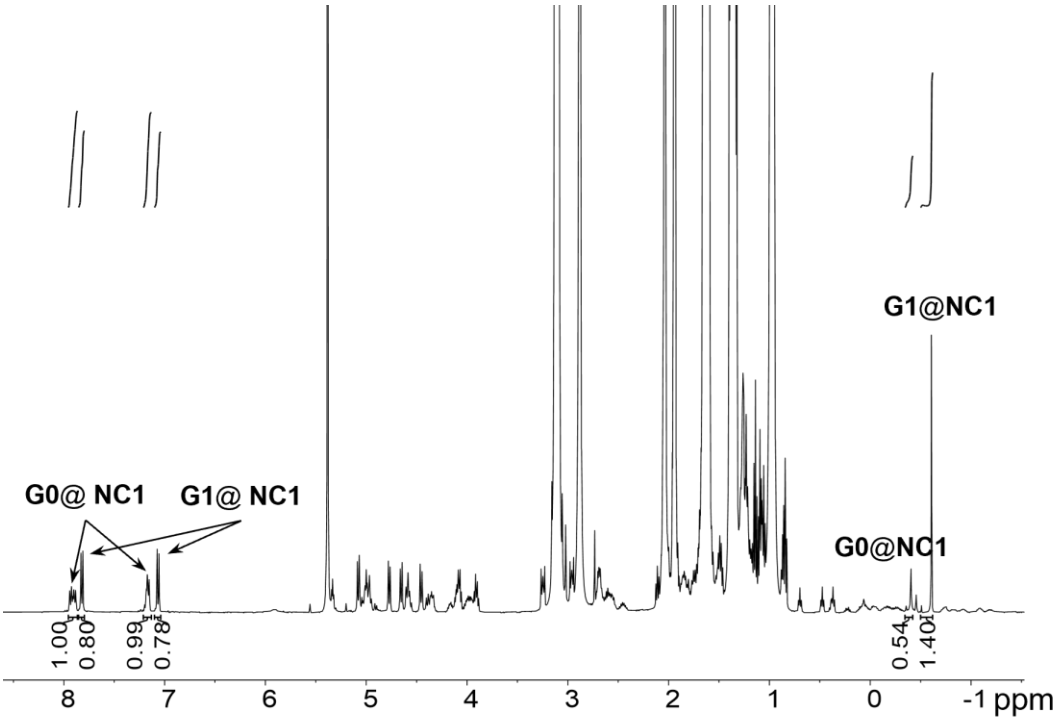

Figure S32. A representative ^{1}H NMR spectrum (500 MHz, CD_2Cl_2:CD_3CN (*v*/*v* = 1:1), 298 K) of an equilibrium mixture containing **NC** (0.50 mM), **G0** (50 mM) and **G1** (0.30 mM).

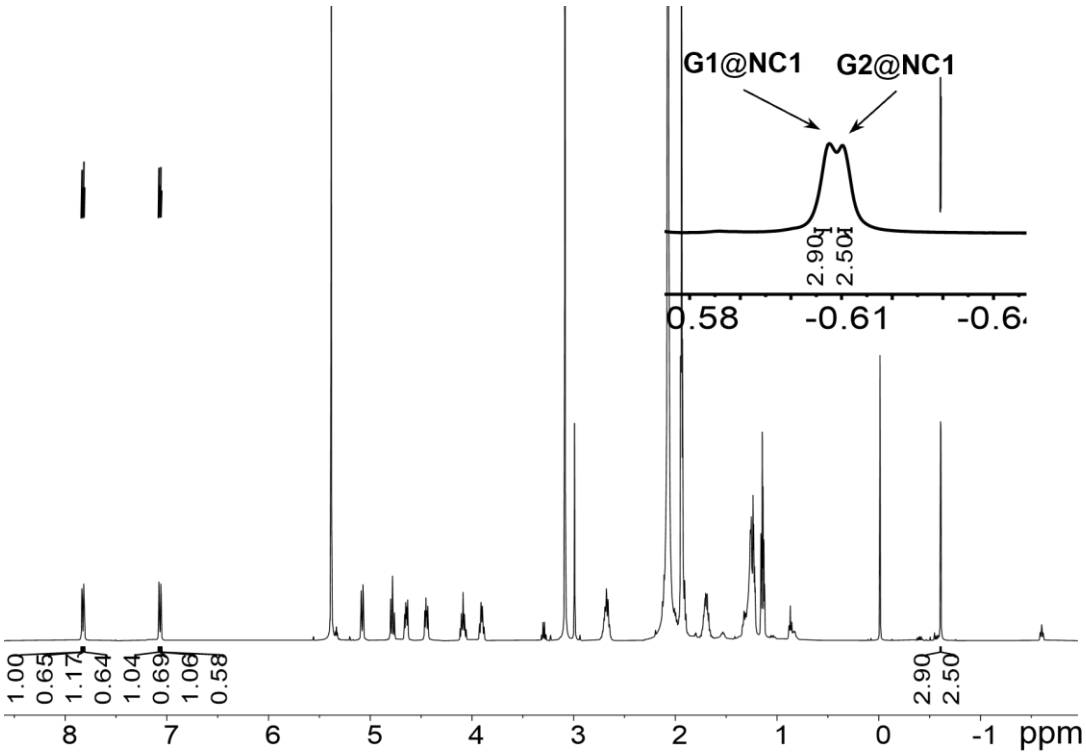

Figure S33. A representative ^{1}H NMR spectrum (500 MHz, CD_2Cl_2:CD_3CN (*v*/*v* = 1:1), 298 K) of an equilibrium mixture containing **NC** (0.56 mM), **G1** (3.5 mM) and **G2** (0.86 mM).

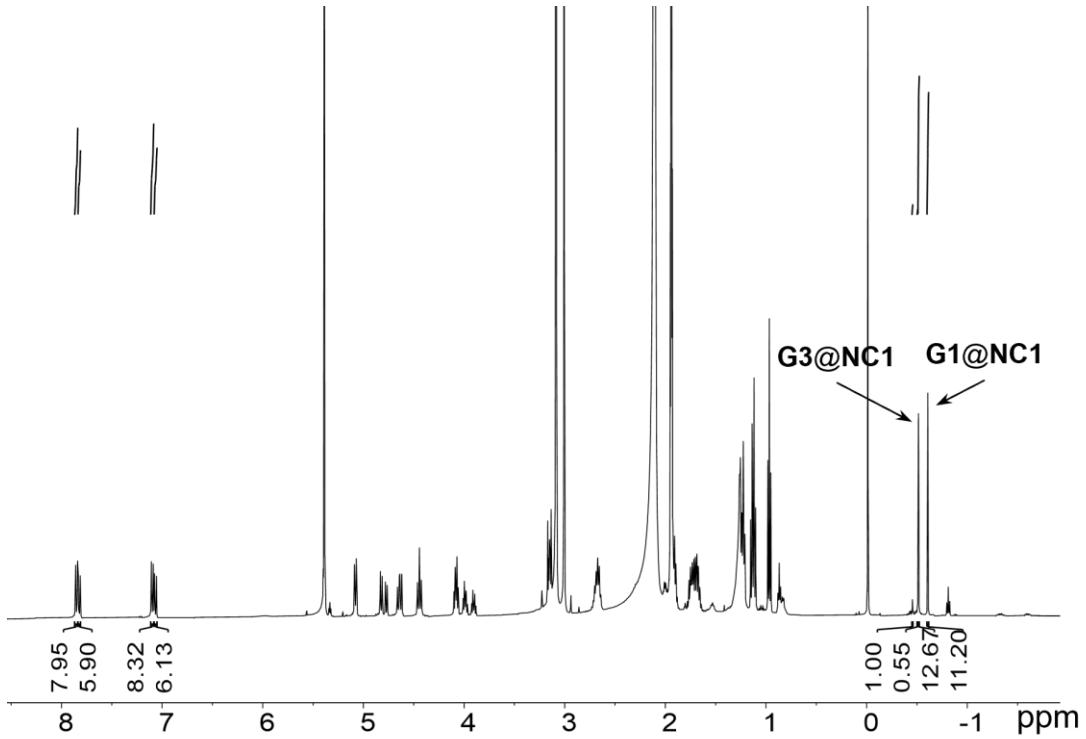

Figure S34. A representative ^{1}H NMR spectrum (500 MHz, CD_2Cl_2:CD_3CN (*v*/*v* = 1:1), 298 K) of an equilibrium mixture containing **NC** (0.43 mM), **G1** (5.8 mM) and **G3** (2.4 mM).

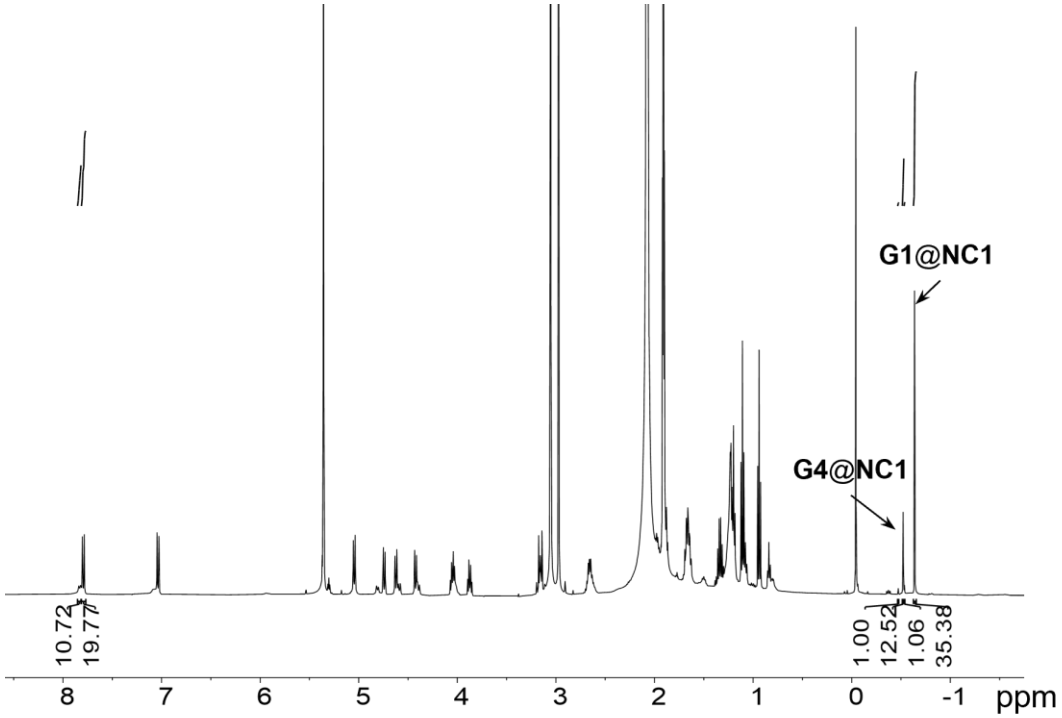

Figure S35. A representative ^{1}H NMR spectrum (500 MHz, CD_2Cl_2:CD_3CN (*v*/*v* = 1:1), 298 K) of an equilibrium mixture containing **NC** (0.47 mM), **G1** (4.9 mM) and **G4** (1.8 mM).

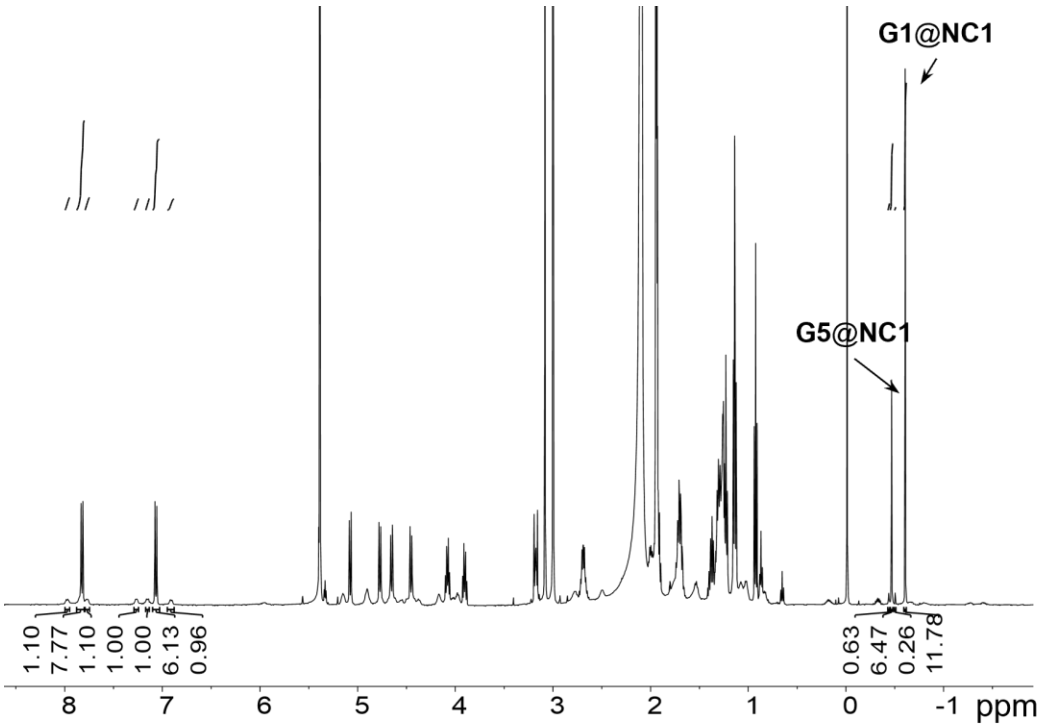

Figure S36. A representative ^{1}H NMR spectrum (500 MHz, CD_2Cl_2:CD_3CN (*v*/*v* = 1:1), 298 K) of an equilibrium mixture containing **NC** (0.47 mM), **G1** (1.3 mM) and **G5** (1.6 mM).

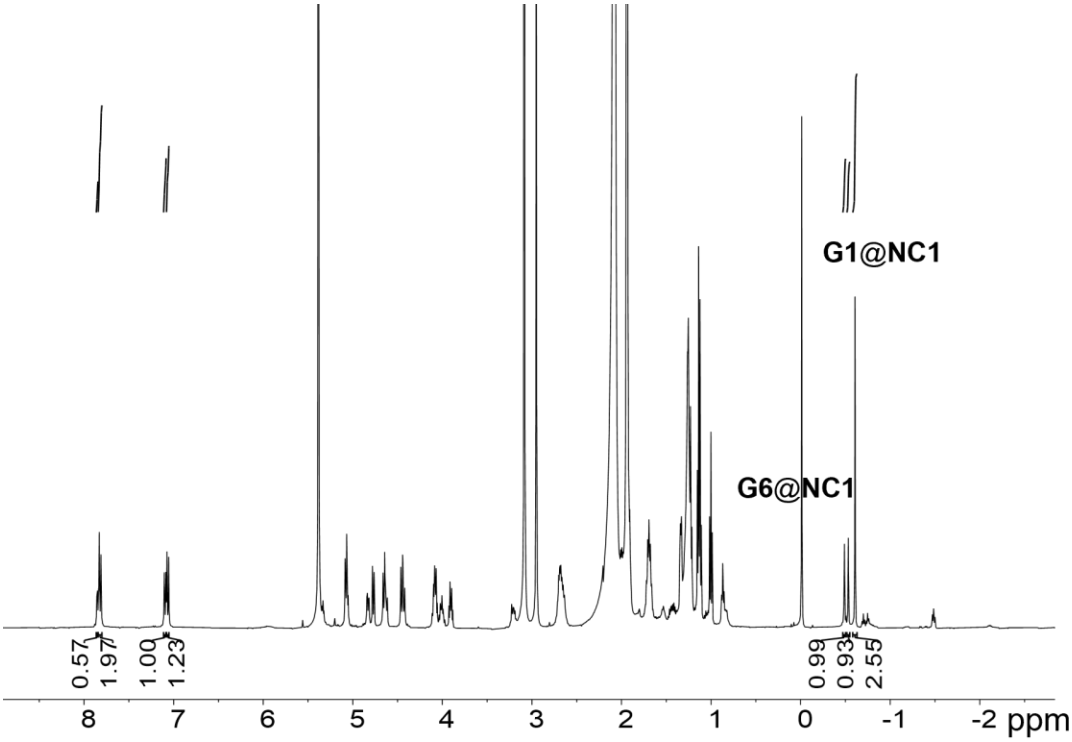

Figure S37. A representative ^{1}H NMR spectrum (500 MHz, CD_2Cl_2:CD_3CN (*v*/*v* = 1:1), 298 K) of an equilibrium mixture containing **NC** (0.52 mM), **G1** (3.3 mM) and **G6** (1.7 mM).

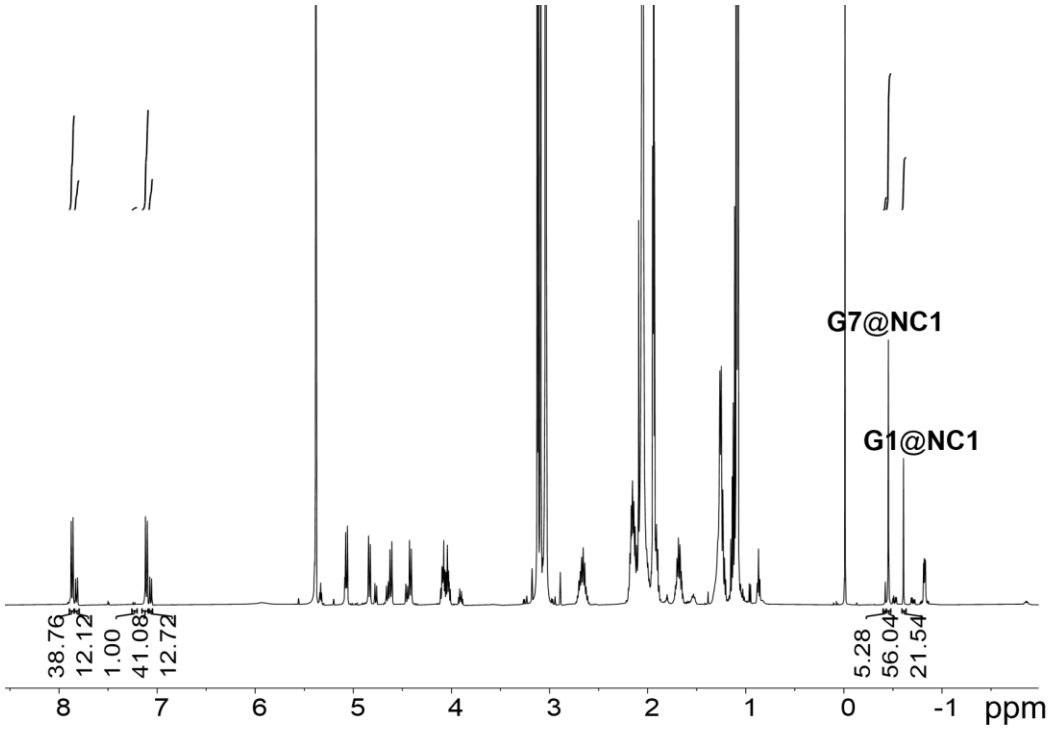

Figure S38. A representative ^{1}H NMR spectrum (500 MHz, CD_2Cl_2:CD_3CN (*v*/*v* = 1:1), 298 K) of an equilibrium mixture containing **NC** (0.62 mM), **G1** (3.6 mM) and **G7** (13 mM).

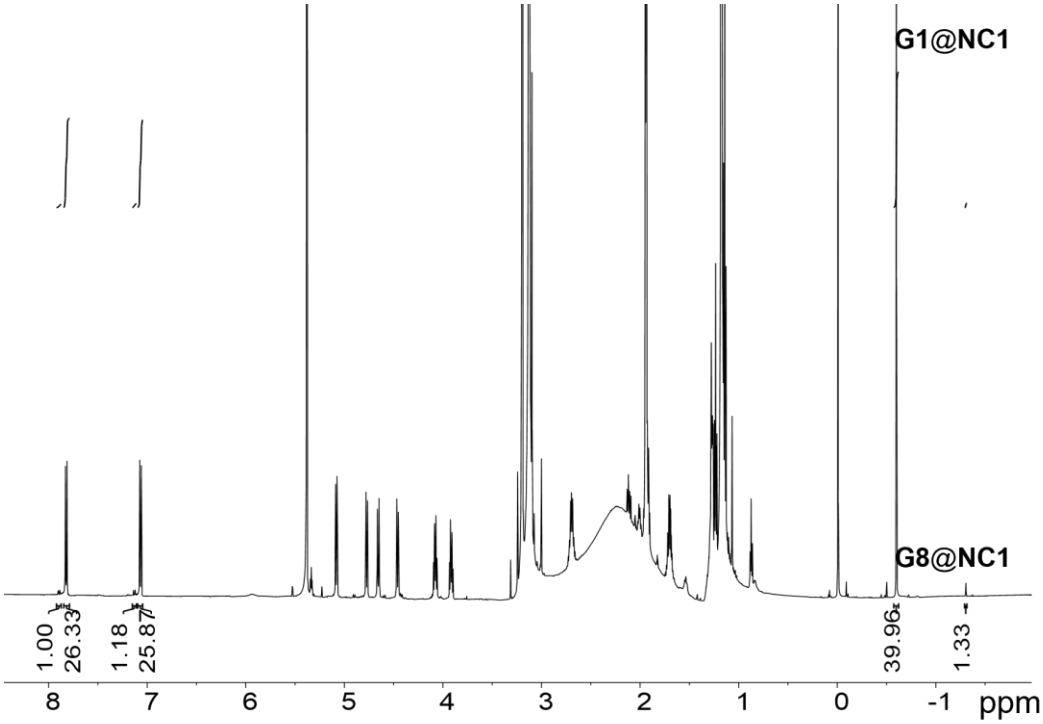

Figure S39. A representative ^{1}H NMR spectrum (500 MHz, CD_2Cl_2:CD_3CN (*v*/*v* = 1:1), 298 K) of an equilibrium mixture containing **NC** (0.43 mM), **G1** (1.1 mM) and **G8** (30 mM).

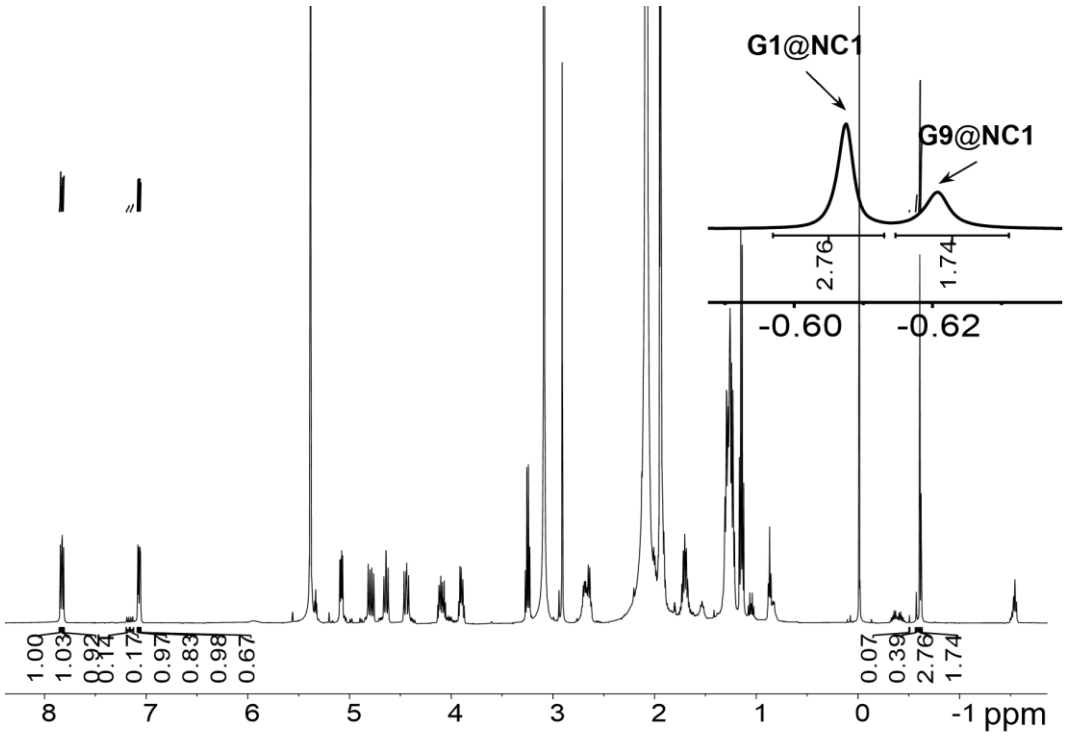

Figure S40. A representative ^{1}H NMR spectrum (500 MHz, CD_2Cl_2:CD_3CN (*v*/*v* = 1:1), 298 K) of an equilibrium mixture containing **NC** (0.40 mM), **G1** (6.5 mM) and **G9** (1.1 mM).

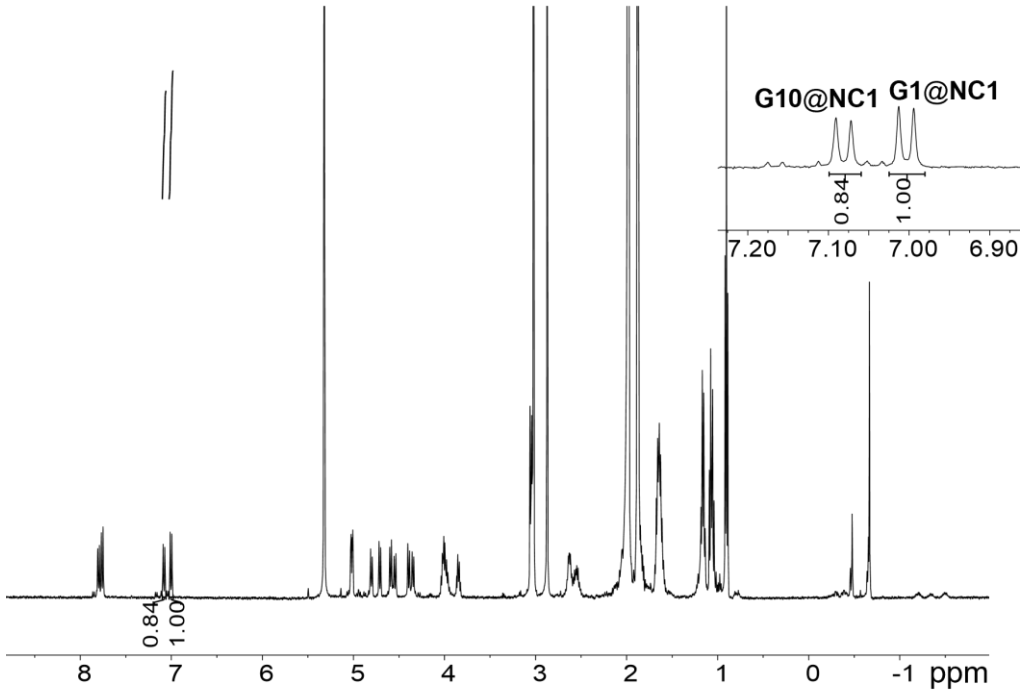

Figure S41. A representative ^{1}H NMR spectrum (500 MHz, CD_2Cl_2:CD_3CN (*v*/*v* = 1:1), 298 K) of an equilibrium mixture containing **NC** (0.49 mM), **G1** (3.8 mM) and **G10** (2.0 mM).

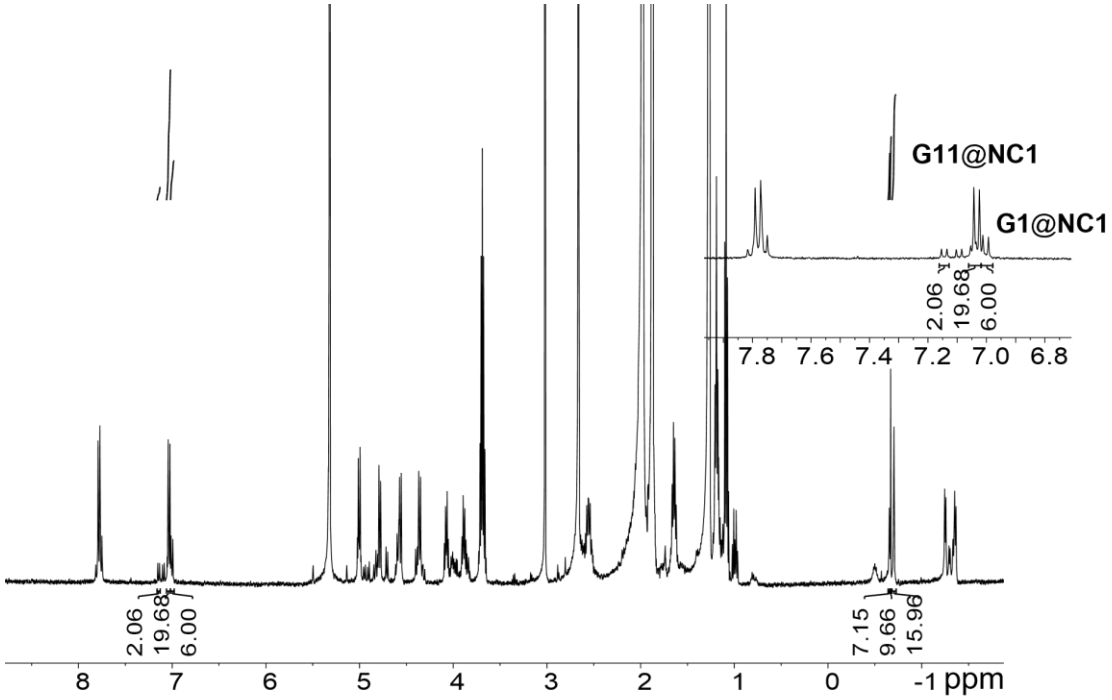

Figure S42. A representative ^{1}H NMR spectrum (500 MHz, CD_2Cl_2:CD_3CN (*v*/*v* = 1:1), 298 K) of an equilibrium mixture containing **NC** (0.46 mM), **G1** (2.5 mM) and **G11** (4.4 mM).

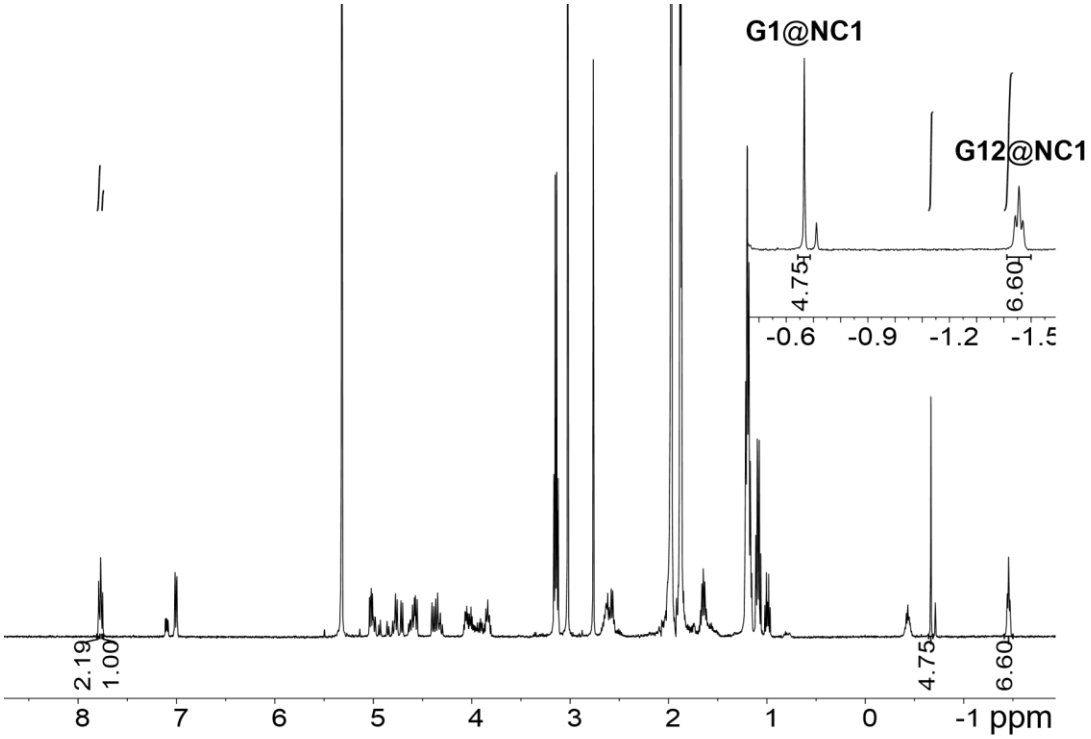

Figure S43. A representative ^{1}H NMR spectrum (500 MHz, CD_2Cl_2:CD_3CN (*v*/*v* = 1:1), 298 K) of an equilibrium mixture containing **NC** (0.50 mM), **G1** (3.7 mM) and **G12** (2.5 mM).

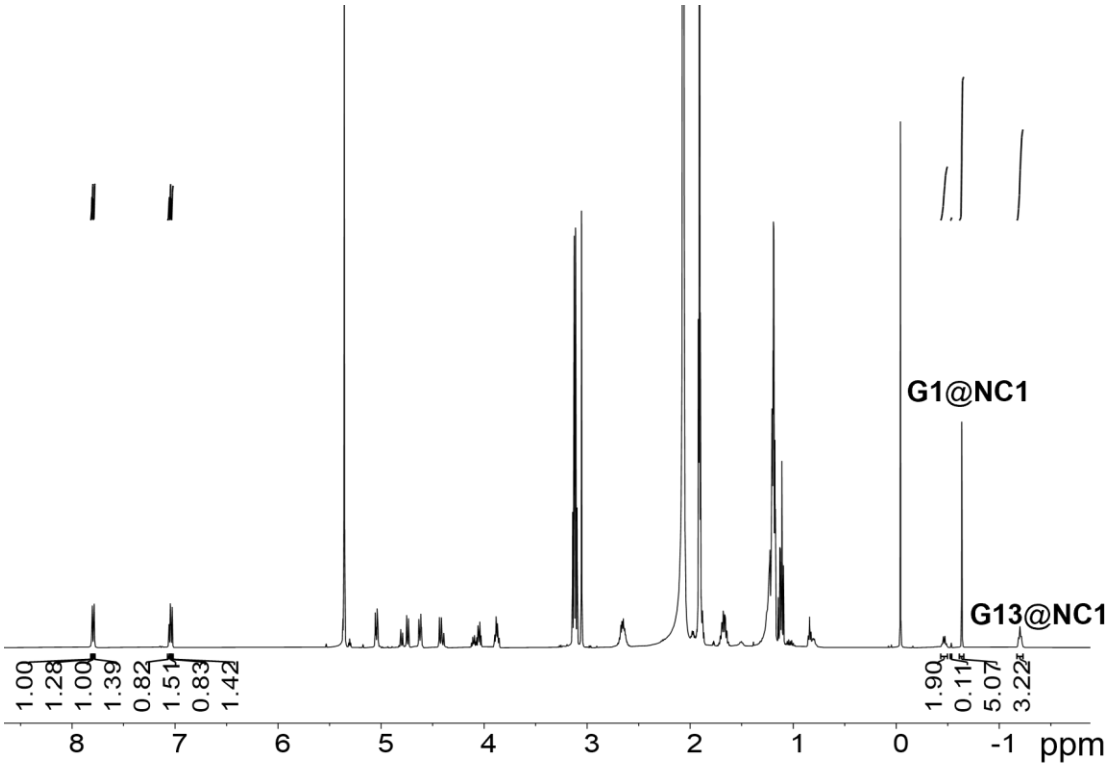

Figure S44. A representative ^{1}H NMR spectrum (500 MHz, CD_2Cl_2:CD_3CN (*v*/*v* = 1:1), 298 K) of an equilibrium mixture containing **NC** (0.43 mM), **G1** (1.4 mM) and **G13** (2.4 mM).

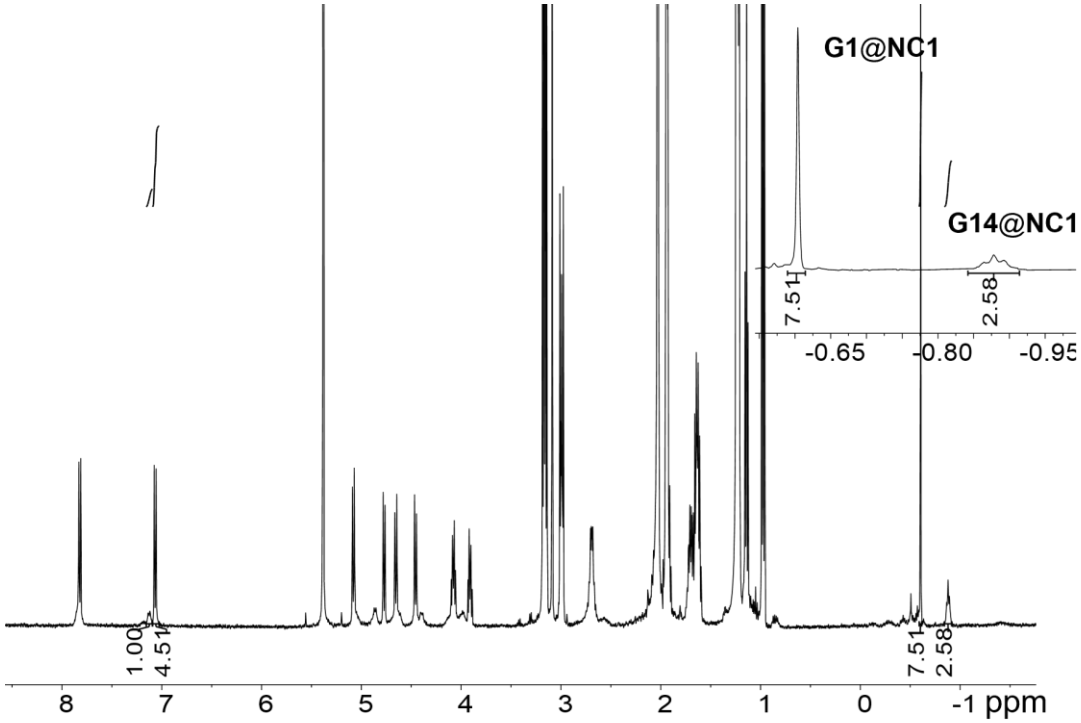

Figure S45. A representative ^{1}H NMR spectrum (500 MHz, CD_2Cl_2:CD_3CN (*v*/*v* = 1:1), 298 K) of an equilibrium mixture containing **NC** (0.52 mM), **G1** (2.2 mM) and **G14** (5.2 mM).

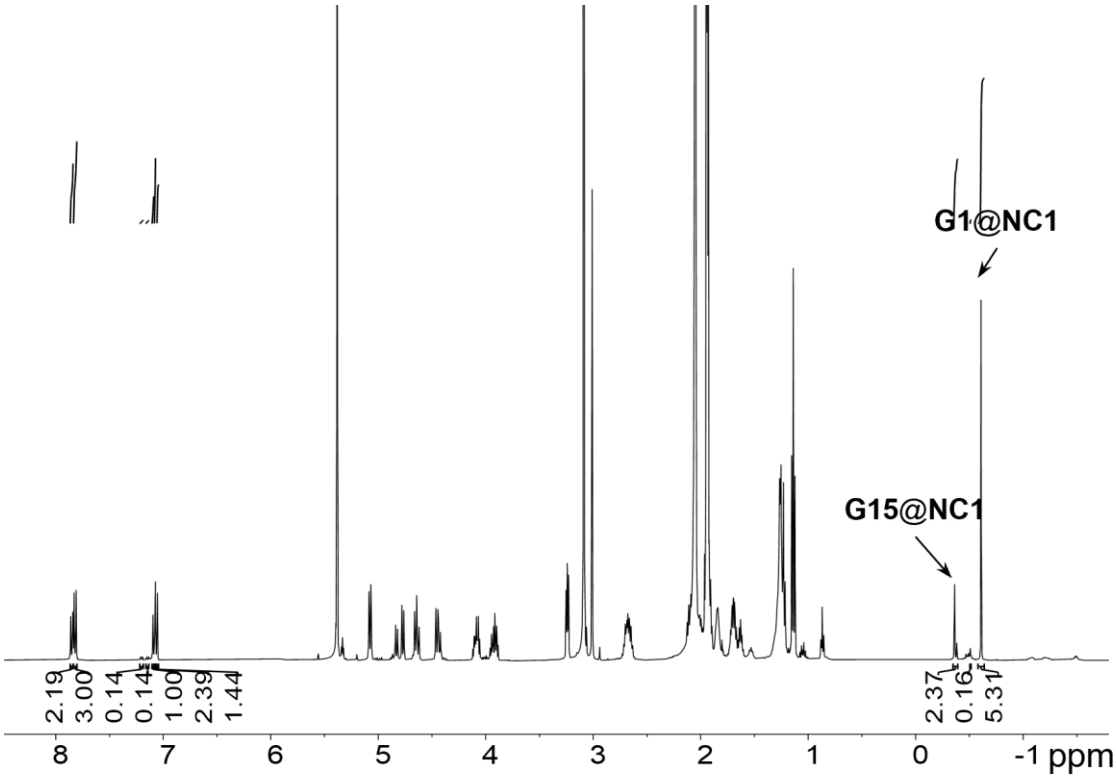

Figure S46. A representative ^{1}H NMR spectrum (500 MHz, CD_2Cl_2:CD_3CN (*v*/*v* = 1:1), 298 K) of an equilibrium mixture containing **NC** (0.56 mM), **G1** (6.6 mM) and **G15** (1.3 mM).

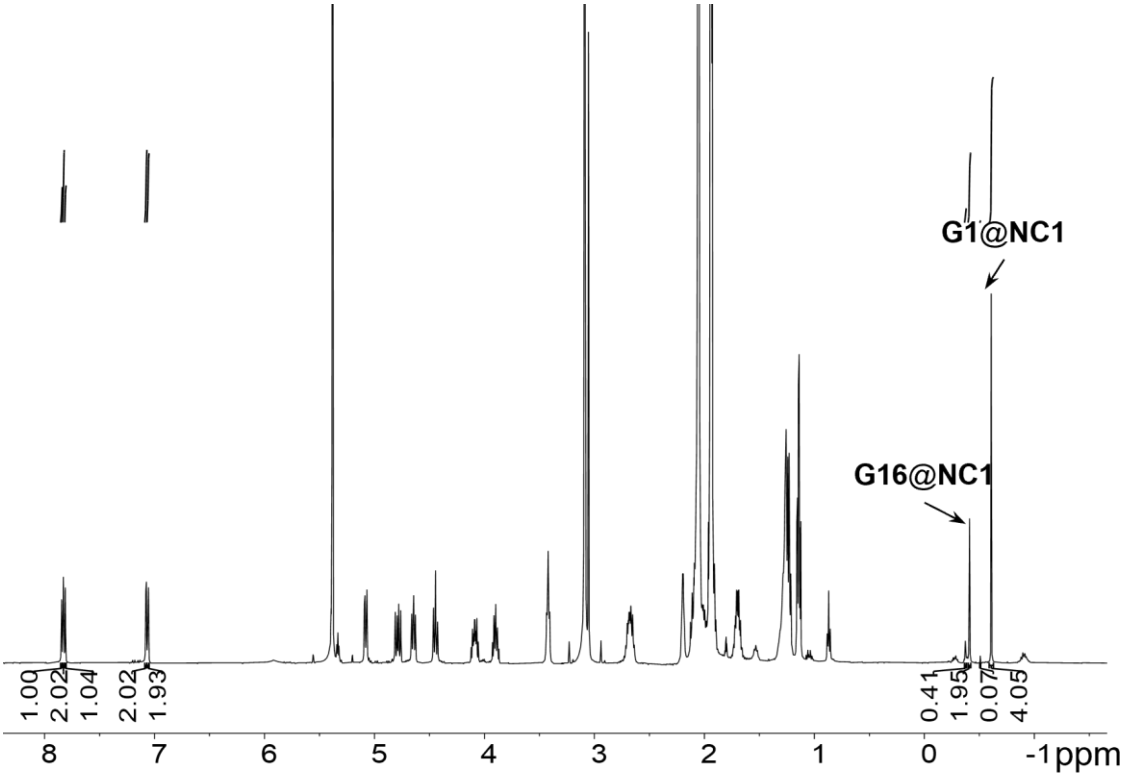

Figure S47. A representative ^{1}H NMR spectrum (500 MHz, CD_2Cl_2:CD_3CN (*v*/*v* = 1:1), 298 K) of an equilibrium mixture containing **NC** (0.55 mM), **G1** (6.5 mM) and **G16** (1.1 mM).

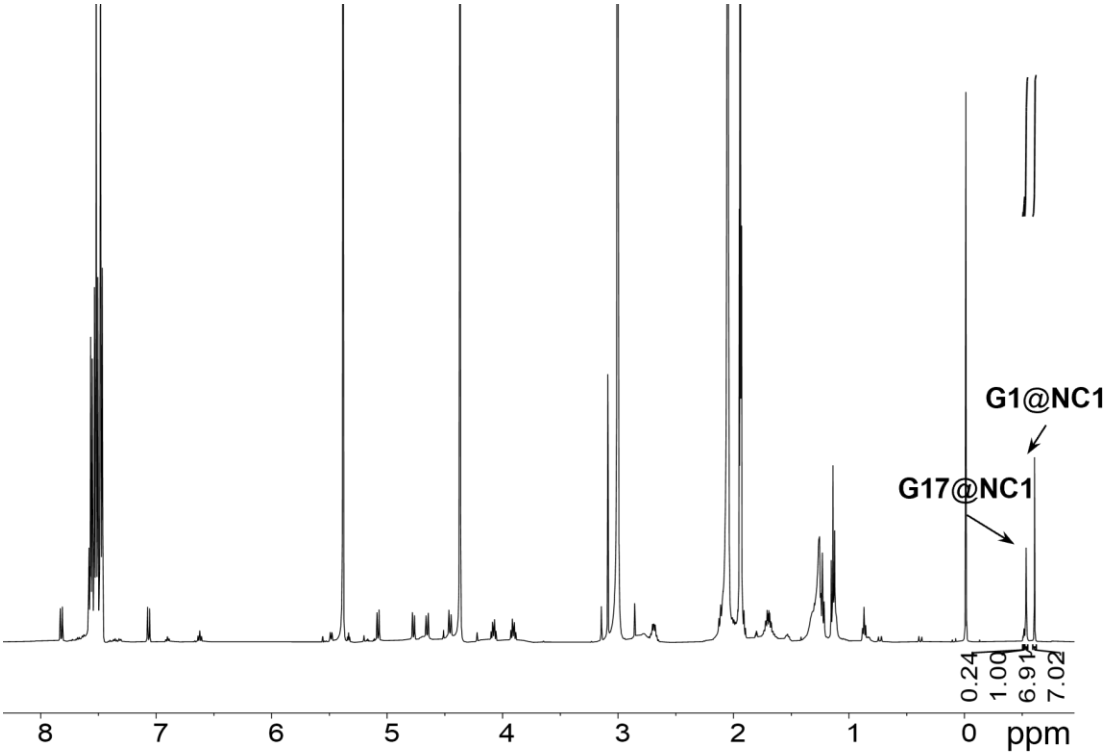

Figure S48. A representative ^{1}H NMR spectrum (500 MHz, CD_2Cl_2:CD_3CN (*v*/*v* = 1:1), 298 K) of an equilibrium mixture containing **NC** (0.46 mM), **G1** (0.71 mM) and **G17** (11 mM).

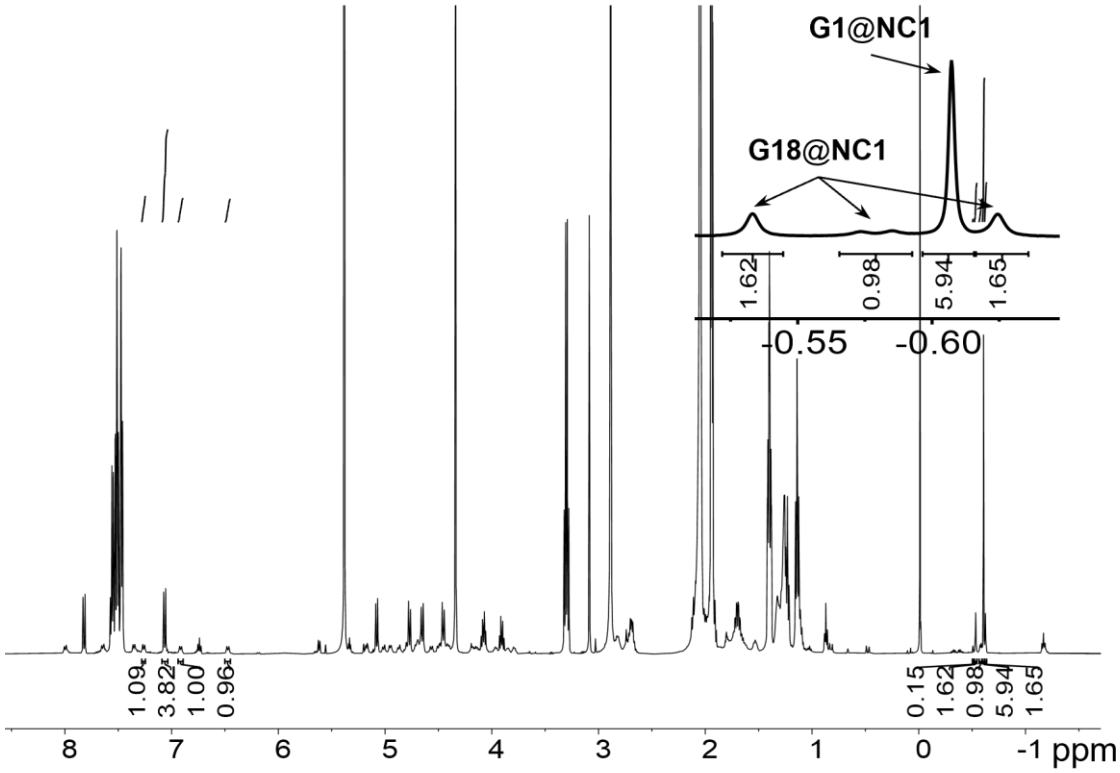

Figure S49. A representative ^{1}H NMR spectrum (500 MHz, CD_2Cl_2:CD_3CN (*v*/*v* = 1:1), 298 K) of an equilibrium mixture containing **NC** (0.55 mM), **G1** (0.93 mM) and **G18** (4.9 mM).

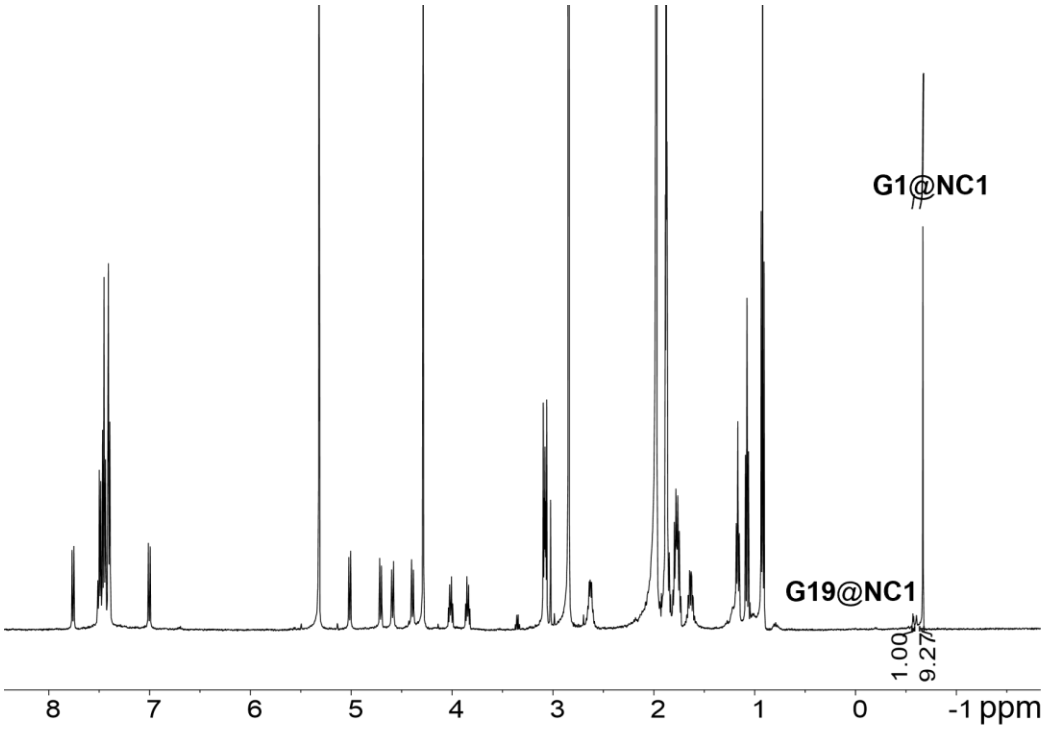

Figure S50. A representative ^{1}H NMR spectrum (500 MHz, CD_2Cl_2:CD_3CN (*v*/*v* = 1:1), 298 K) of an equilibrium mixture containing **NC** (0.46 mM), **G1** (1.6 mM) and **G19** (6.4 mM).

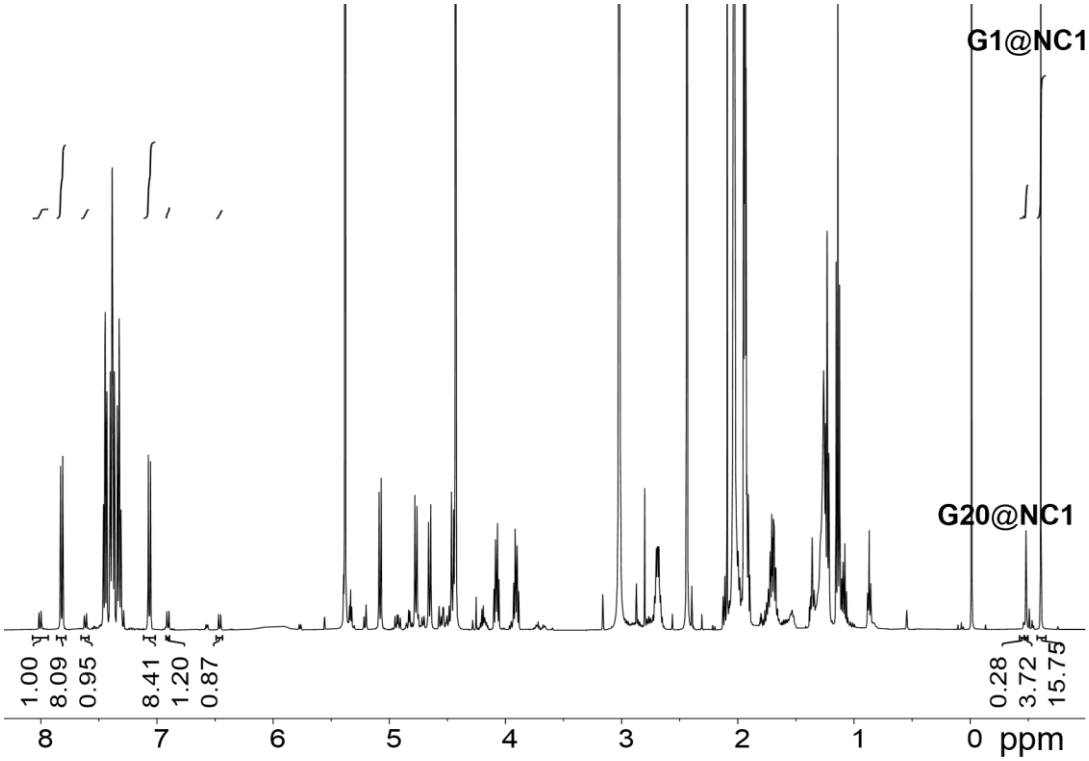

Figure S51. A representative ^{1}H NMR spectrum (500 MHz, CD_2Cl_2:CD_3CN (*v*/*v* = 1:1), 298 K) of an equilibrium mixture containing **NC** (0.55 mM), **G1** (0.44 mM) and **G20** (7.3 mM).

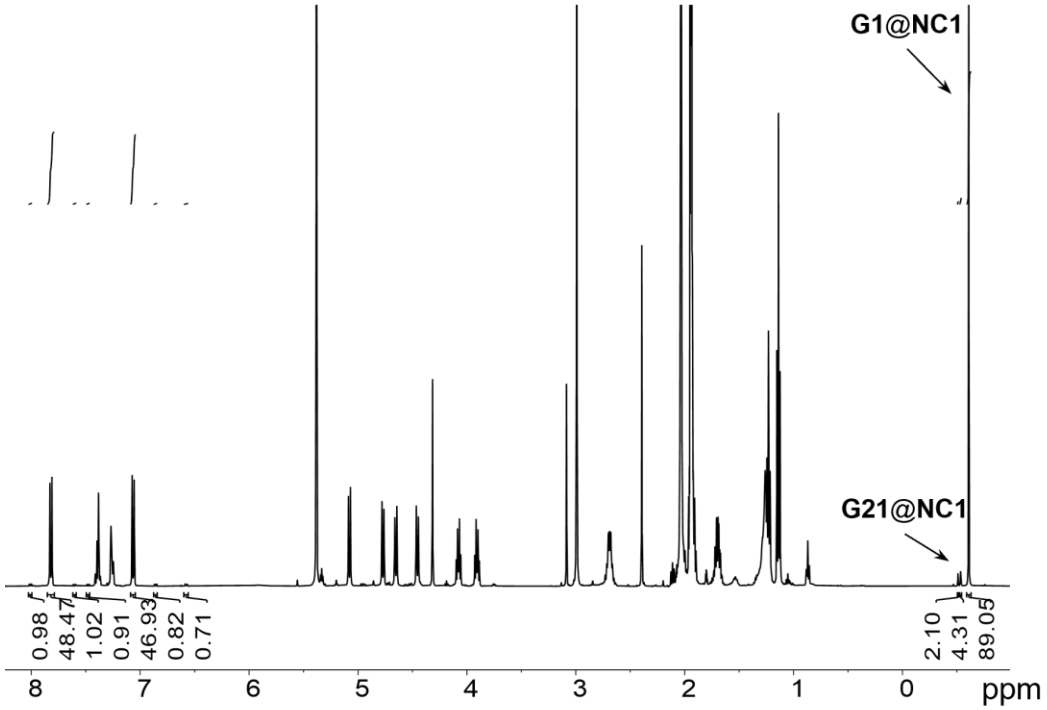

Figure S52. A representative ^{1}H NMR spectrum (500 MHz, CD_2Cl_2:CD_3CN (*v*/*v* = 1:1), 298 K) of an equilibrium mixture containing **NC** (0.55 mM), **G1** (1.0 mM) and **G21** (1.6 mM).

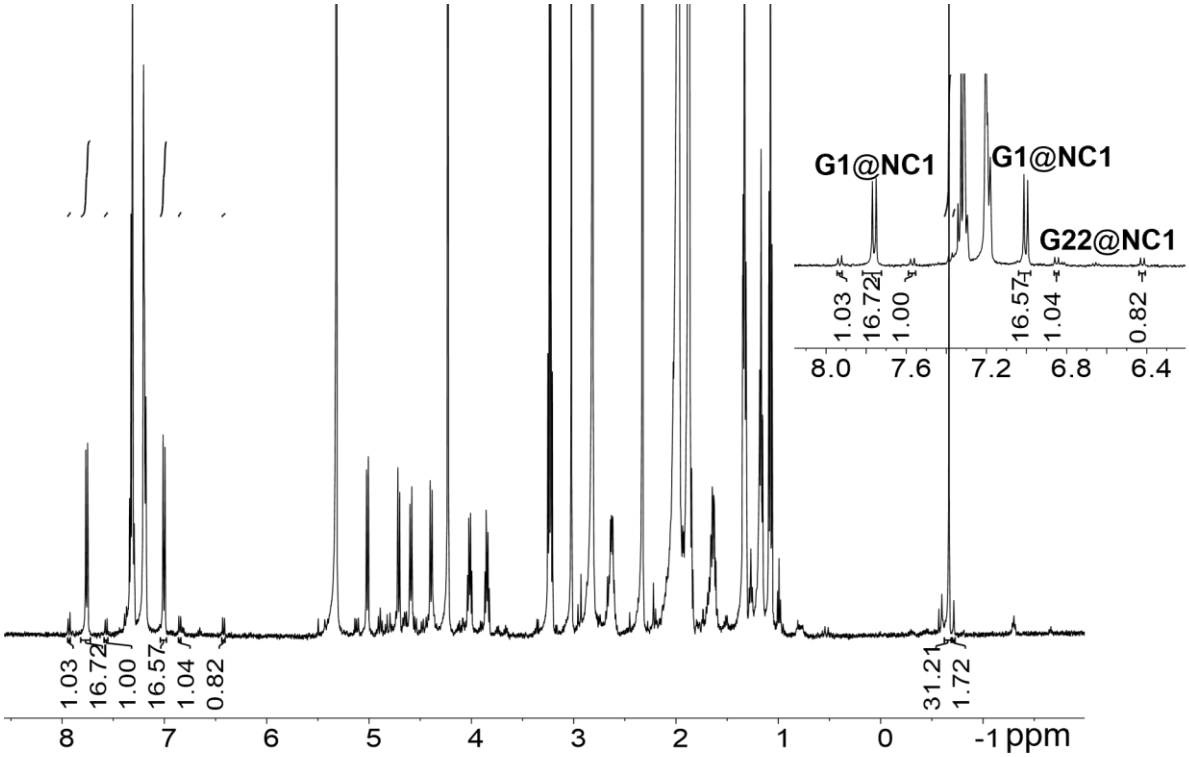

Figure S53. A representative ^{1}H NMR spectrum (500 MHz, CD_2Cl_2:CD_3CN (*v*/*v* = 1:1), 298 K) of an equilibrium mixture containing **NC** (0.47 mM), **G1** (1.6 mM) and **G22** (9.8 mM).

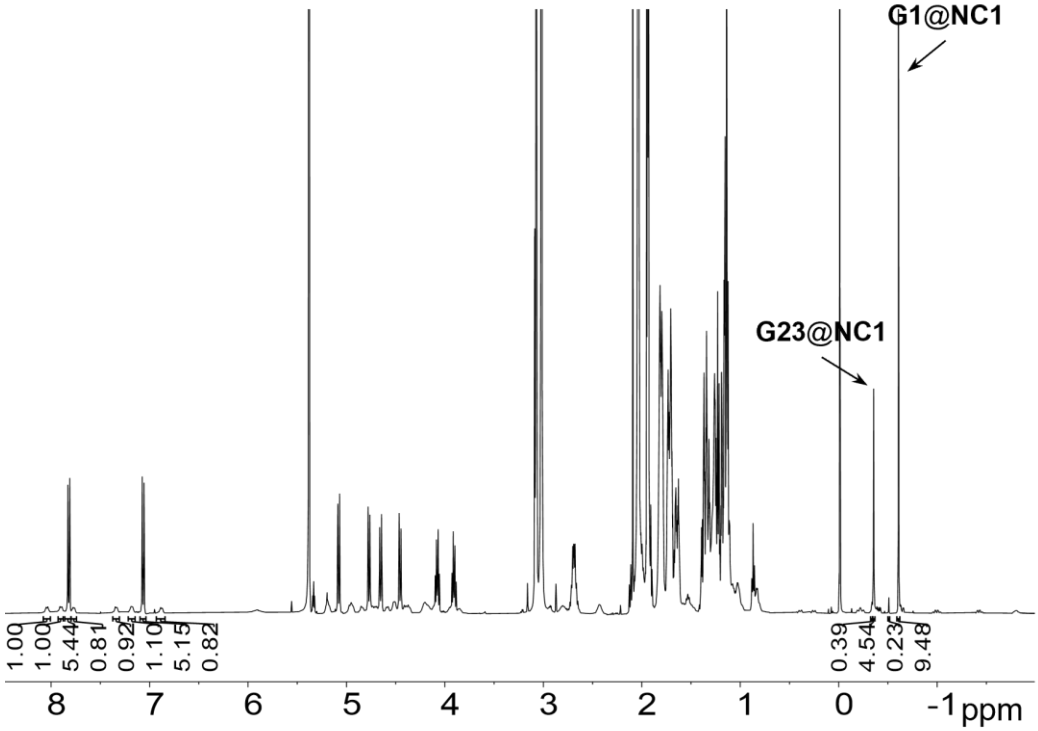

Figure S54. A representative ^{1}H NMR spectrum (500 MHz, CD_2Cl_2:CD_3CN (*v*/*v* = 1:1), 298 K) of an equilibrium mixture containing **NC** (0.52 mM), **G1** (0.99 mM) and **G23** (6.6 mM).

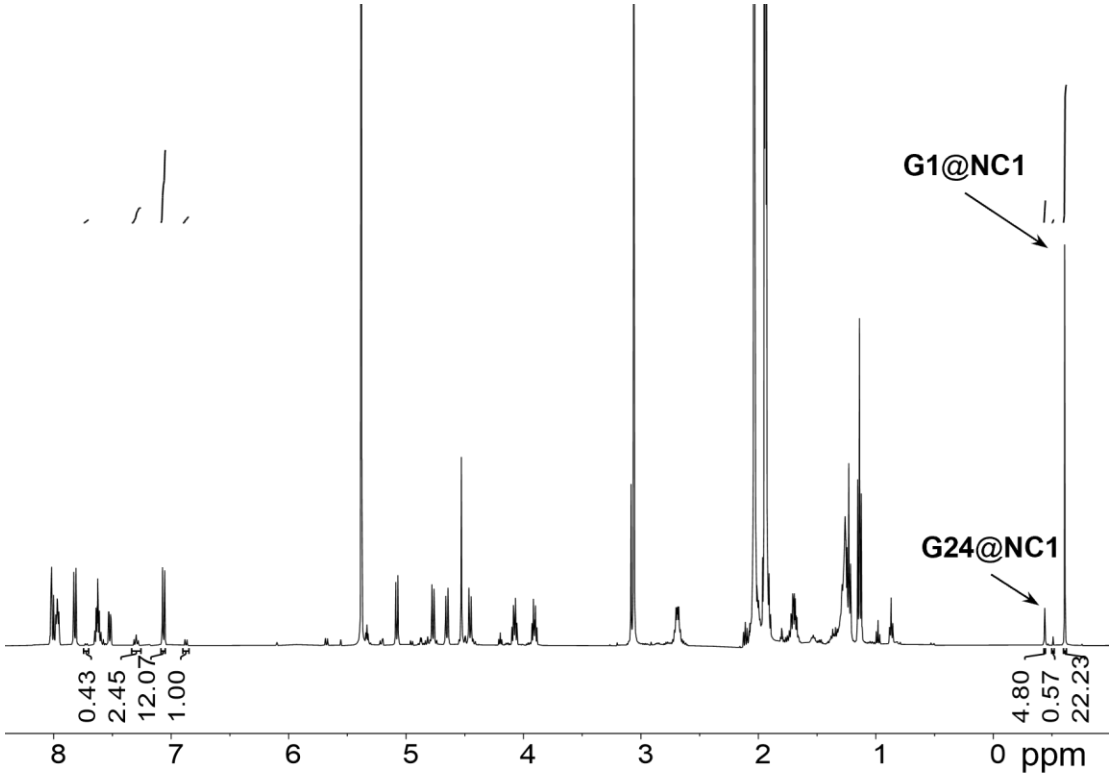

Figure S55. A representative ^{1}H NMR spectrum (500 MHz, CD_2Cl_2:CD_3CN (*v*/*v* = 1:1), 298 K) of an equilibrium mixture containing **NC** (0.50 mM), **G1** (0.88 mM) and **G24** (1.5 mM).

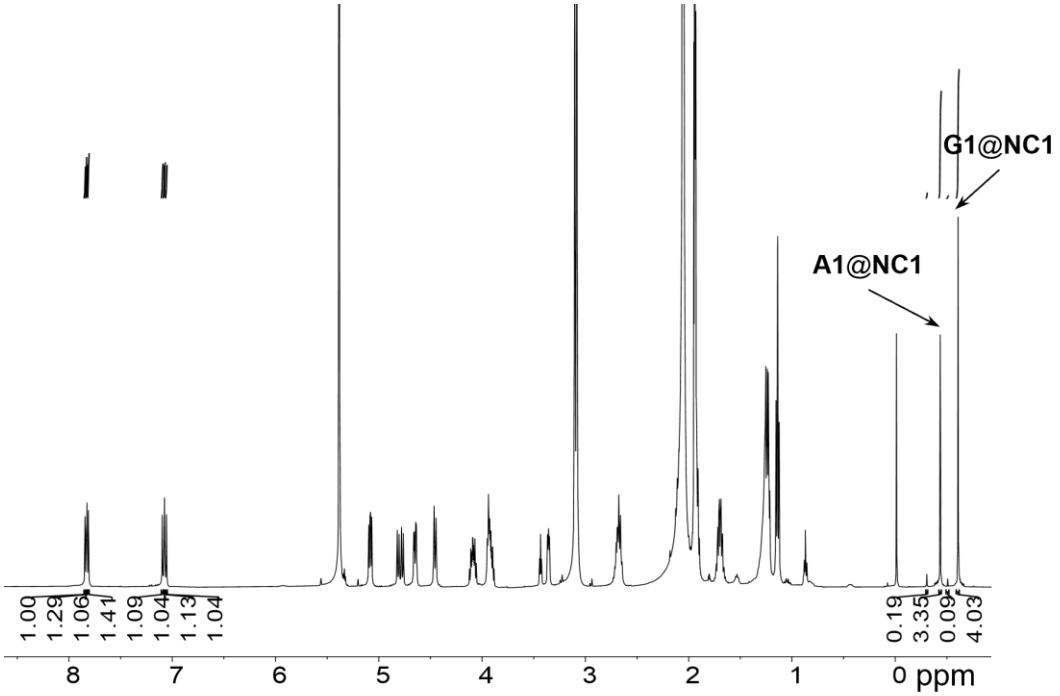

Figure S56. A representative ^{1}H NMR spectrum (500 MHz, CD_2Cl_2:CD_3CN (*v*/*v* = 1:1), 298 K) of an equilibrium mixture containing **NC** (0.50 mM), **G1** (2.2 mM) and **A1** (1.4 mM).

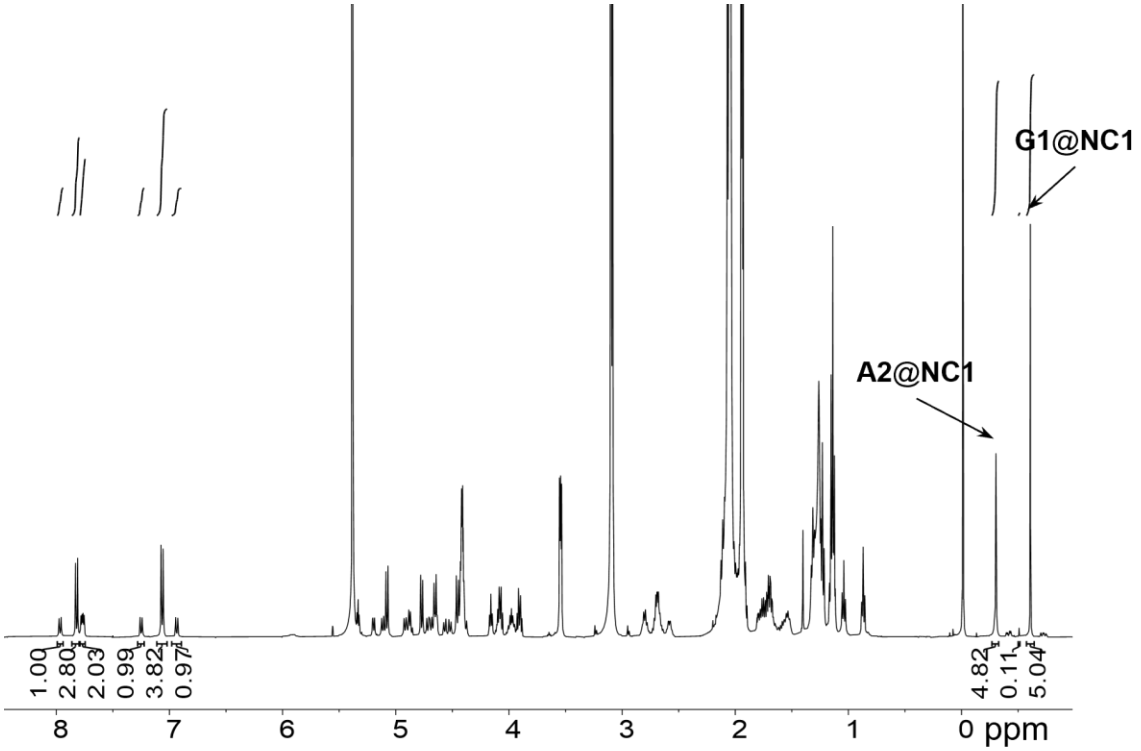

Figure S57. A representative ^{1}H NMR spectrum (500 MHz, CD_2Cl_2:CD_3CN (*v*/*v* = 1:1), 298 K) of an equilibrium mixture containing **NC** (0.45 mM), **G1** (1.5 mM) and **A2** (2.3 mM).

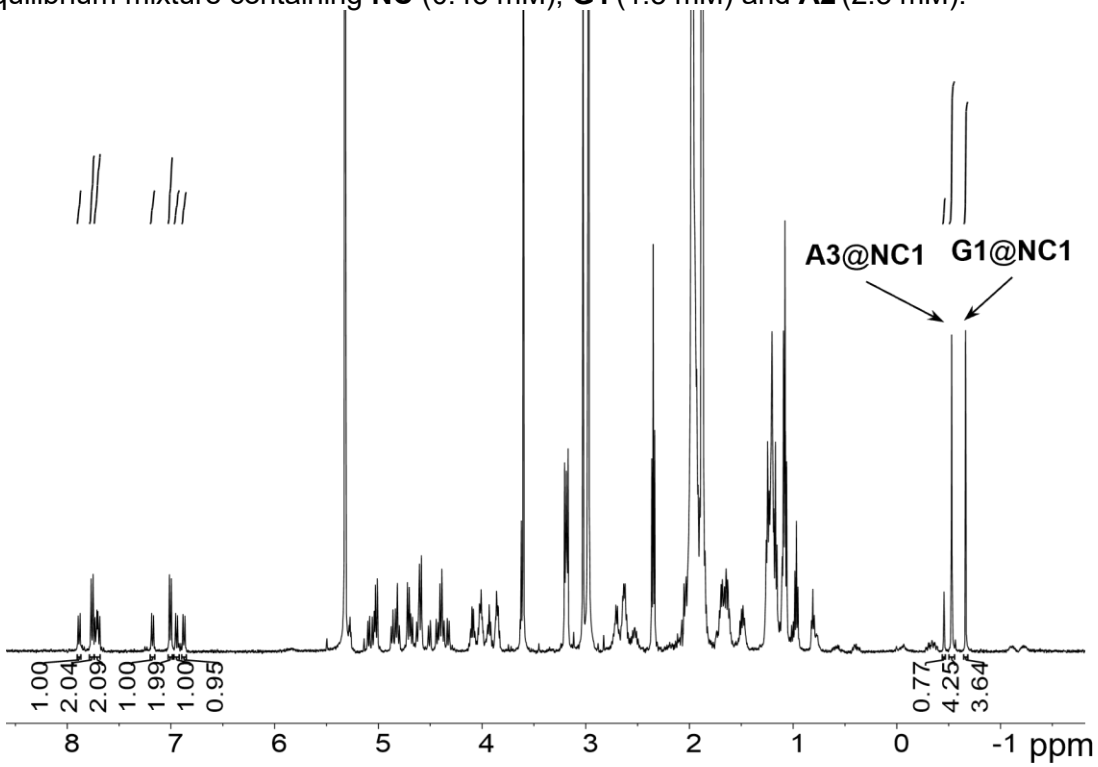

Figure S58. A representative ^{1}H NMR spectrum (500 MHz, CD_2Cl_2:CD_3CN (*v*/*v* = 1:1), 298 K) of an equilibrium mixture containing **NC** (0.50 mM), **G1** (1.1 mM) and **A3** (3.5 mM).

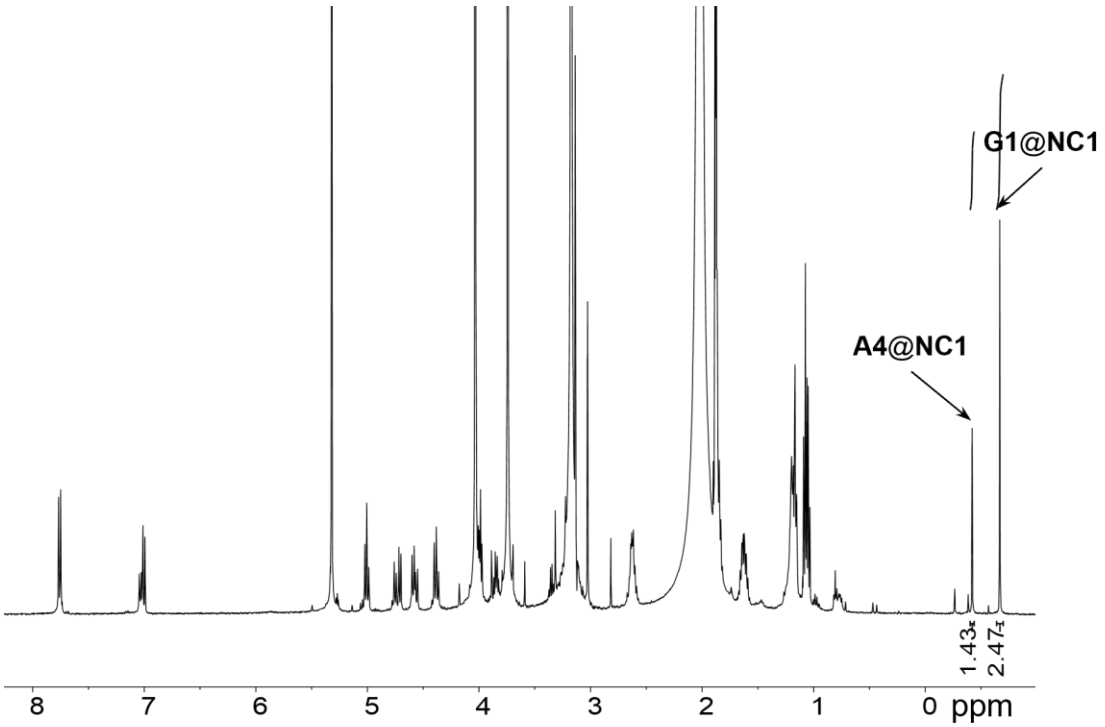

Figure S59. A representative ^{1}H NMR spectrum (500 MHz, CD_2Cl_2:CD_3CN (*v*/*v* = 1:1), 298 K) of an equilibrium mixture containing **NC** (0.53 mM), **G1** (0.82 mM) and **A4** (27 mM).

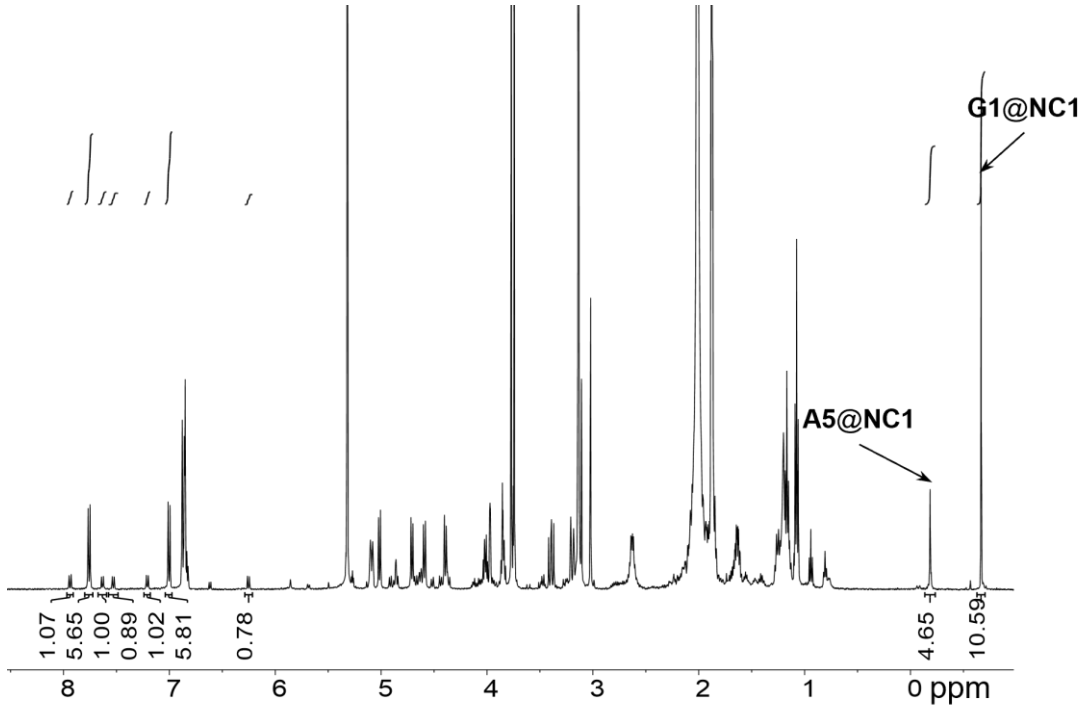

Figure S60. A representative ^{1}H NMR spectrum (500 MHz, CD_2Cl_2:CD_3CN (*v*/*v* = 1:1), 298 K) of an equilibrium mixture containing **NC** (0.56 mM), **G1** (1.2 mM) and **A5** (2.6 mM).

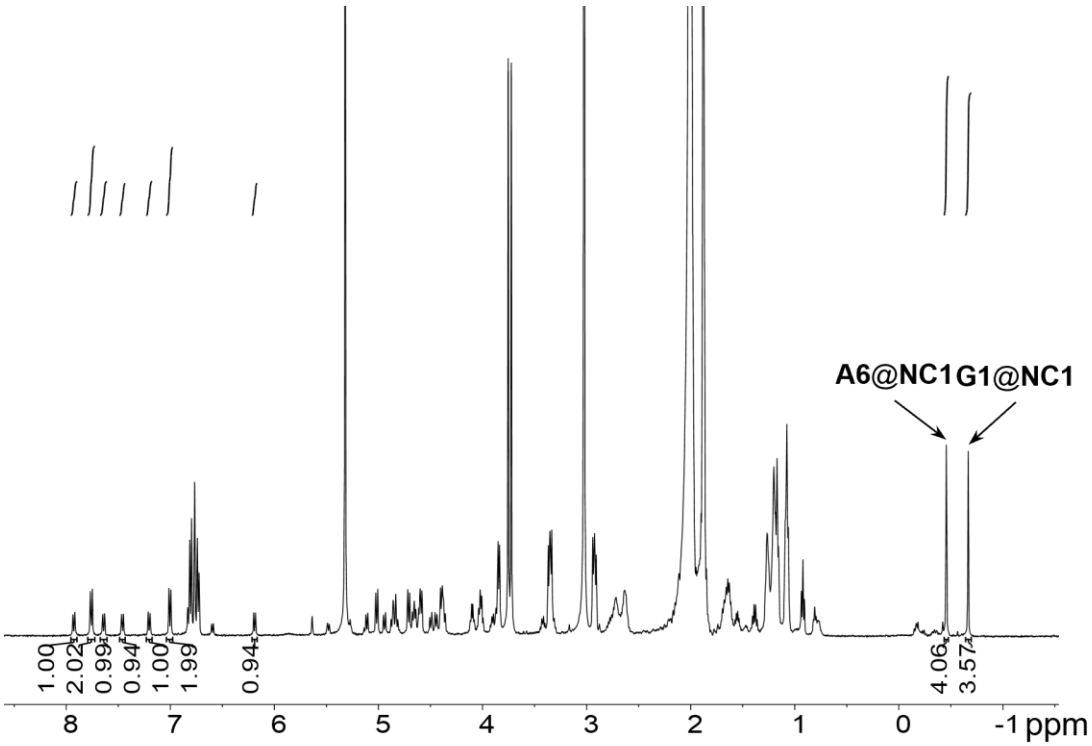

Figure S61. A representative ^{1}H NMR spectrum (500 MHz, CD_2Cl_2:CD_3CN (*v*/*v* = 1:1), 298 K) of an equilibrium mixture containing **NC** (0.62 mM), **G1** (1.3 mM) and **A6** (3.1 mM).

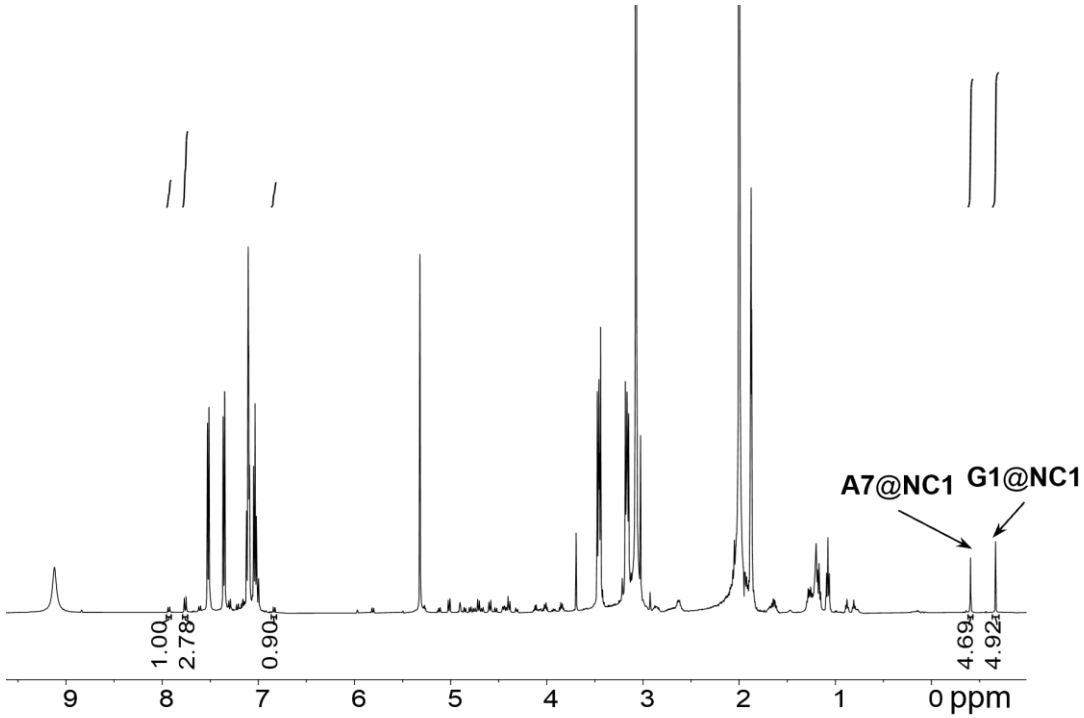

Figure S62. A representative ^{1}H NMR spectrum (500 MHz, CD_2Cl_2:CD_3CN (*v*/*v* = 1:1), 298 K) of an equilibrium mixture containing **NC** (0.57 mM), **G1** (1.1 mM) and **A7** (14 mM).

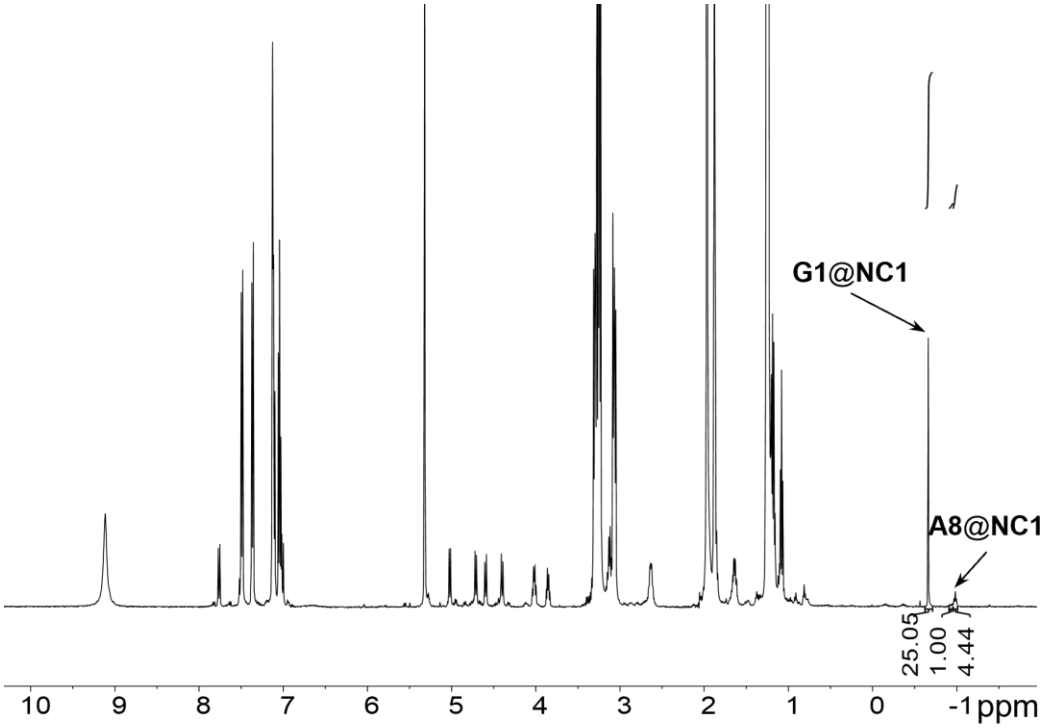

Figure S63. A representative ^{1}H NMR spectrum (500 MHz, CD_2Cl_2:CD_3CN (*v*/*v* = 1:1), 298 K) of an equilibrium mixture containing **NC** (0.50 mM), **G1** (1.1 mM) and **A8** (16 mM).

3. Kinetic Experiments

General. ^{1}H NMR spectra were recorded on Bruker Avance 400 or 500 spectrometers. All chemical shifts are reported in *ppm* with residual solvents or TMS (tetramethylsilane) signals as the internal standards. The following abbreviations are used for signal multiplicities: s, singlet; d, doublet; t triplet; m, multiplet. Host-guest complexes were prepared by mixing the host and excess guest in CD_2Cl_2/CD_3CN (*v*/*v* = 1:1). Counterions of the guests are PF_6^-.

For a typical kinetic experiment, a solution of **NC** (2.0 mM, CD_2Cl_2:CD_3CN (*v*:*v* = 1:1), 0.25 mL) was added a solution of an ammonium guest (2.0 mM, CD_2Cl_2:CD_3CN (*v*:*v* = 1:1), 0.25 mL,) such that the final concentrations of both the host and guest are 1.0 mM. The sample was quickly mixed in an NMR tube and transferred into the NMR spectrometer. ^{1}H NMR spectra were recorded at certain time intervals at room temperature.

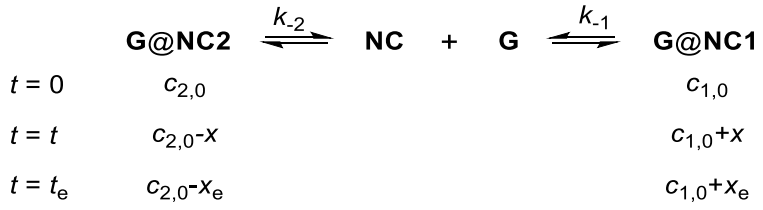

$c_{1,0}$ = initial concentration of **G@NC1**

$c_{2,0}$ = initial concentration of **G@NC2**

x = change in concentration at time t

x_e = change in concentration at equilibrium

t_e = time to reach equilibrium

The equilibrium reaction kinetic equation is

$$x = -x_e e^{-(k_{-1}+k_{-2})t} + x_e \qquad (S6)$$

Derivation of equation *S*6:

The net forward reaction rate depends is the sum of the forward and reverse reaction rates:

$$r = \frac{dx}{dt} = r_2 - r_1 = k_{-2}\left(c_{2,0} - x\right) - k_{-1}(c_{1,0} + x) \qquad (S7)$$

Integration of *S*7 gives

$$\int_0^x \frac{dx}{k_{-2}\left(c_{2,0} - x\right) - k_{-1}(c_{1,0} + x)} = \int_0^t dt \qquad (S8)$$

$$\int_0^x \frac{dx}{-(k_{-1} + k_{-2})x + k_{-2}c_{2,0} - k_{-1}c_{1,0}} = \int_0^t dt \qquad (S9)$$

$$-\frac{ln\left(k_{-2}\left(c_{2,0} - x\right) - k_{-1}(c_{1,0} + x)\right)}{k_{-1} + k_{-2}} + \frac{ln\left(k_{-2}c_{2,0} - k_{-1}c_{1,0}\right)}{k_{-1} + k_{-2}} = t \qquad (S10)$$

$$ln\frac{k_{-2}c_{2,0} - k_{-1}c_{1,0}}{k_{-2}\left(c_{2,0} - x\right) - k_{-1}(c_{1,0} + x)} = (k_{-1} + k_{-2})t \qquad (S11)$$

$$\frac{k_{-2}c_{2,0} - k_{-1}c_{1,0}}{k_{-2}\left(c_{2,0} - x\right) - k_{-1}(c_{1,0} + x)} = e^{(k_{-1}+k_{-2})t} \qquad (S12)$$

$$\frac{k_{-2}c_{2,0} - k_{-1}c_{1,0}}{\left(k_{-2}c_{2,0} - k_{-2}x\right) - (k_{-1}c_{1,0} + k_{-1}x)} = e^{(k_{-1}+k_{-2})t} \qquad (S13)$$

$$\left(k_{-2}c_{2,0} - k_{-1}c_{1,0}\right)e^{-(k_{-1}+k_{-2})t} = k_{-2}c_{2,0} - k_{-1}c_{1,0} - (k_{-1} + k_{-2})x \qquad (S14)$$

which can be simplified to

$$x = -\frac{k_{-2}c_{2,0} - k_{-1}c_{1,0}}{k_{-1} + k_{-2}}e^{-(k_{-1}+k_{-2})t} + \frac{k_{-2}c_{2,0} - k_{-1}c_{1,0}}{k_{-1} + k_{-2}} \qquad (S15)$$

At equilibrium,

$$r = \frac{dx}{dt} = 0 \qquad (S16)$$

so that,

$$k_{-2}\left(c_{2,0} - x_e\right) = k_{-1}(c_{1,0} + x_e) \qquad (S17)$$

$$k_{-1} = \frac{c_{2,0} - x_e}{c_{1,0} + x_e} k_{-2} \qquad (S18)$$

$$x_e = \frac{k_{-2}c_{2,0} - k_{-1}c_{1,0}}{k_{-1} + k_{-2}} \qquad (S19)$$

Substituting *S*19 to *S*15 gives,

$$x = -x_e e^{-(k_{-1}+k_{-2})t} + x_e \qquad (S6)$$

At time t,

$$x = c_{1,t} - c_{1,0} \qquad (S20)$$

$$c_{1,t} = c_{1,0} + x \qquad (S21)$$

by substituting *S*1 to *S*21,

$$c_{1,t} = c_{1,0} - x_e e^{-(k_{-1}+k_{-2})t} + x_e \qquad (S22)$$

fitting of the NMR data to the equation:

$$C = Ae^{-kt} + B \qquad (S23)$$

in which

$$C = c_{1,t}$$

$$A = -x_e$$

$$k = k_{-1} + k_{-2} = \frac{c_{2,0} + c_{1,0}}{c_{1,0} + x_e} k_{-2}$$

$$B = c_{1,0} + x_e$$

A, B and k were obtained, and $c_{1,0}$, $c_{2,0}$, k_{-1}, k_{-2}, x_e can be calculated.

Table S3. Overall rate constant k, dissociation rate constants k_{-1} and k_{-2}, initial concentration of **G@NC1** ($c_{1,0}$) and **G@NC2** ($c_{2,0}$), and the equilibrium concentration of **G@NC1** ($c_{1,e}$) obtained from fitting the ^{1}H NMR data.

	A	k/s^{-1}	B	R^2	k_{-1}/s^{-1}	k_{-2}/s^{-1}	$c_{1,0}$/mM	$c_{2,0}$/mM	$c_{1,e}$/mM
G1	-6.5×10^{-4}	2.9×10^{-4}	9.8×10^{-4}	0.9999	4.7×10^{-6}	2.9×10^{-4}	0.33	0.67	0.98
G2	-6.0×10^{-4}	2.2×10^{-5}	9.6×10^{-4}	0.9998	9.3×10^{-7}	2.1×10^{-5}	0.36	0.64	0.96
G3	-5.7×10^{-4}	1.9×10^{-5}	9.1×10^{-4}	0.9999	1.9×10^{-6}	1.8×10^{-5}	0.34	0.66	0.90
G4	-6.2×10^{-4}	4.7×10^{-5}	9.4×10^{-4}	0.9999	2.8×10^{-6}	4.4×10^{-5}	0.32	0.68	0.94
G5	-5.9×10^{-4}	1.1×10^{-4}	9.2×10^{-4}	0.9996	8.9×10^{-6}	1.1×10^{-4}	0.34	0.66	0.92
G6	-5.5×10^{-4}	1.5×10^{-5}	9.1×10^{-4}	0.9991	1.3×10^{-6}	1.3×10^{-5}	0.36	0.64	0.91
G7	-5.7×10^{-4}	5.3×10^{-5}	9.1×10^{-4}	0.9999	4.7×10^{-6}	4.8×10^{-5}	0.34	0.66	0.91
G8	/	/	/	/	/	/	/	/	/
G9	-5.3×10^{-4}	2.6×10^{-6}	9.5×10^{-4}	0.9999	1.4×10^{-7}	2.4×10^{-6}	0.41	0.59	0.95
G10	/	/	/	/	/	/	/	/	/
G11	/	/	/	/	/	/	/	/	/
G12	-3.1×10^{-4}	6.0×10^{-7}	9.8×10^{-4}	0.9980	1.3×10^{-8}	5.9×10^{-7}	0.67	0.33	0.98
G13	-2.1×10^{-4}	6.3×10^{-6}	8.6×10^{-4}	0.9992	8.7×10^{-7}	5.4×10^{-6}	0.65	0.35	0.86
G14	/	/	/	/	/	/	/	/	/
G15	-6.2×10^{-4}	1.0×10^{-5}	9.3×10^{-4}	0.9981	7.1×10^{-7}	9.6×10^{-6}	0.31	0.69	0.93
G16	-6.6×10^{-4}	1.3×10^{-5}	9.8×10^{-4}	0.9980	3.1×10^{-7}	1.3×10^{-5}	0.31	0.69	0.98
G17	-5.9×10^{-4}	8.5×10^{-4}	8.7×10^{-4}	0.9965	1.1×10^{-4}	7.4×10^{-4}	0.28	0.72	0.87
G18	-2.1×10^{-4}	5.4×10^{-5}	8.8×10^{-4}	0.9996	6.7×10^{-6}	4.8×10^{-5}	0.67	0.33	0.88
G19	/	/	/	/	/	/	/	/	/
G20	/	/	/	/	/	/	/	/	/
G21	-4.4×10^{-4}	2.4×10^{-3}	9.0×10^{-4}	0.9980	2.3×10^{-4}	2.1×10^{-3}	0.46	0.54	0.90
G22	-1.5×10^{-4}	1.9×10^{-4}	9.3×10^{-4}	0.9836	1.4×10^{-5}	1.8×10^{-4}	0.77	0.23	0.93
G23	-4.4×10^{-4}	1.4×10^{-3}	9.4×10^{-4}	0.9960	8.4×10^{-5}	1.3×10^{-3}	0.50	0.50	0.94
G24	-6.1×10^{-4}	1.2×10^{-3}	9.6×10^{-4}	0.9975	5.3×10^{-5}	1.1×10^{-3}	0.35	0.65	0.96

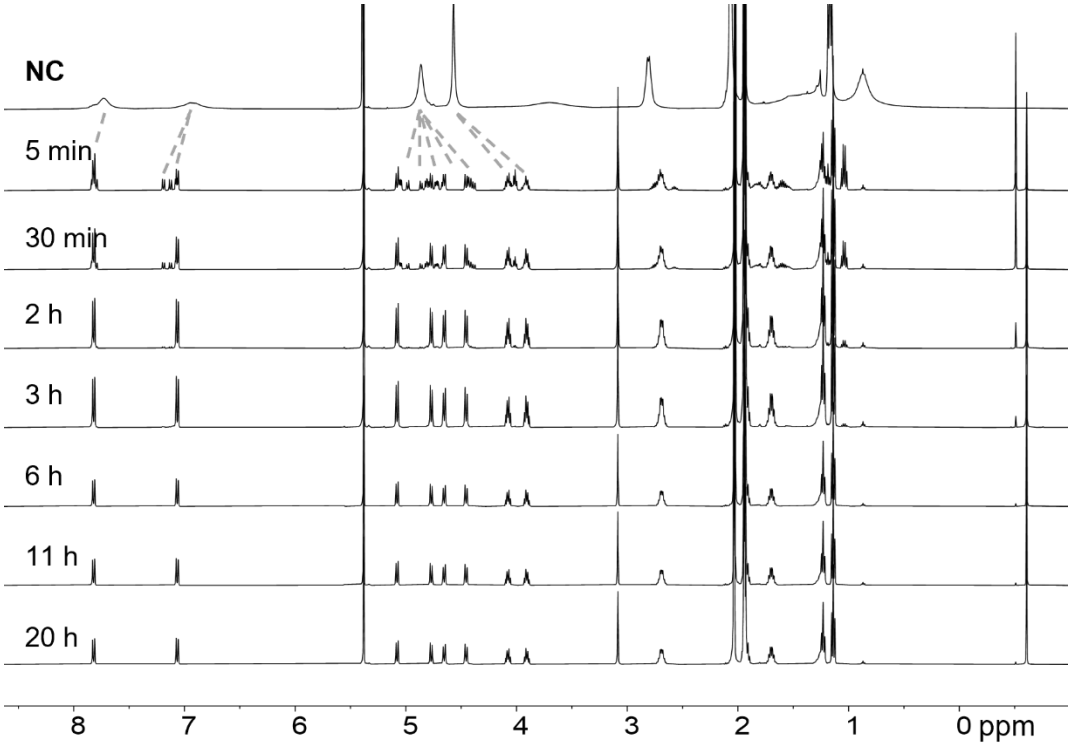

Figure S64. ^{1}H NMR spectra (500 MHz, CD_2Cl_2:CD_3CN (*v*/*v* = 1:1), 1.0 mM, 298 K) of **NC** after addition of **G1** at different time.

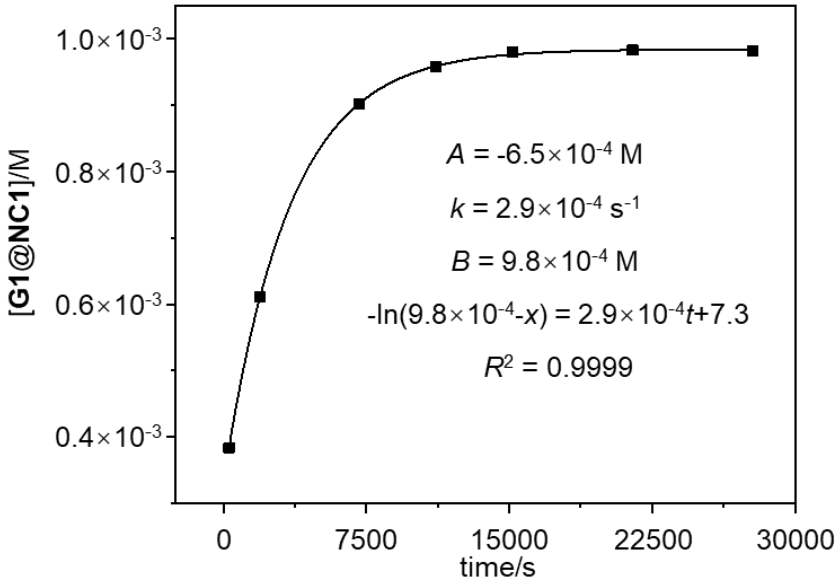

Figure S65. Change in concentration of **G1@NC1** against time and the fitted kinetic data.

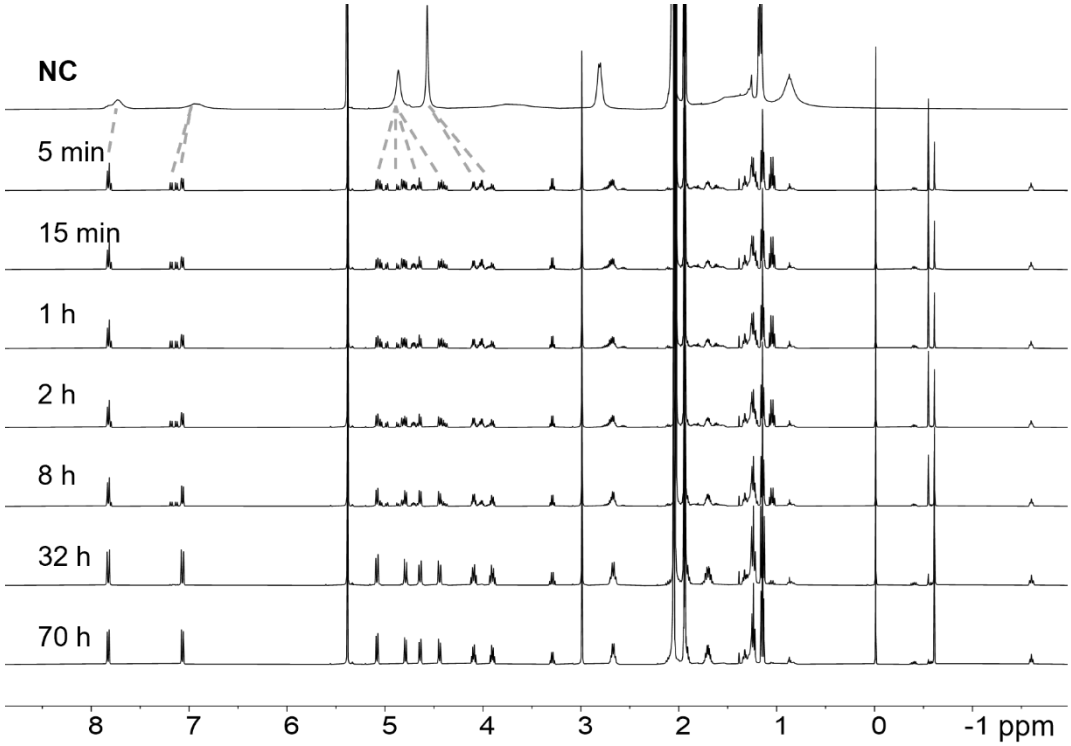

Figure S66. ^{1}H NMR spectra (500 MHz, CD_2Cl_2:CD_3CN (*v*/*v* = 1:1), 1.0 mM, 298 K) of **NC** after addition of **G2** at different time.

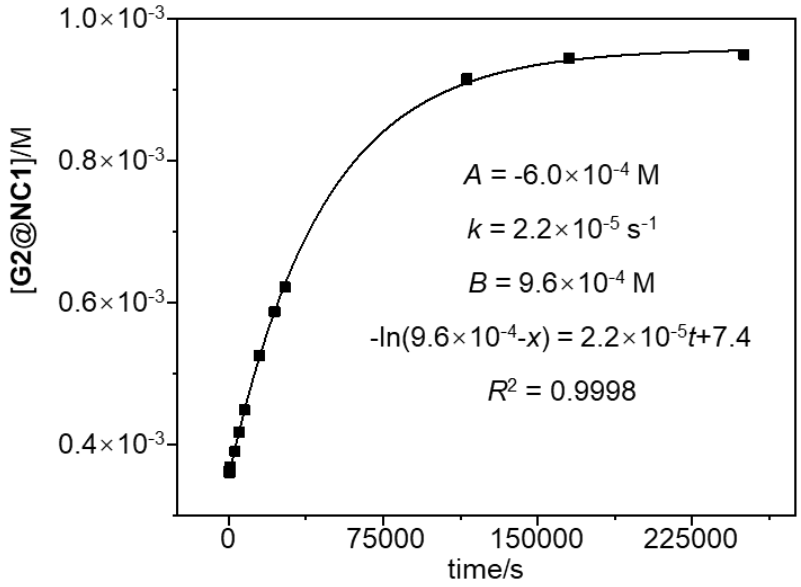

Figure S67. Change in concentration of **G2@NC1** against time and the fitted kinetic data.

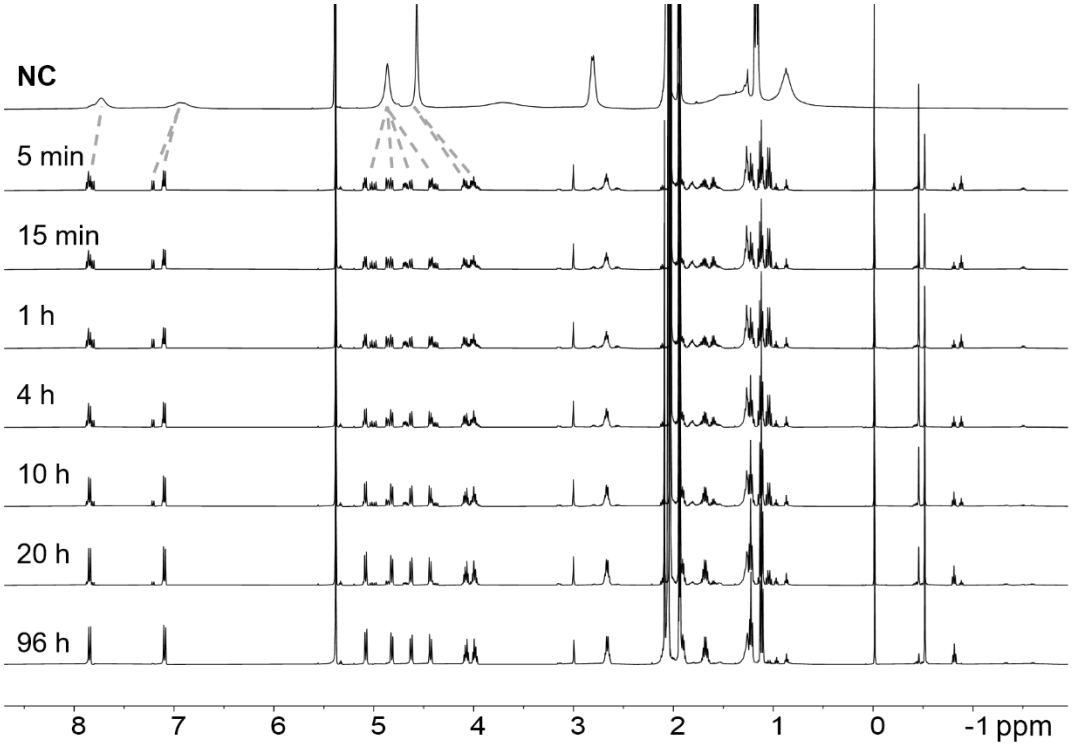

Figure S68. ^{1}H NMR spectra (500 MHz, CD_2Cl_2:CD_3CN (*v*/*v* = 1:1), 1.0 mM, 298 K) of **NC** after addition of **G3** at different time.

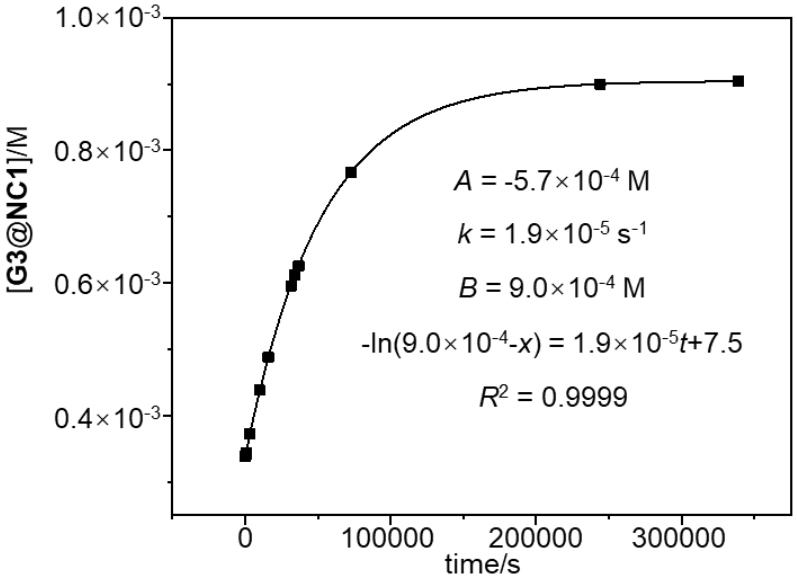

Figure S69. Change in concentration of **G3@NC1** against time and the fitted kinetic data.

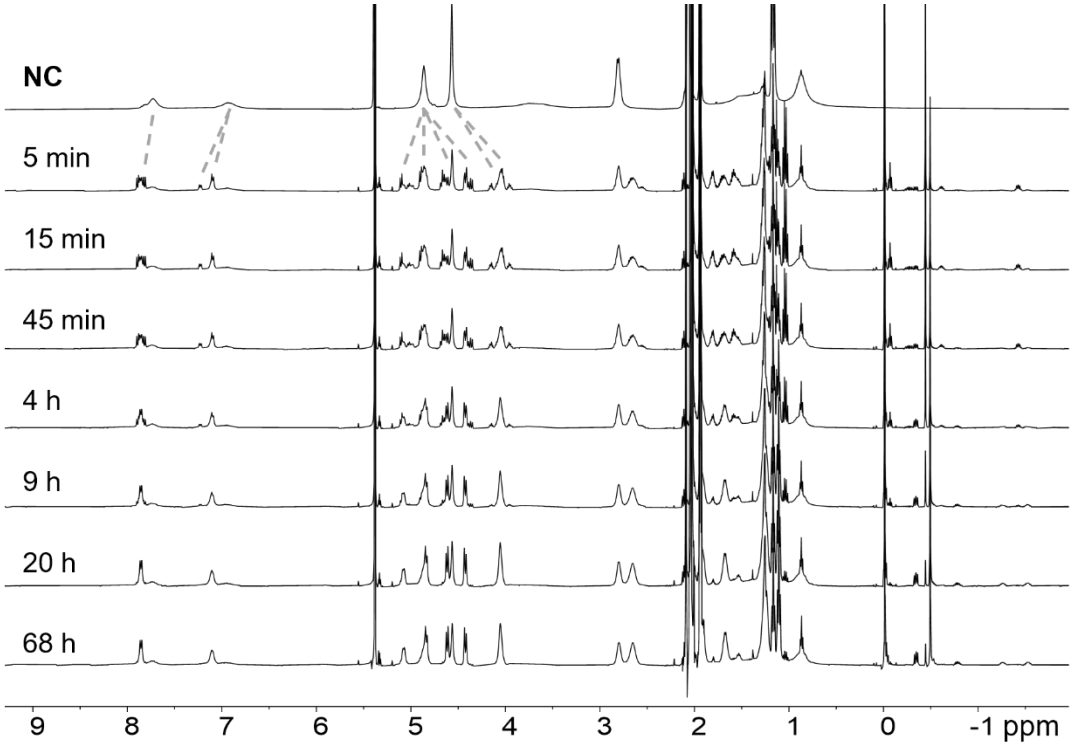

Figure S70. ^{1}H NMR spectra (500 MHz, CD_2Cl_2:CD_3CN (*v*/*v* = 1:1), 1.0 mM, 298 K) of **NC** after addition of **G4** at different time.

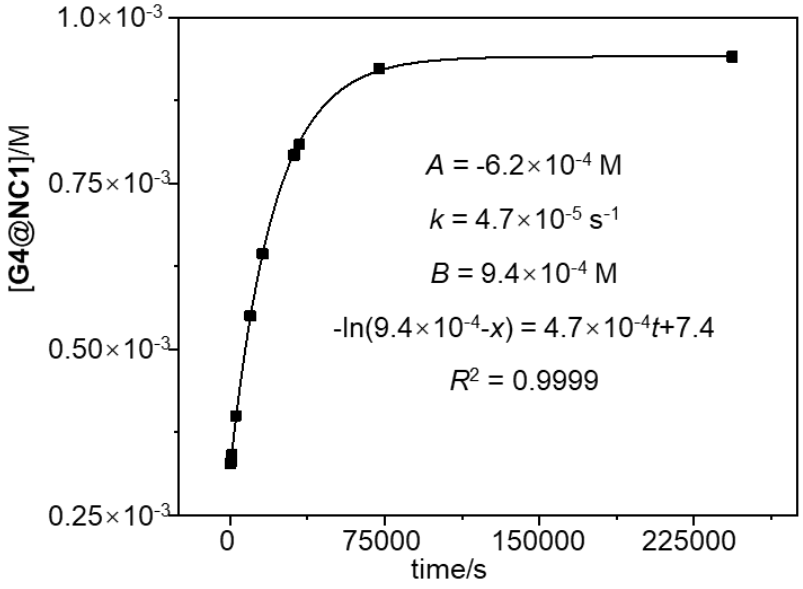

Figure S71. Change in concentration of **G4@NC1** against time and the fitted kinetic data.

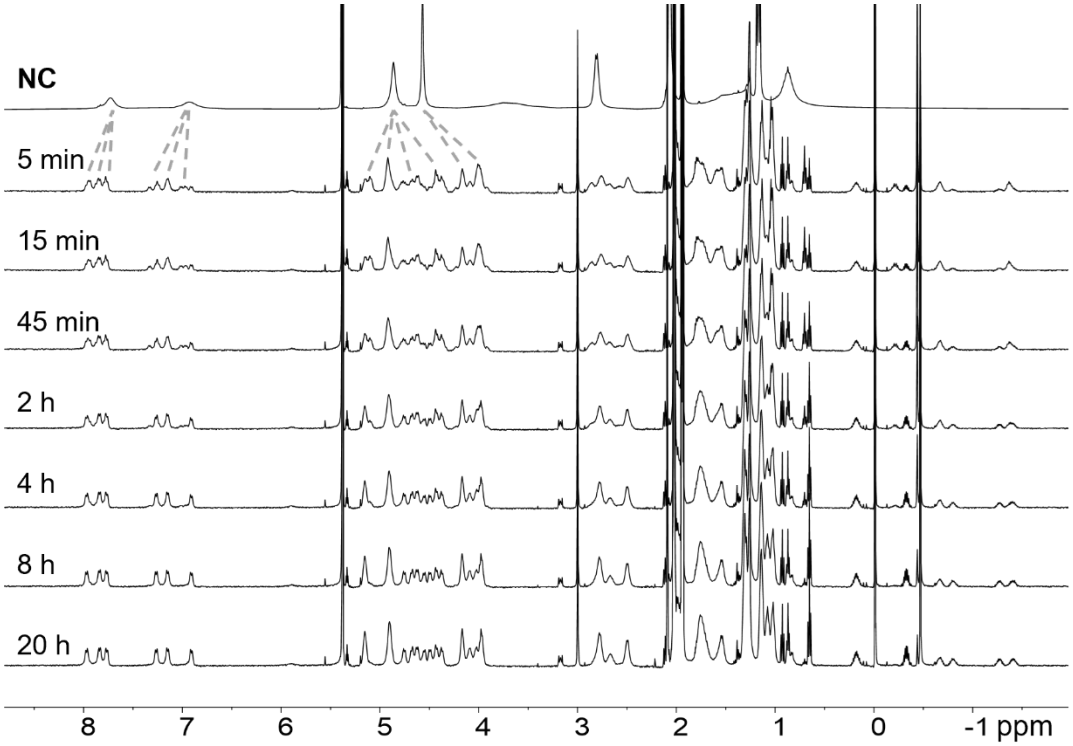

Figure S72. ^{1}H NMR spectra (500 MHz, CD_2Cl_2:CD_3CN (*v*/*v* = 1:1), 1.0 mM, 298 K) of **NC** after addition of **G5** at different time.

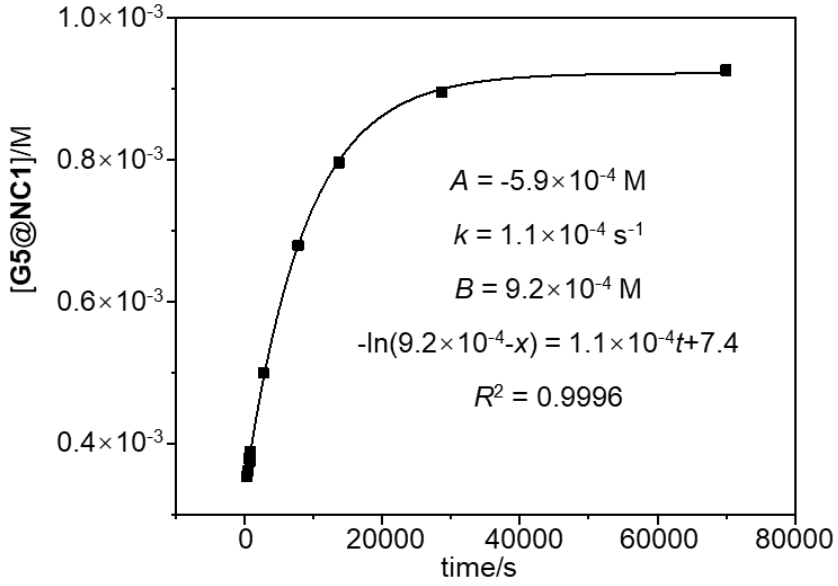

Figure S73. Change in concentration of **G5@NC1** against time and the fitted kinetic data.

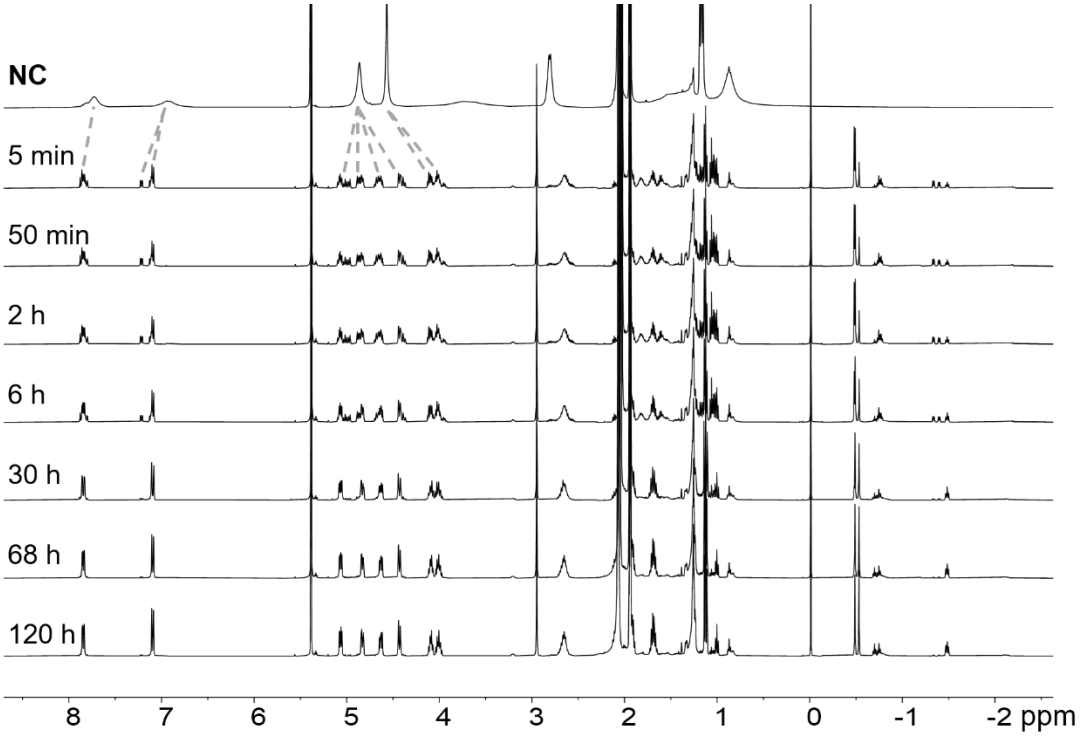

Figure S74. ^{1}H NMR spectra (500 MHz, CD_2Cl_2:CD_3CN (*v*/*v* = 1:1), 1.0 mM, 298 K) of **NC** after addition of **G6** at different time.

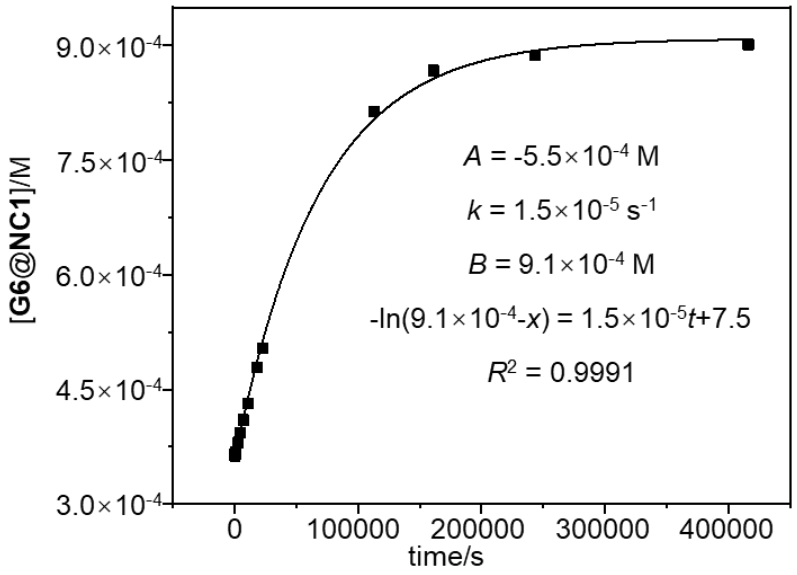

Figure S75. Change in concentration of **G6@NC1** against time and the fitted kinetic data.

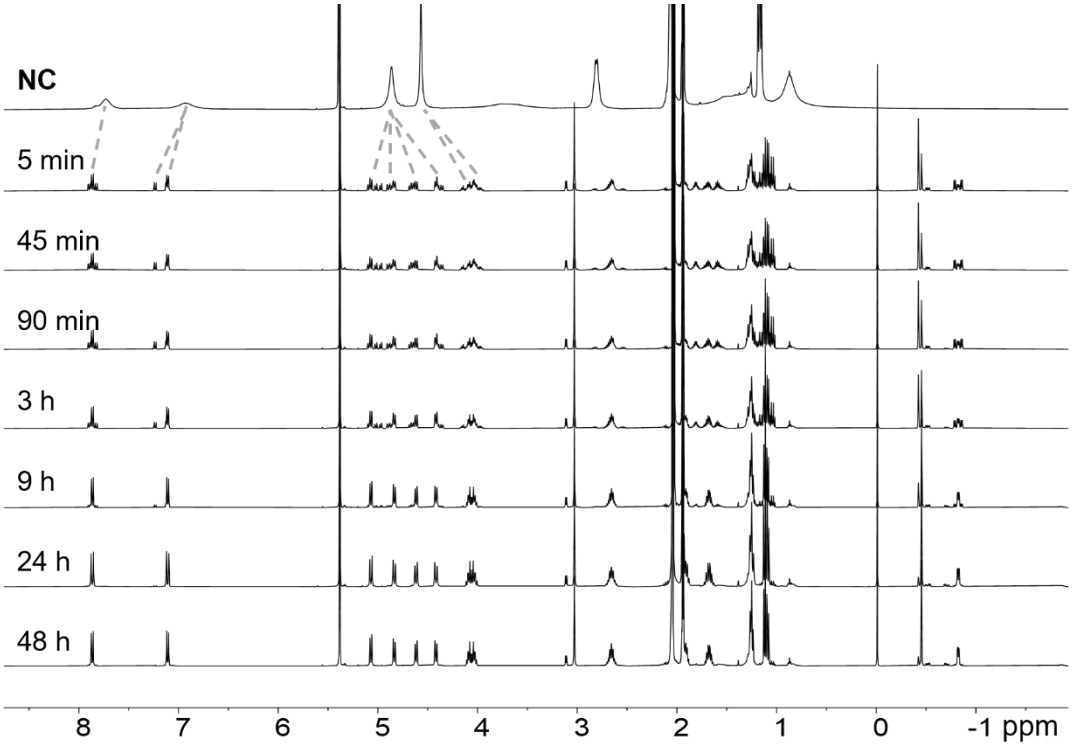

Figure S76. ^{1}H NMR spectra (500 MHz, CD_2Cl_2:CD_3CN (*v*/*v* = 1:1), 1.0 mM, 298 K) of **NC** after addition of **G7** at different time.

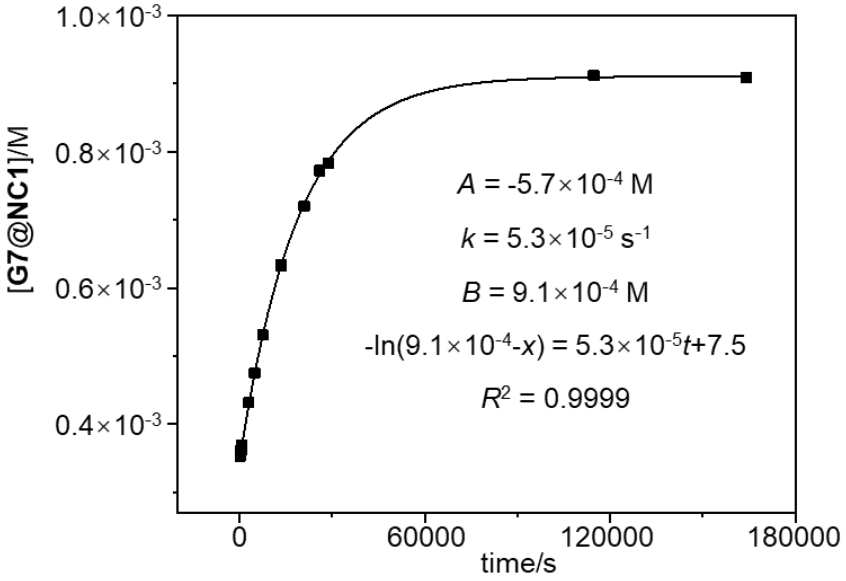

Figure S77. Change in concentration of **G7@NC1** against time and the fitted kinetic data.

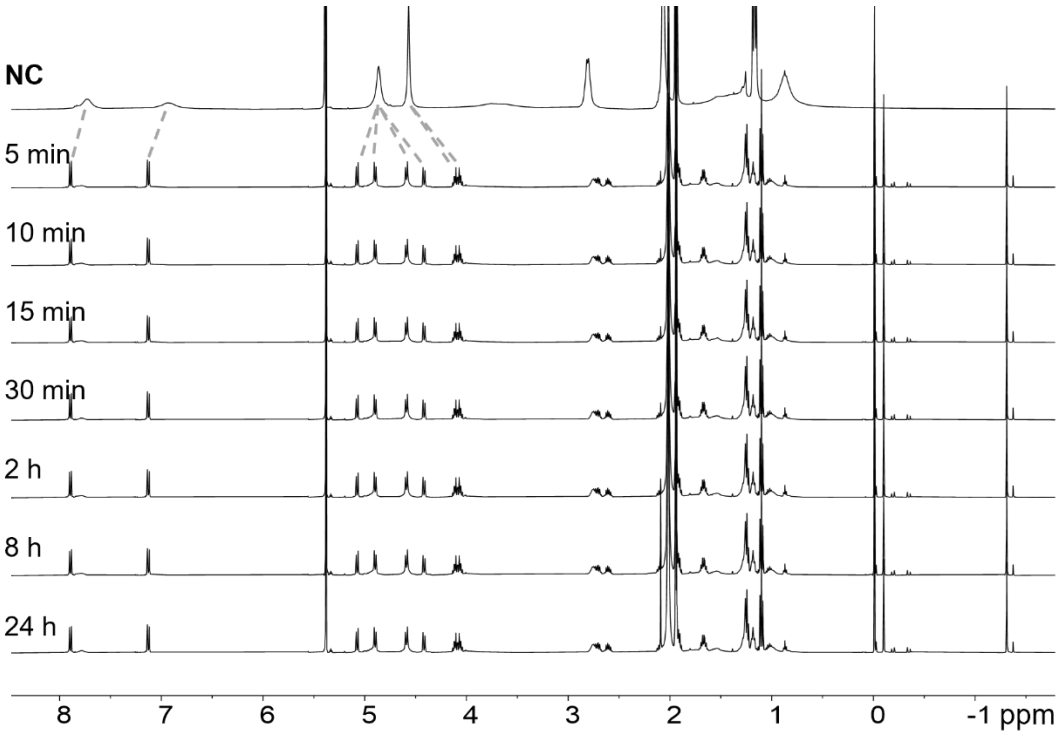

Figure S78. ^{1}H NMR spectra (500 MHz, CD_2Cl_2:CD_3CN (*v*/*v* = 1:1), 1.0 mM, 298 K) of **NC** after addition of **G8** at different time.

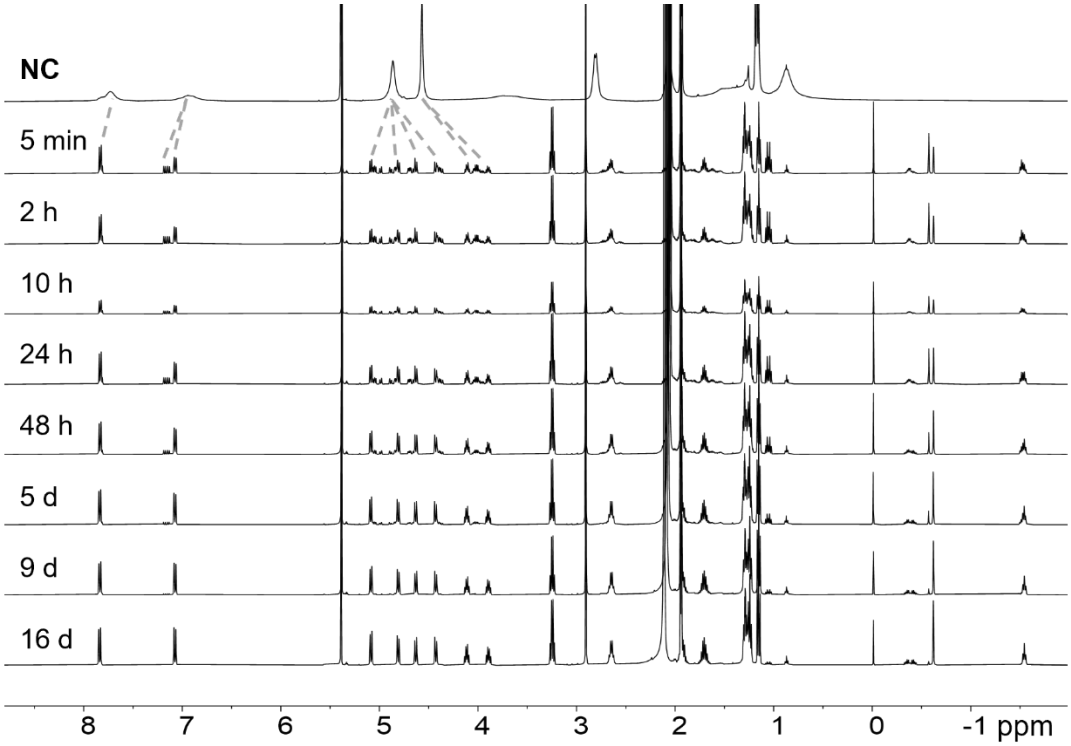

Figure S79. ^{1}H NMR spectra (500 MHz, CD_2Cl_2:CD_3CN (*v*/*v* = 1:1), 1.0 mM, 298 K) of **NC** after addition of **G9** at different time.

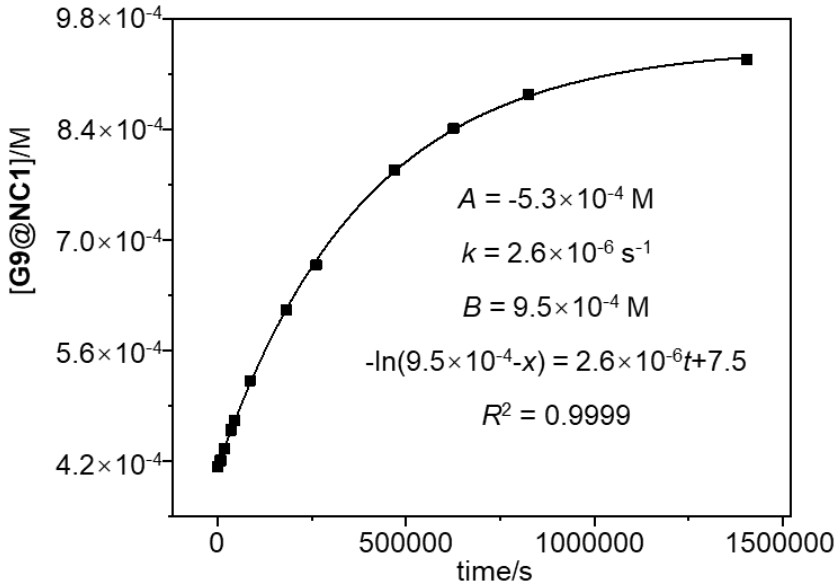

Figure S80. Change in concentration of **G9@NC1** against time and the fitted kinetic data.

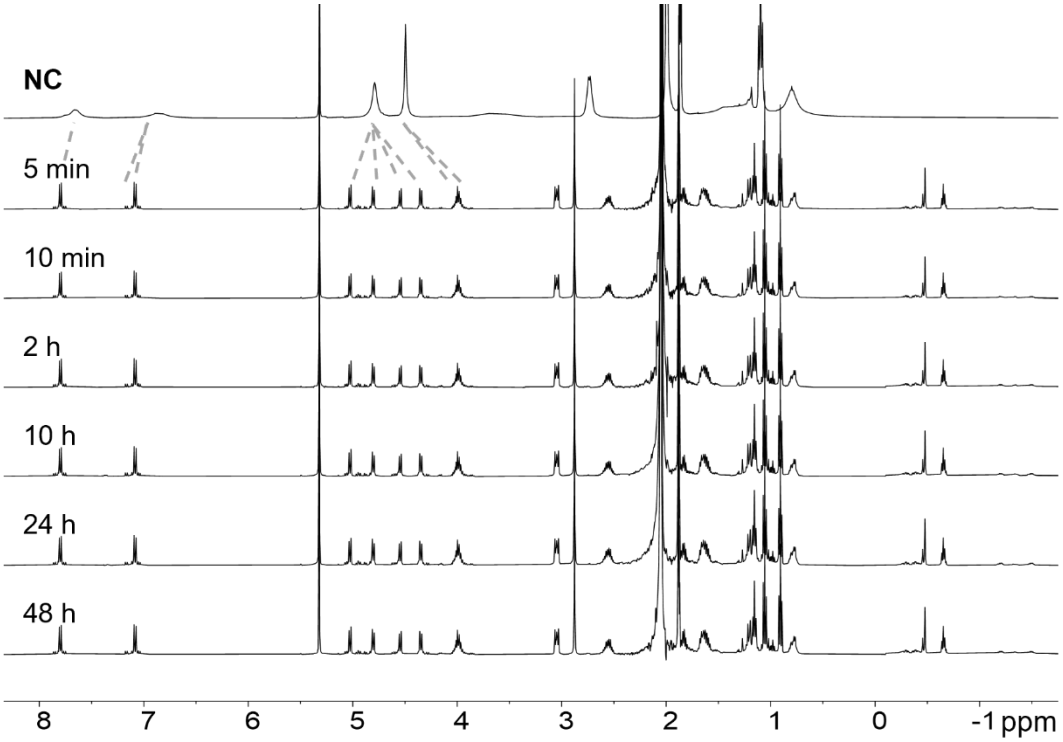

Figure S81. ^{1}H NMR spectra (500 MHz, CD_2Cl_2:CD_3CN (*v*/*v* = 1:1), 1.0 mM, 298 K) of **NC** after addition of **G10** at different time.

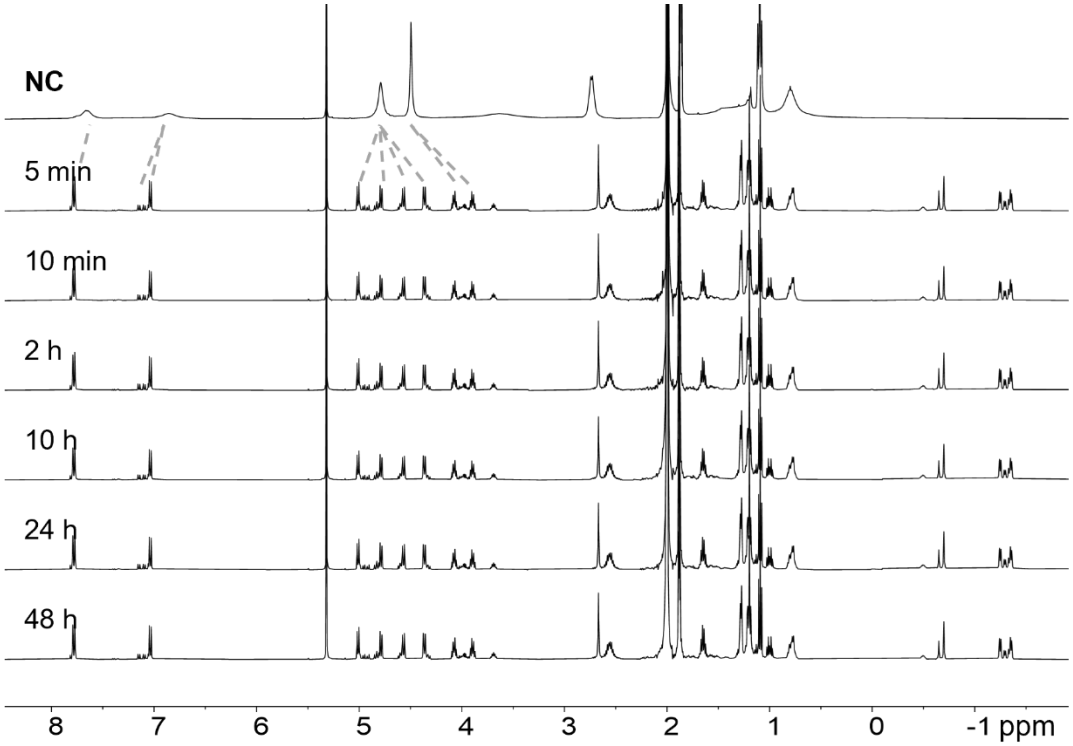

Figure S82. ^{1}H NMR spectra (500 MHz, CD_2Cl_2:CD_3CN (*v*/*v* = 1:1), 1.0 mM, 298 K) of **NC** after addition of **G11** at different time.

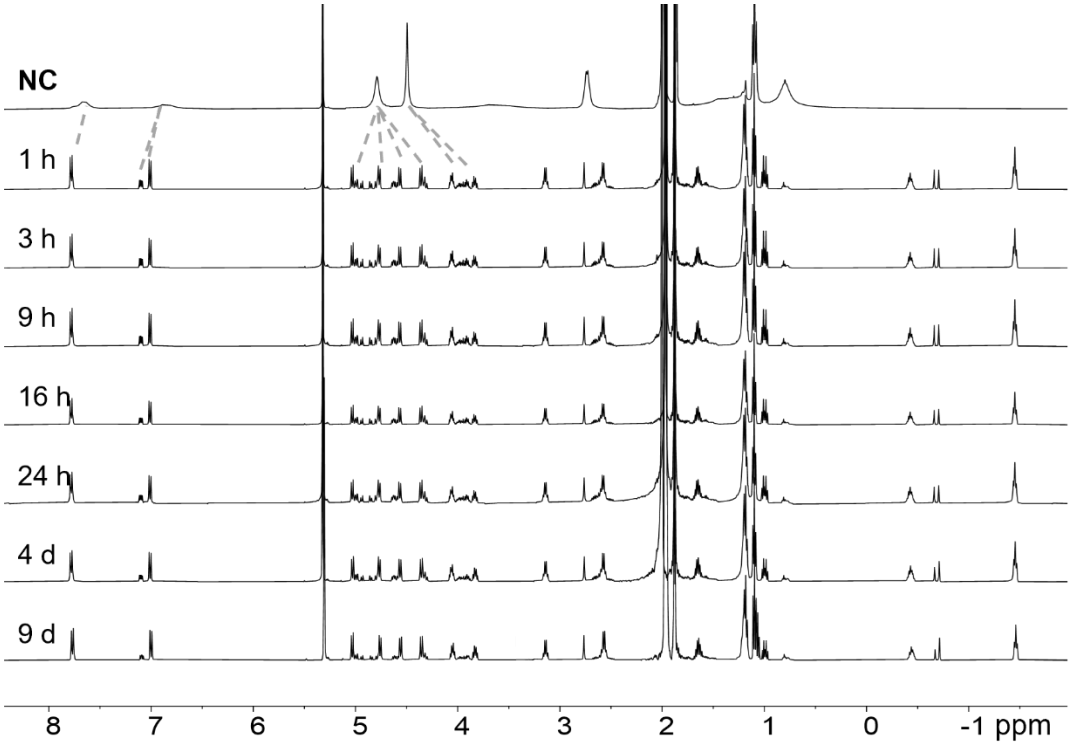

Figure S83. ^{1}H NMR spectra (500 MHz, CD_2Cl_2:CD_3CN (*v*/*v* = 1:1), 1.0 mM, 298 K) of **NC** after addition of **G12** at different time.

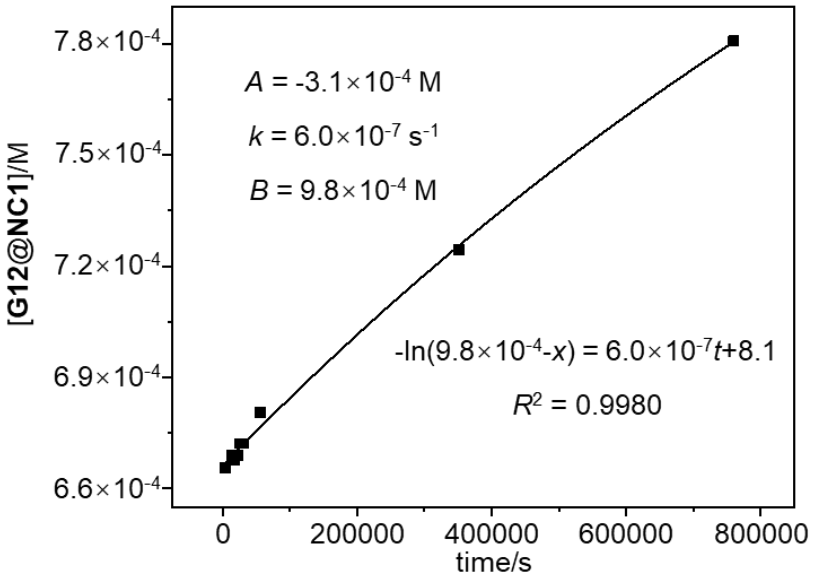

Figure S84. Change in concentration of **G9@NC1** against time and the fitted kinetic data.

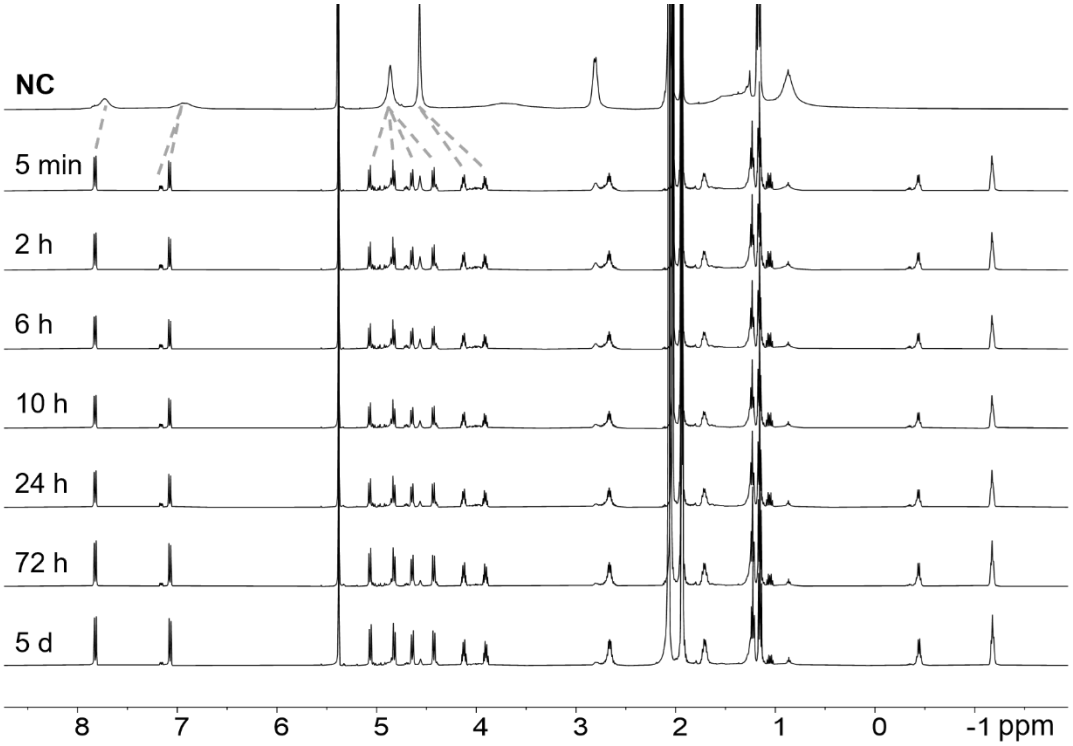

Figure S85. ^{1}H NMR spectra (500 MHz, CD_2Cl_2:CD_3CN (*v*/*v* = 1:1), 1.0 mM, 298 K) of **NC** after addition of **G13** at different time.

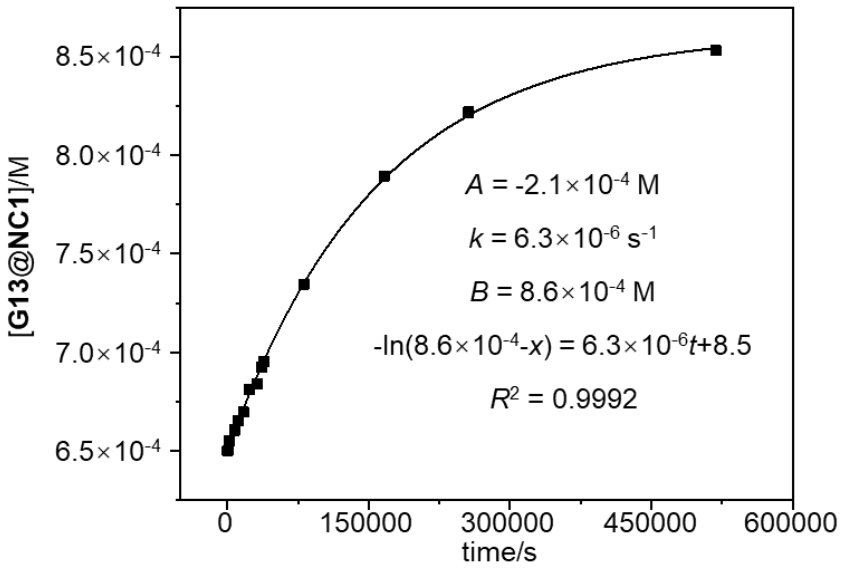

Figure S86. Change in concentration of **G13@NC1** against time and the fitted kinetic data.

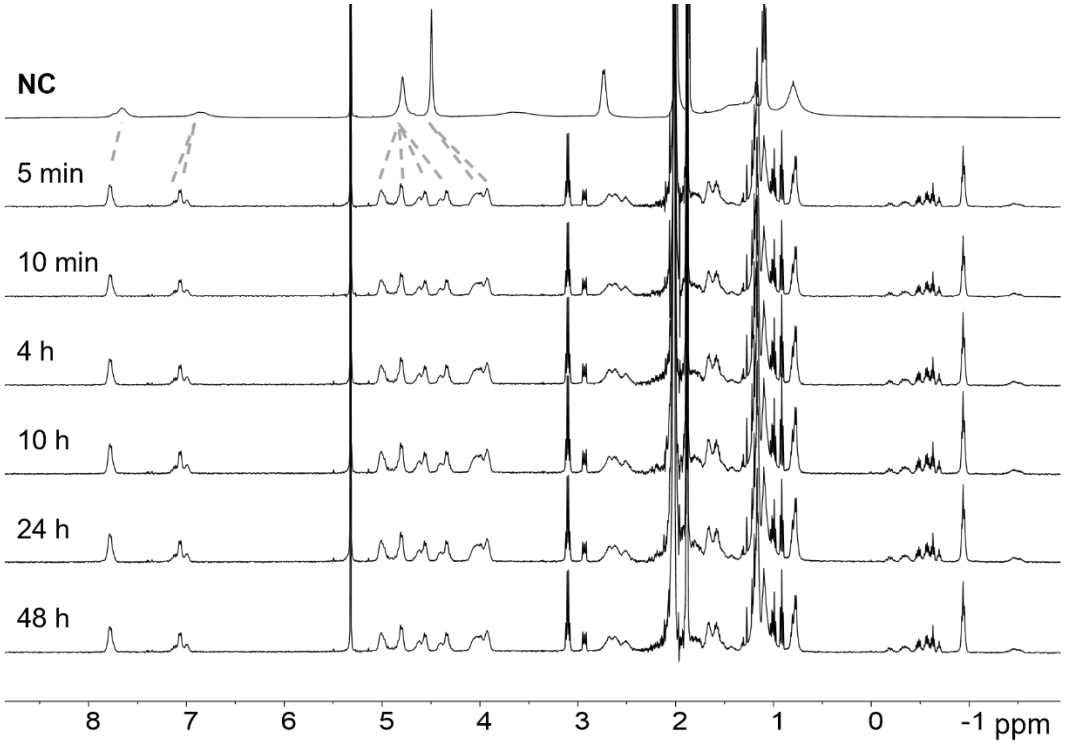

Figure S87. ^{1}H NMR spectra (500 MHz, CD_2Cl_2:CD_3CN (*v*/*v* = 1:1), 1.0 mM, 298 K) of **NC** after addition of **G14** at different time.

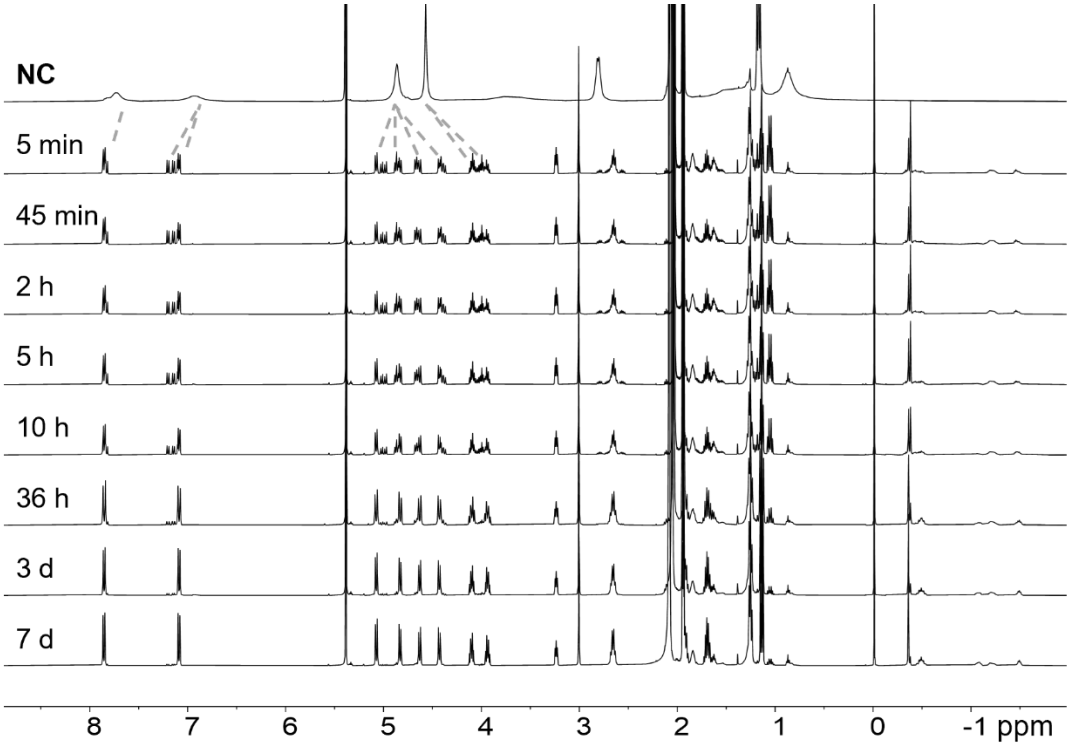

Figure S88. ^{1}H NMR spectra (500 MHz, CD_2Cl_2:CD_3CN (*v*/*v* = 1:1), 1.0 mM, 298 K) of **NC** after addition of **G15** at different time.

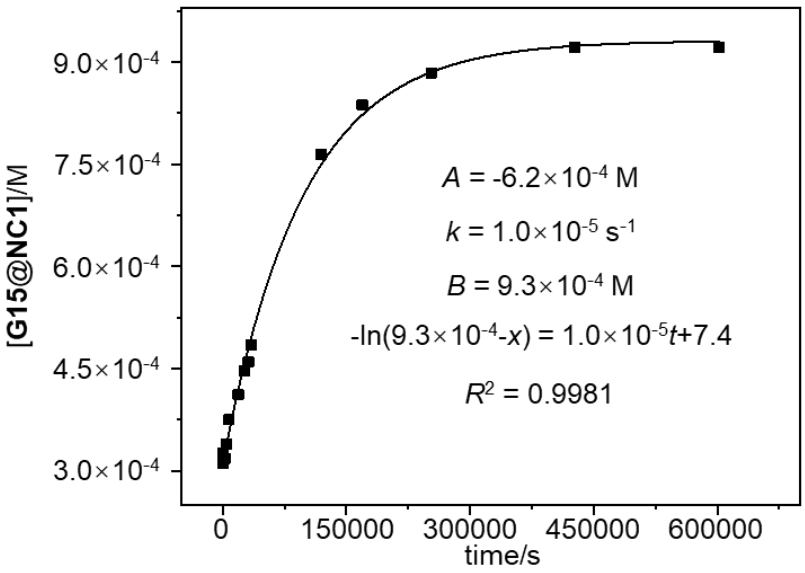

Figure S89. Change in concentration of **G15@NC1** against time and the fitted kinetic data.

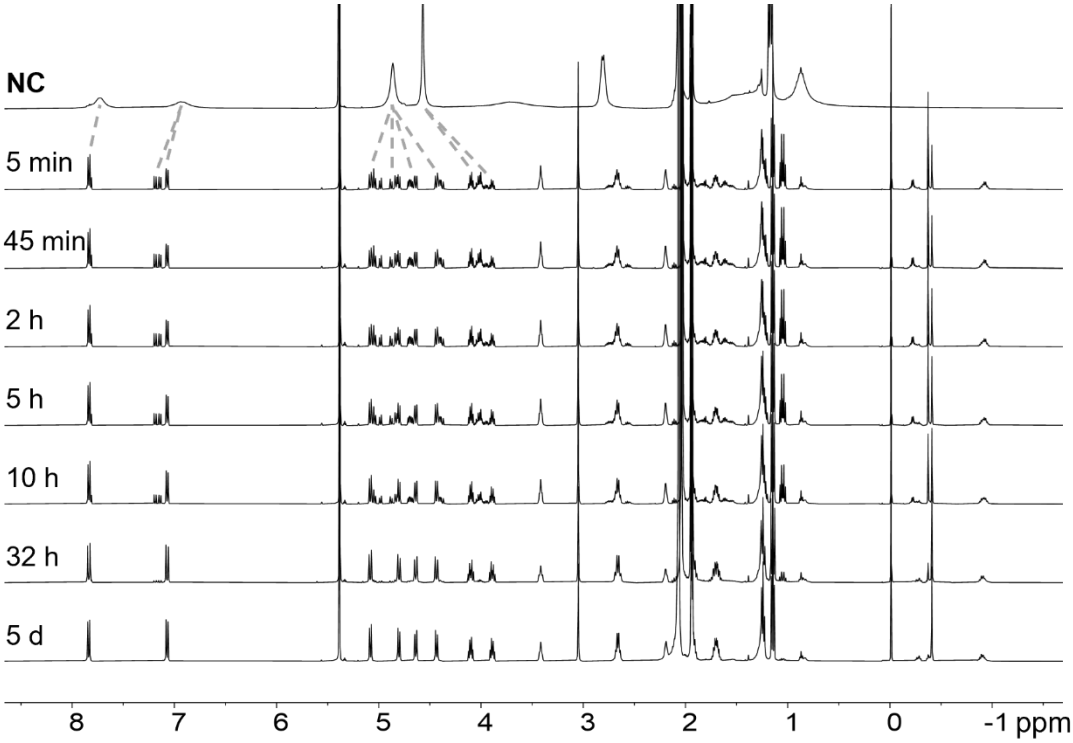

Figure S90. ^{1}H NMR spectra (500 MHz, CD_2Cl_2:CD_3CN (*v*/*v* = 1:1), 1.0 mM, 298 K) of **NC** after addition of **G16** at different time.

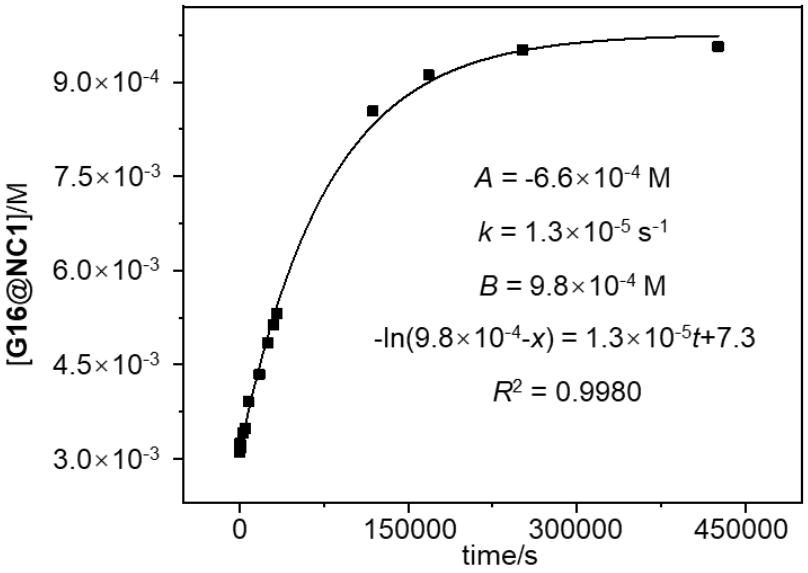

Figure S91. Change in concentration of **G16@NC1** against time and the fitted kinetic data.

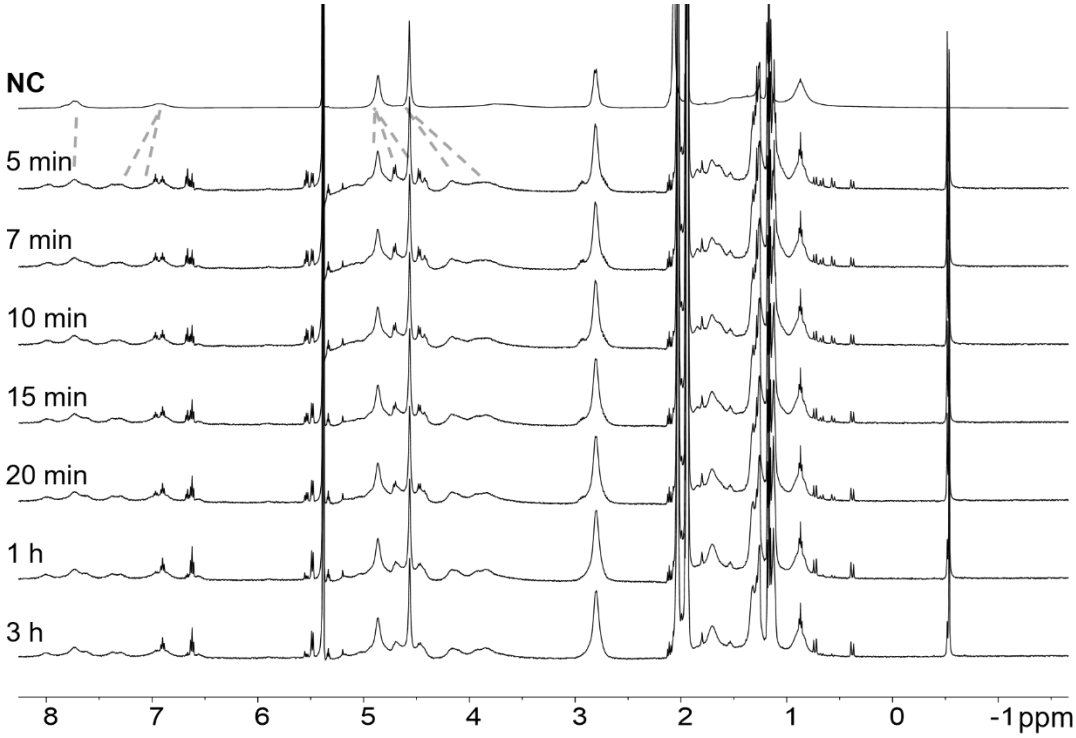

Figure S92. ^{1}H NMR spectra (500 MHz, CD_2Cl_2:CD_3CN (*v*/*v* = 1:1), 1.0 mM, 298 K) of **NC** after addition of **G17** at different time.

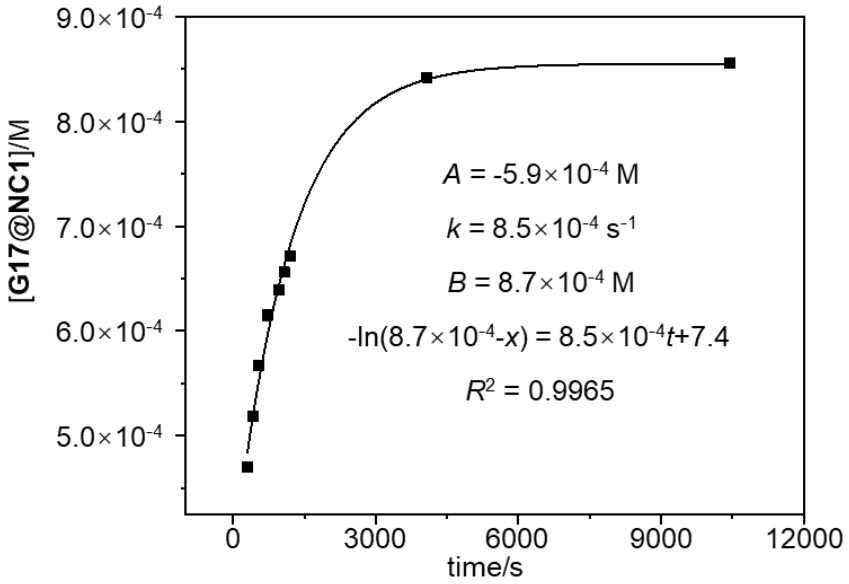

Figure S93. Change in concentration of **G17@NC1** against time and the fitted kinetic data.

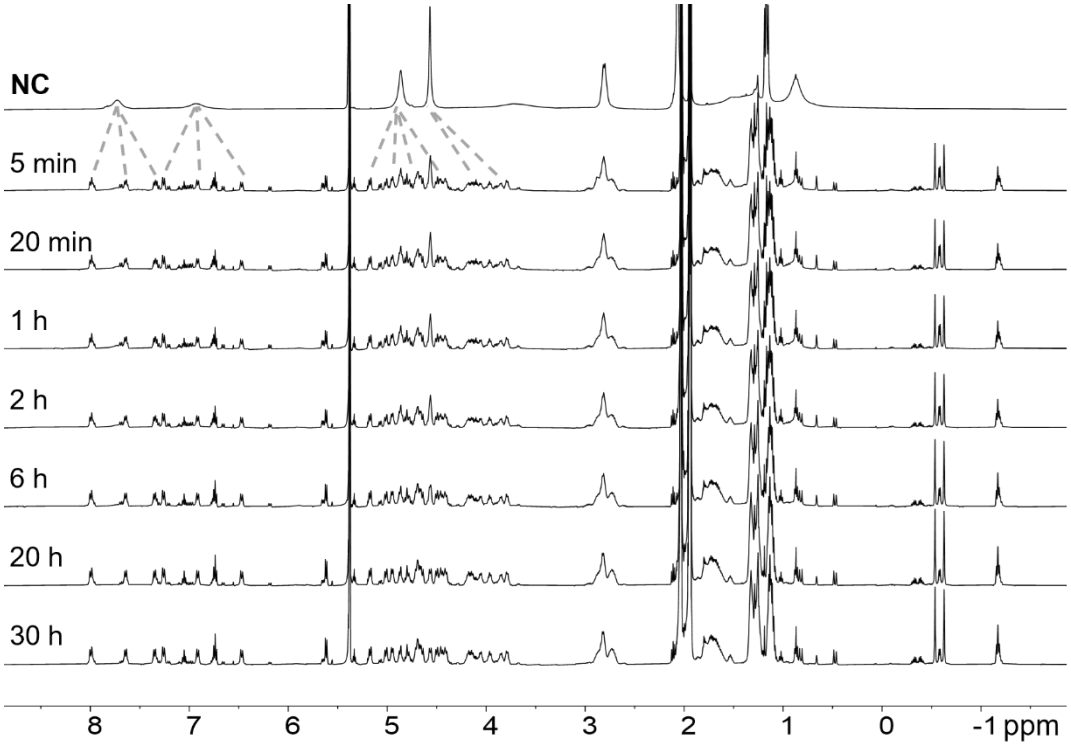

Figure S94. ^{1}H NMR spectra (500 MHz, CD_2Cl_2:CD_3CN (*v*/*v* = 1:1), 1.0 mM, 298 K) of **NC** after addition of **G18** at different time.

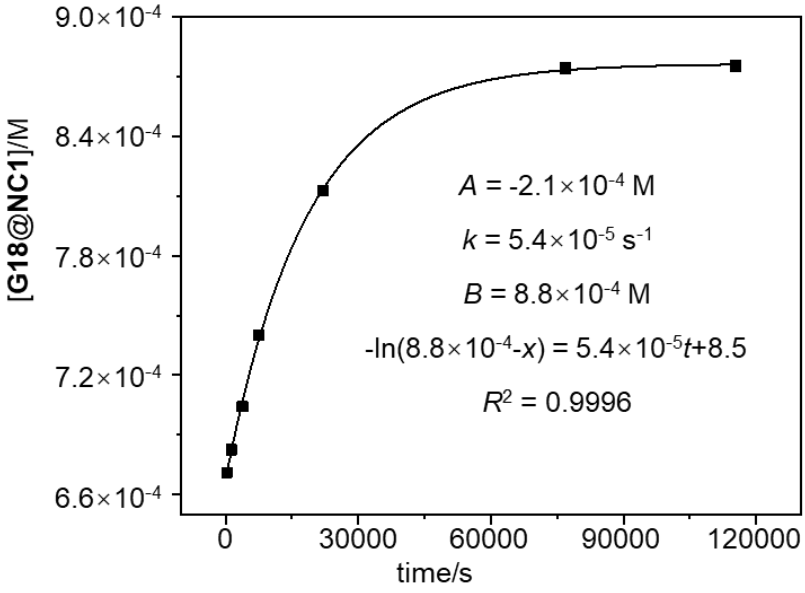

Figure S95. Change in concentration of **G18@NC1** against time and the fitted kinetic data.

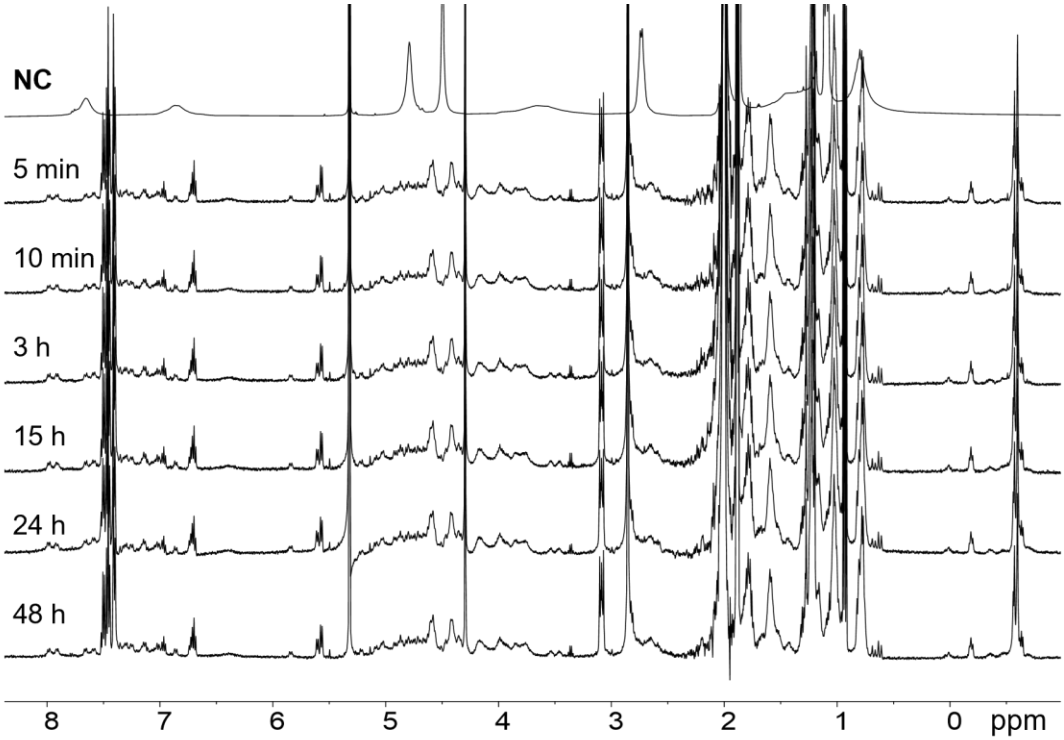

Figure S96. ^{1}H NMR spectra (500 MHz, CD_2Cl_2:CD_3CN (*v*/*v* = 1:1), 1.0 mM, 298 K) of **NC** after addition of **G19** at different time.

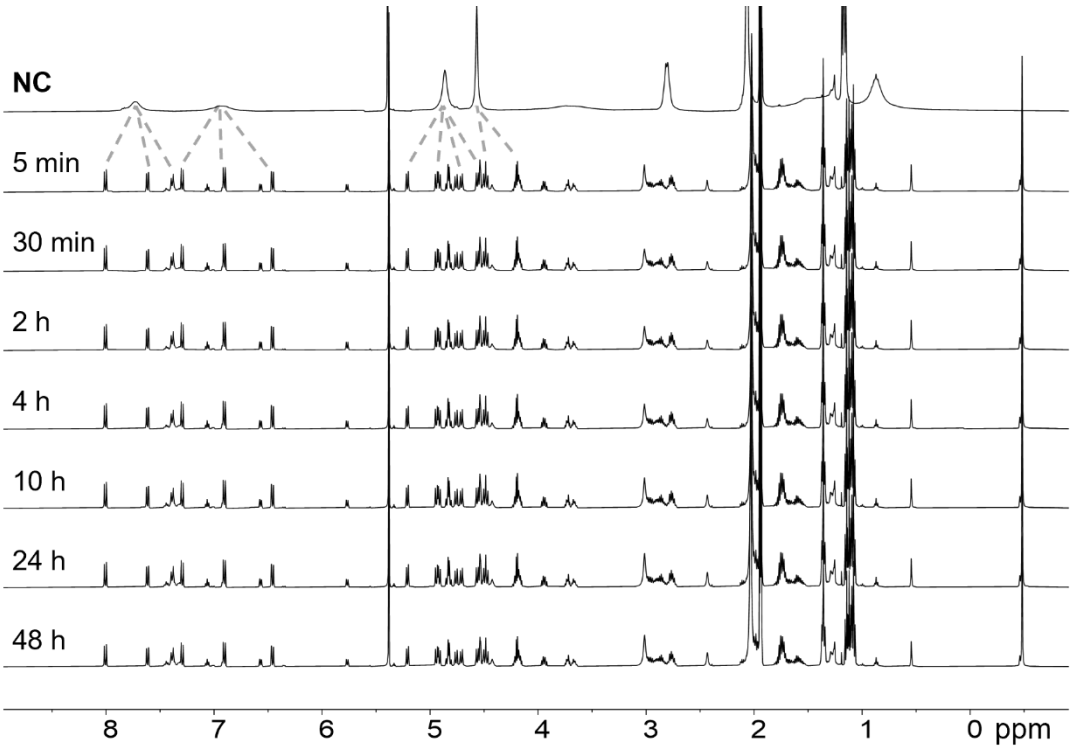

Figure S97. ^{1}H NMR spectra (500 MHz, CD_2Cl_2:CD_3CN (*v*/*v* = 1:1), 1.0 mM, 298 K) of **NC** after addition of **G20** at different time.

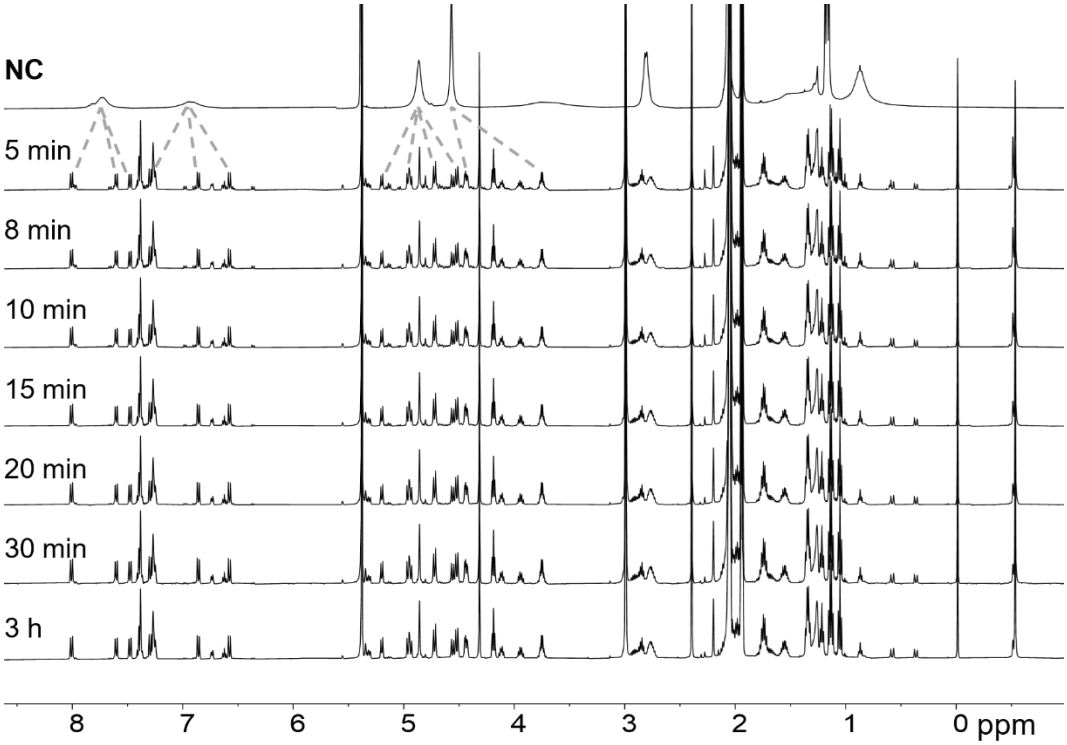

Figure S98. ^{1}H NMR spectra (500 MHz, CD_2Cl_2:CD_3CN (*v*/*v* = 1:1), 1.0 mM, 298 K) of **NC** after addition of **G21** at different time.

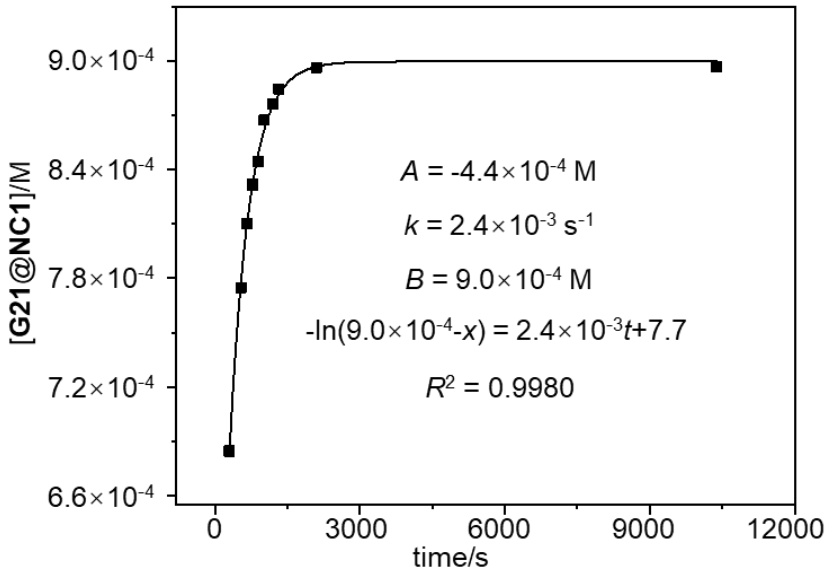

Figure S99. Change in concentration of **G21@NC1** against time and the fitted kinetic data.

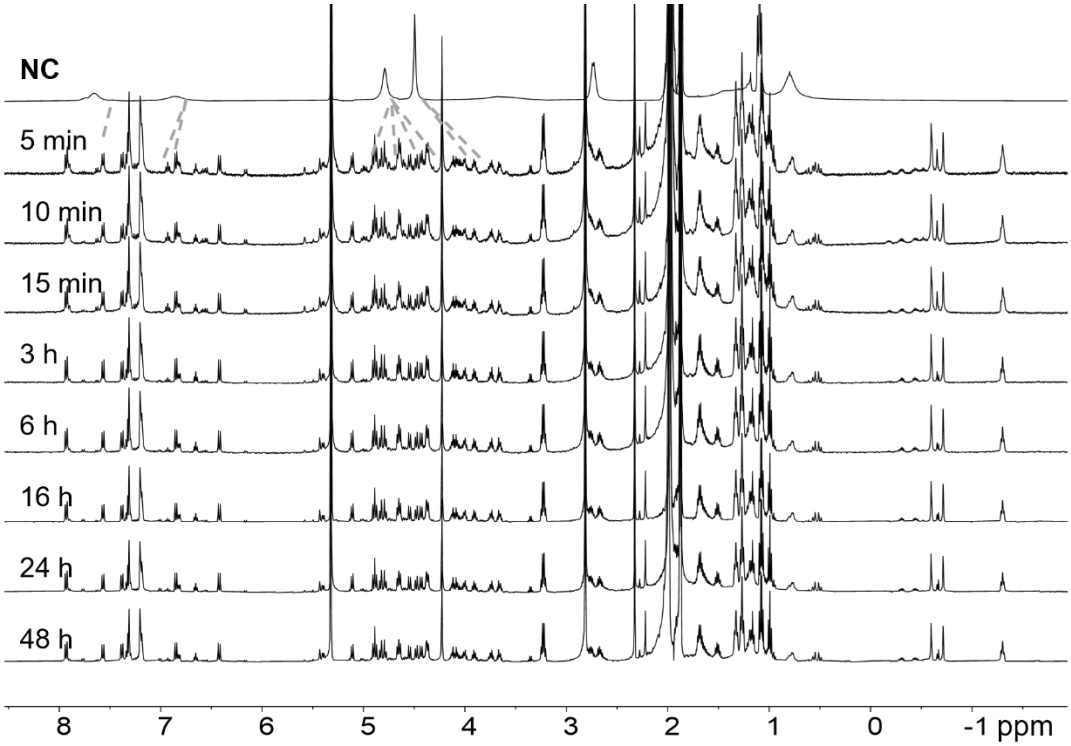

Figure S100. ^{1}H NMR spectra (500 MHz, CD_2Cl_2:CD_3CN (*v*/*v* = 1:1), 1.0 mM, 298 K) of **NC** after addition of **G22** at different time.

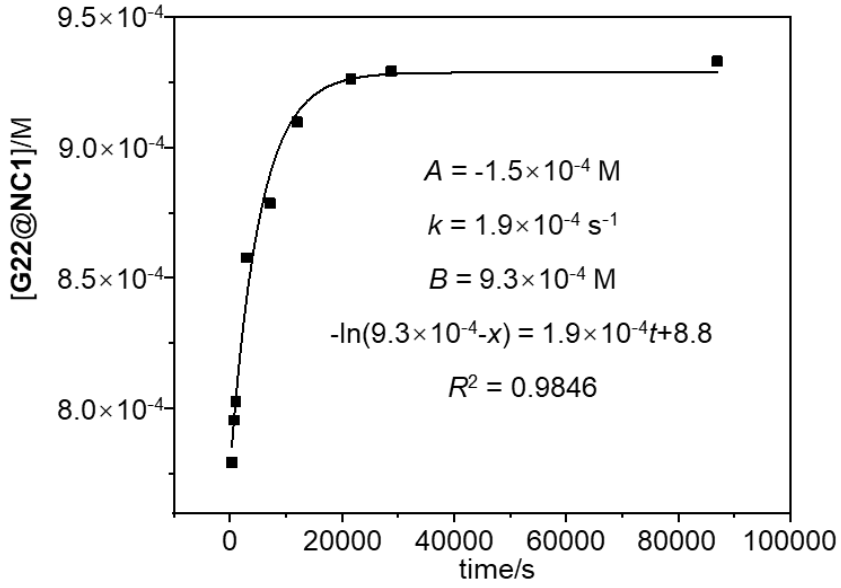

Figure S101. Change in concentration of **G9@NC1** against time and the fitted kinetic data.

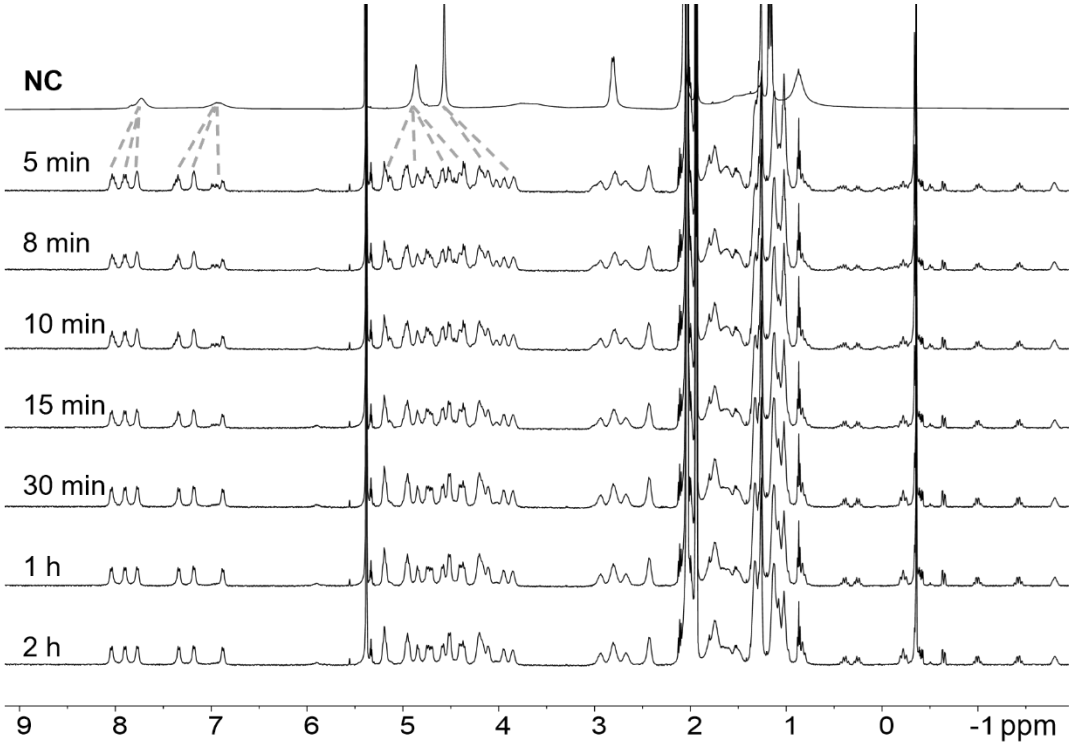

Figure S102. ^{1}H NMR spectra (500 MHz, CD_2Cl_2:CD_3CN (*v*/*v* = 1:1), 1.0 mM, 298 K) of **NC** after addition of **G23** at different time.

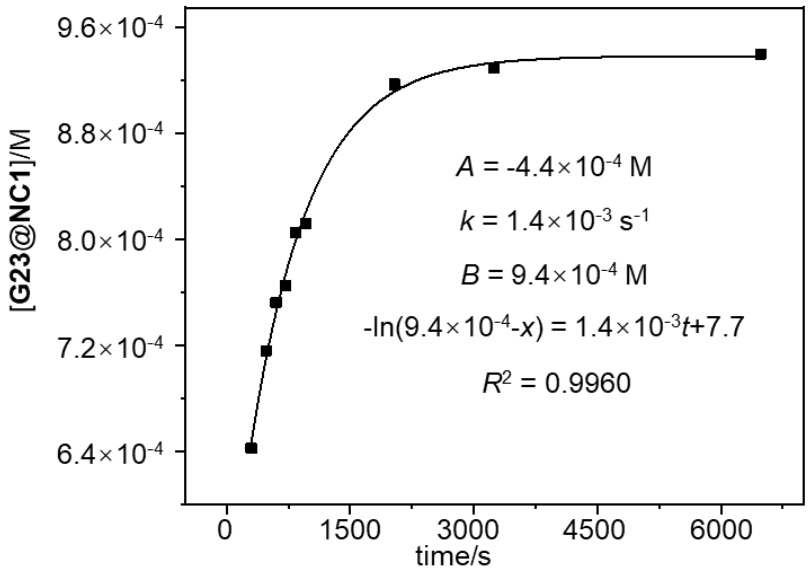

Figure S103. Change in concentration of **G23@NC1** against time and the fitted kinetic data.

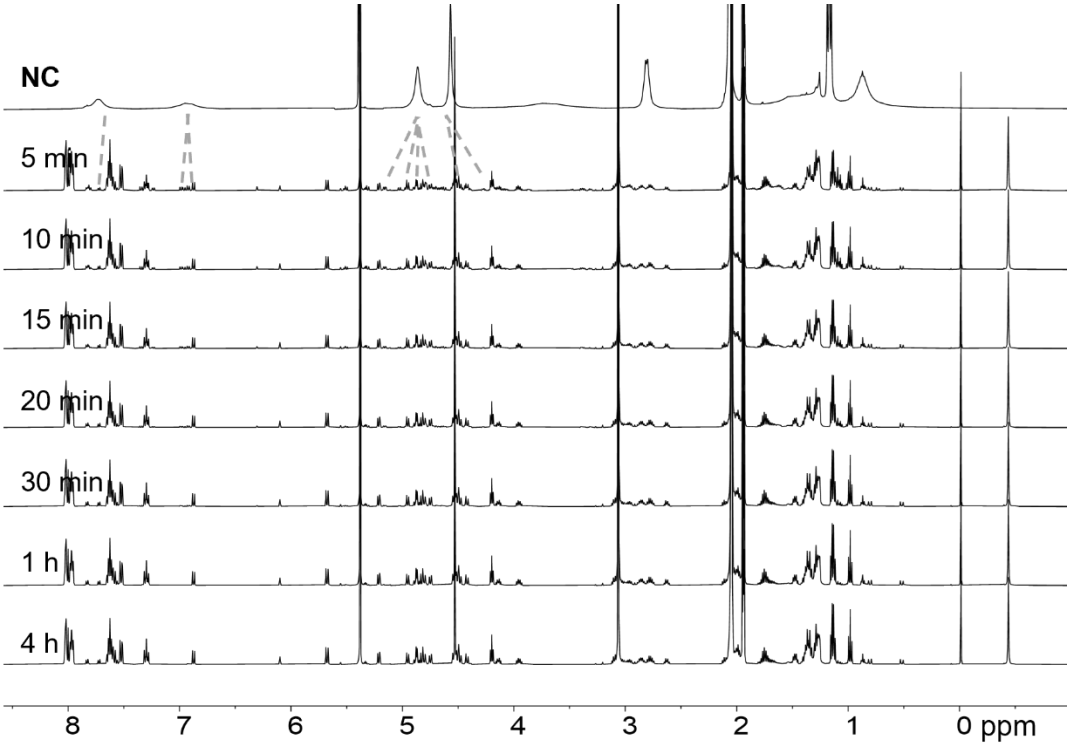

Figure S104. ^{1}H NMR spectra (500 MHz, CD_2Cl_2:CD_3CN (*v*/*v* = 1:1), 1.0 mM, 298 K) of **NC** after addition of **G24** at different time.

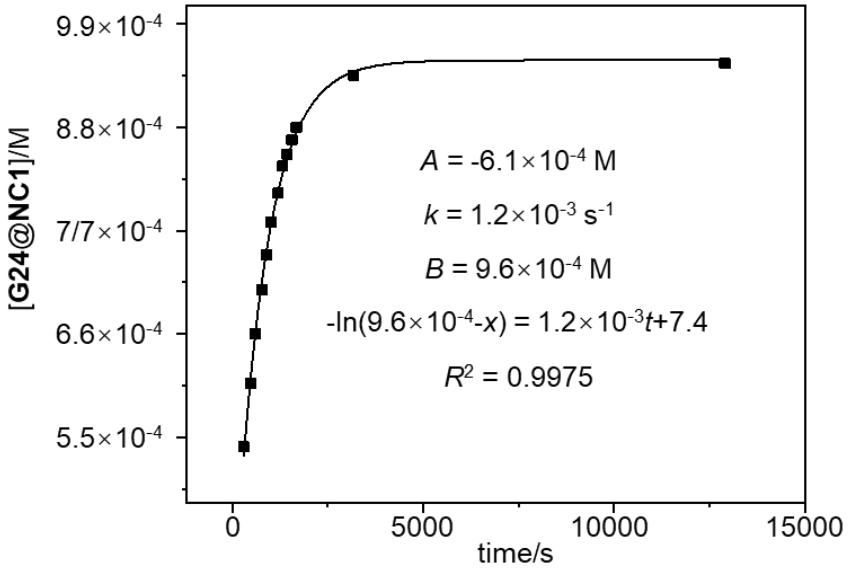

Figure S105. Change in concentration of **G24@NC1** against time and the fitted kinetic data.

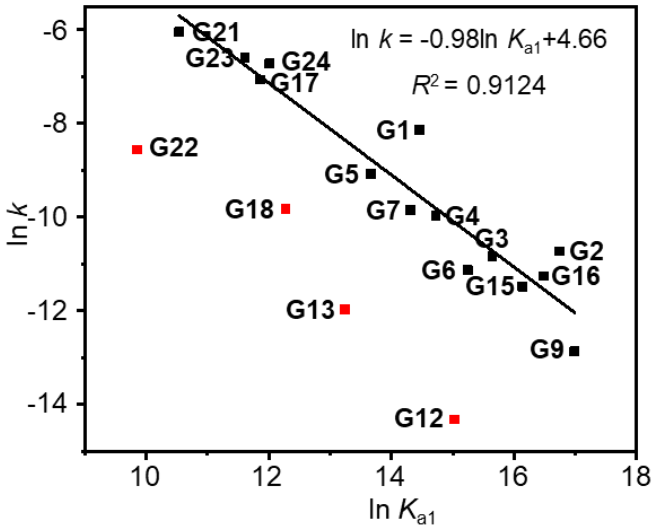

Figure S106. Correlation between the dissociation rate constant and the thermodynamic stability of the host-guest complex of **NC** and **G1** to **G24**.

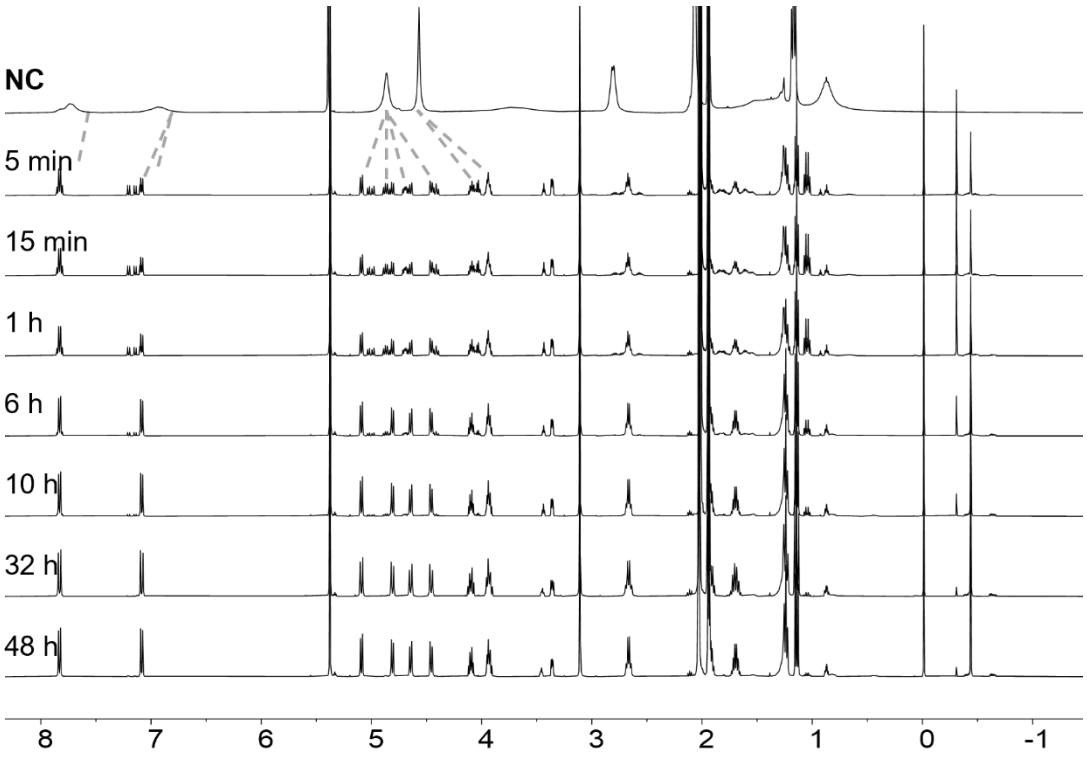

Figure S107. ^{1}H NMR spectra (500 MHz, CD_2Cl_2:CD_3CN (*v*/*v* = 1:1), 1.0 mM, 298 K) of **NC** after addition of **A1** at different time.

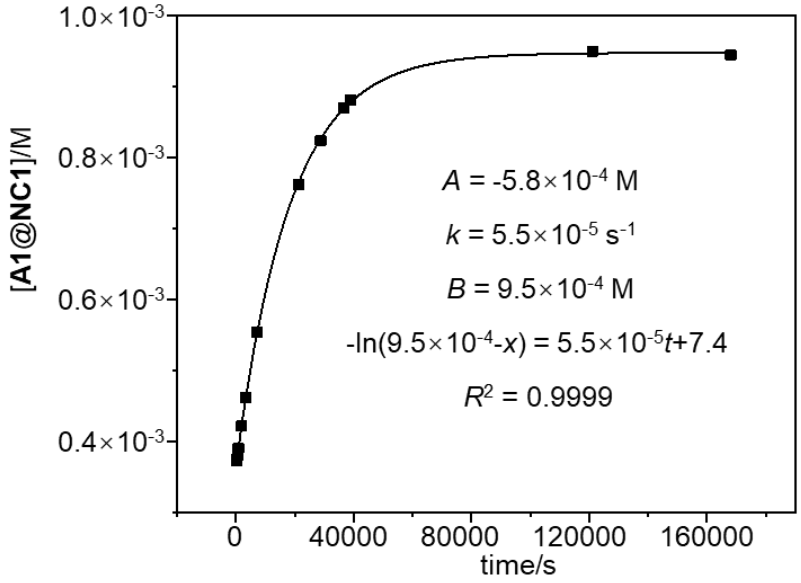

Figure S108. Change in concentration of **A1@NC1** against time and the fitted kinetic data.

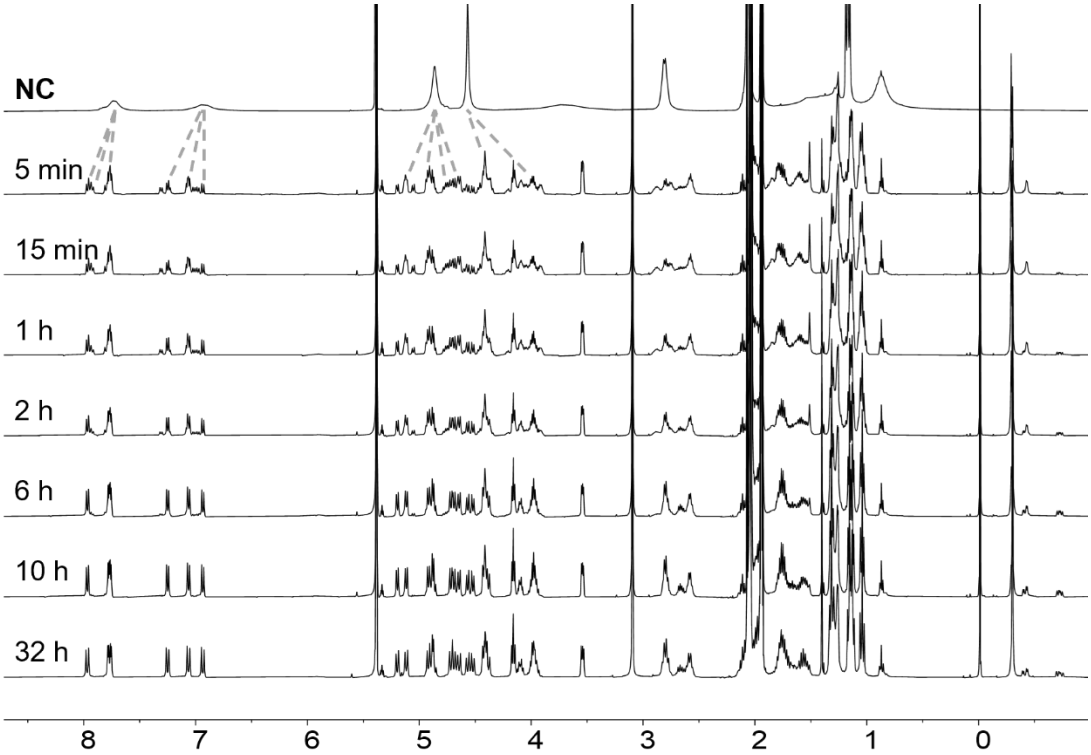

Figure S109. ^{1}H NMR spectra (500 MHz, CD_2Cl_2:CD_3CN (*v*/*v* = 1:1), 1.0 mM, 298 K) of **NC** after addition of **A2** at different time.

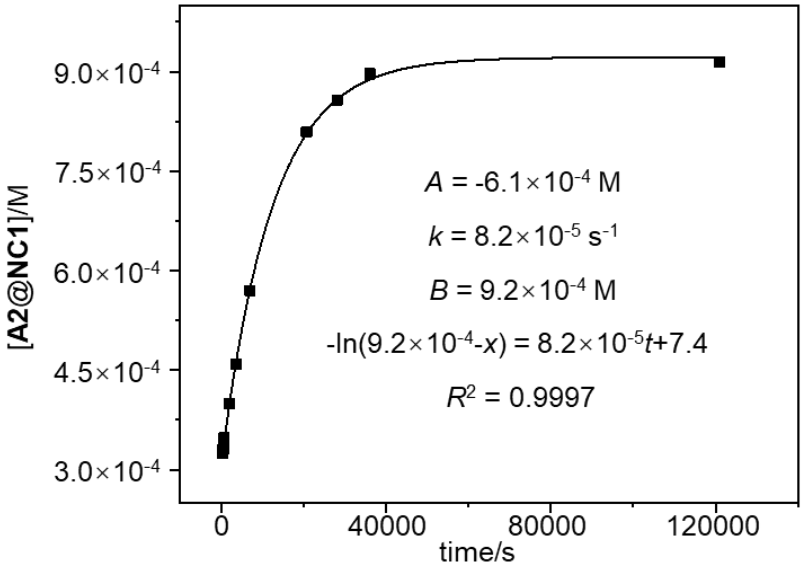

Figure S110. Change in concentration of **A2@NC1** against time and the fitted kinetic data.

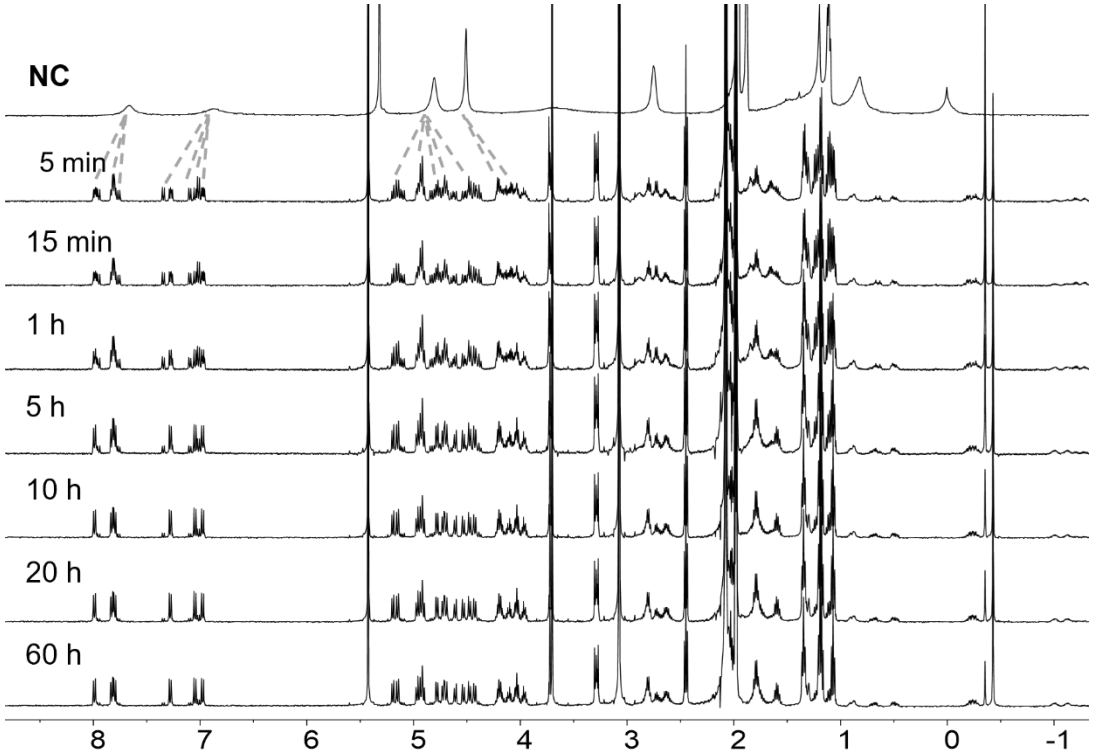

Figure S111. ^{1}H NMR spectra (500 MHz, CD_2Cl_2:CD_3CN (*v*/*v* = 1:1), 1.0 mM, 298 K) of **NC** after addition of **A3** at different time.

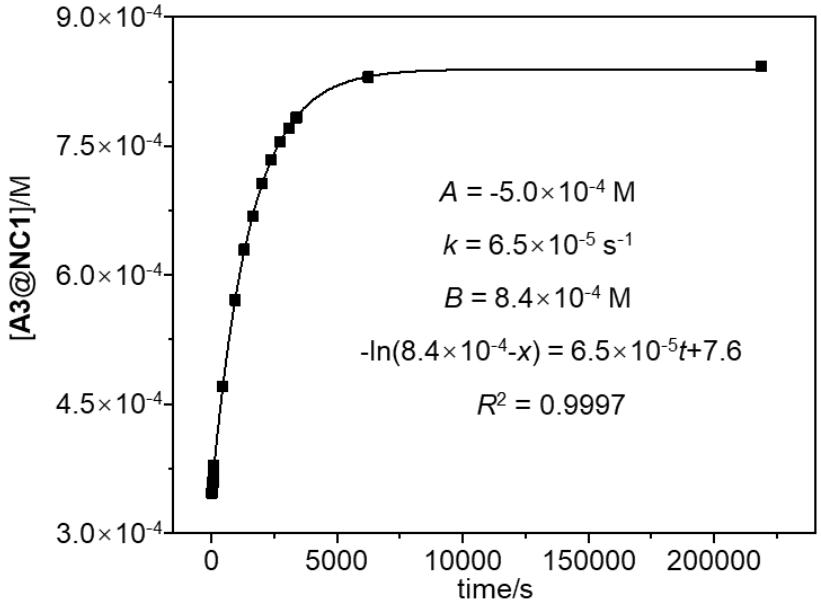

Figure S112. Change in concentration of **A3@NC1** against time and the fitted kinetic data.

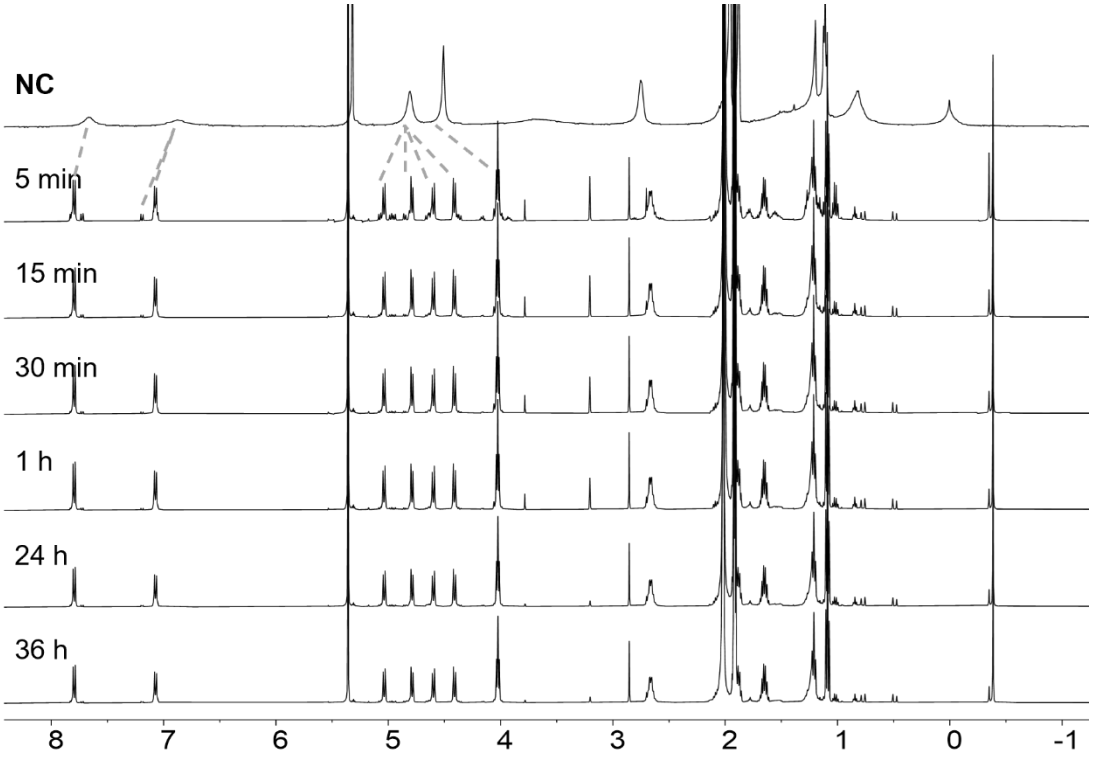

Figure S113. ^{1}H NMR spectra (500 MHz, CD_2Cl_2:CD_3CN (*v*/*v* = 1:1), 1.0 mM, 298 K) of **NC** after addition of **A4** at different time.

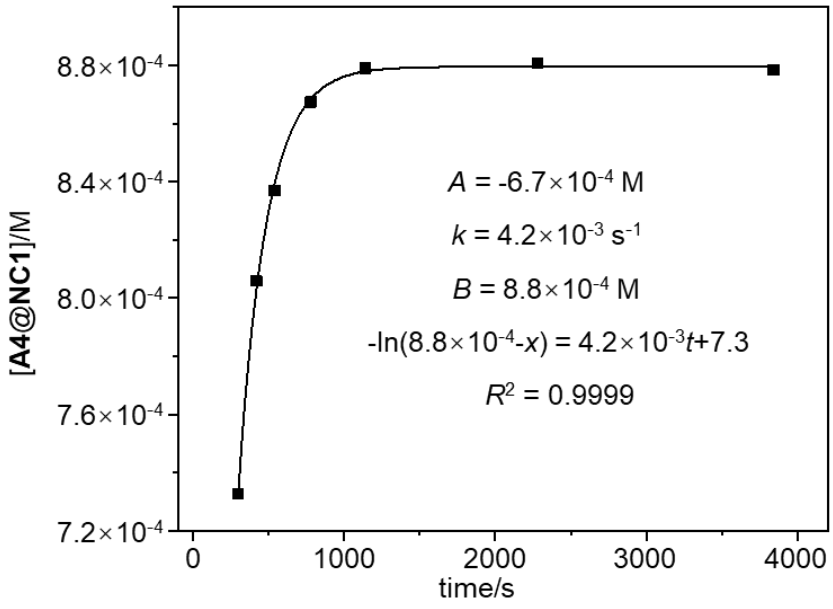

Figure 114. Change in concentration of **A4@NC1** against time and the fitted kinetic data.

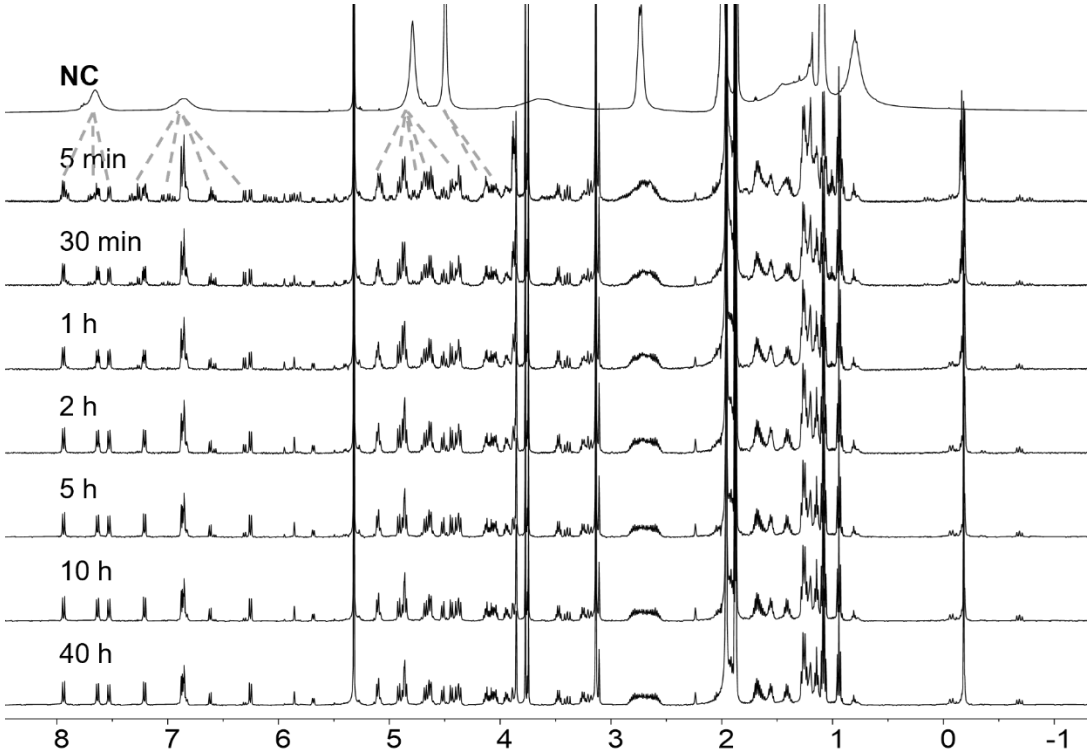

Figure S115. ^{1}H NMR spectra (500 MHz, CD_2Cl_2:CD_3CN (*v*/*v* = 1:1), 1.0 mM, 298 K) of **NC** after addition of **A5** at different time.

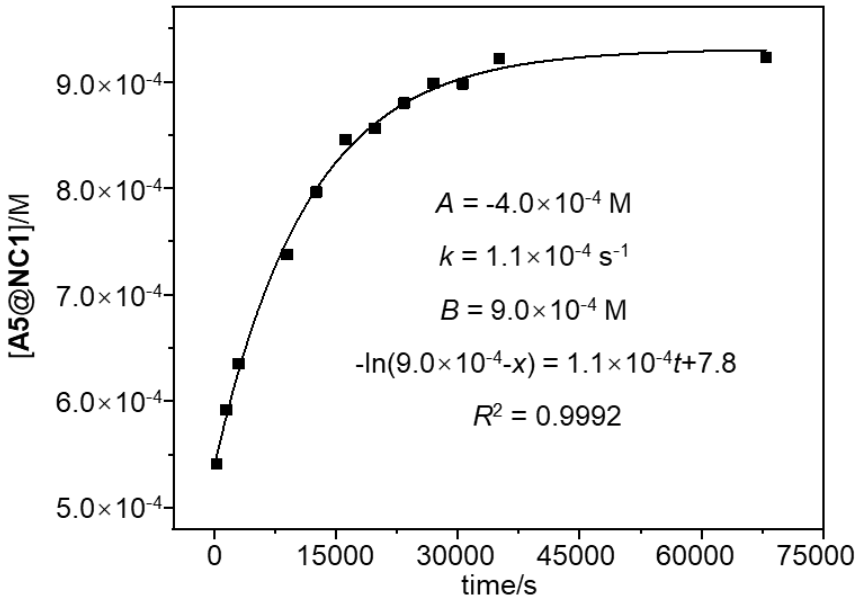

Figure S116. Change in concentration of **A5@NC1** against time and the fitted kinetic data.

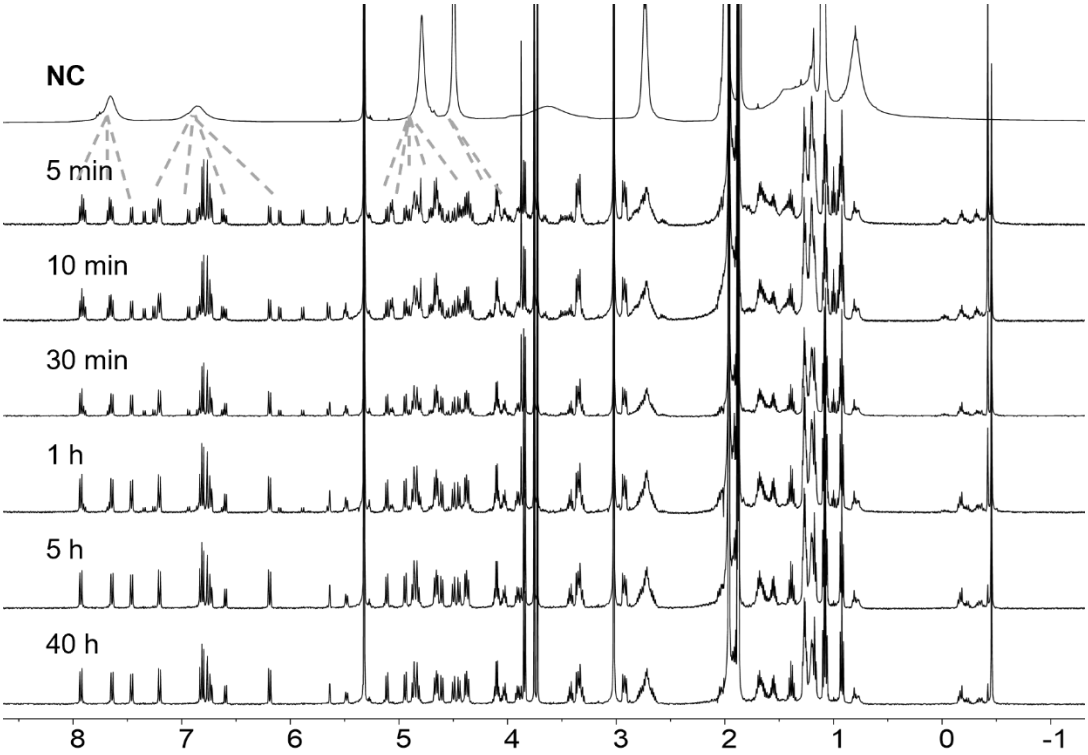

Figure S117. ^{1}H NMR spectra (500 MHz, CD_2Cl_2:CD_3CN (*v*/*v* = 1:1), 1.0 mM, 298 K) of **NC** after addition of **A6** at different time.

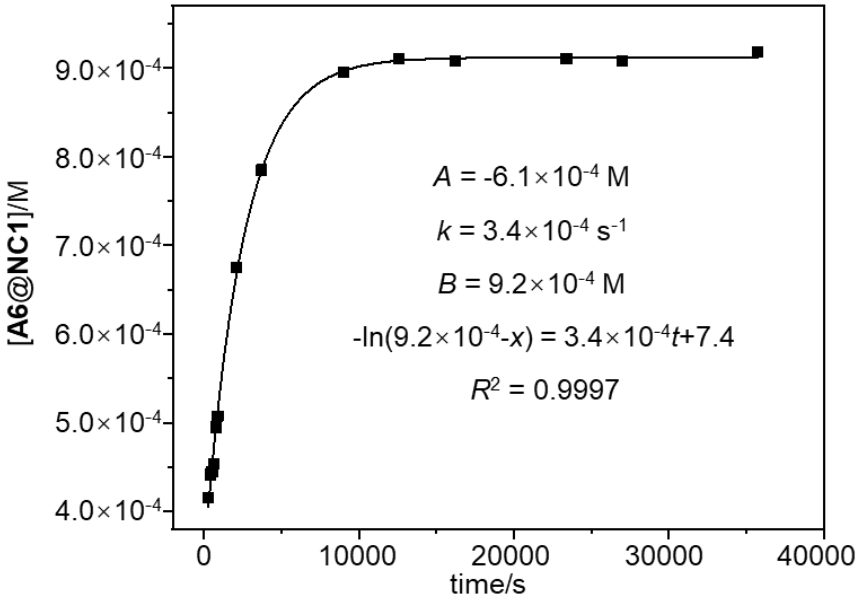

Figure S118. Change in concentration of **A6@NC1** against time and the fitted kinetic data.

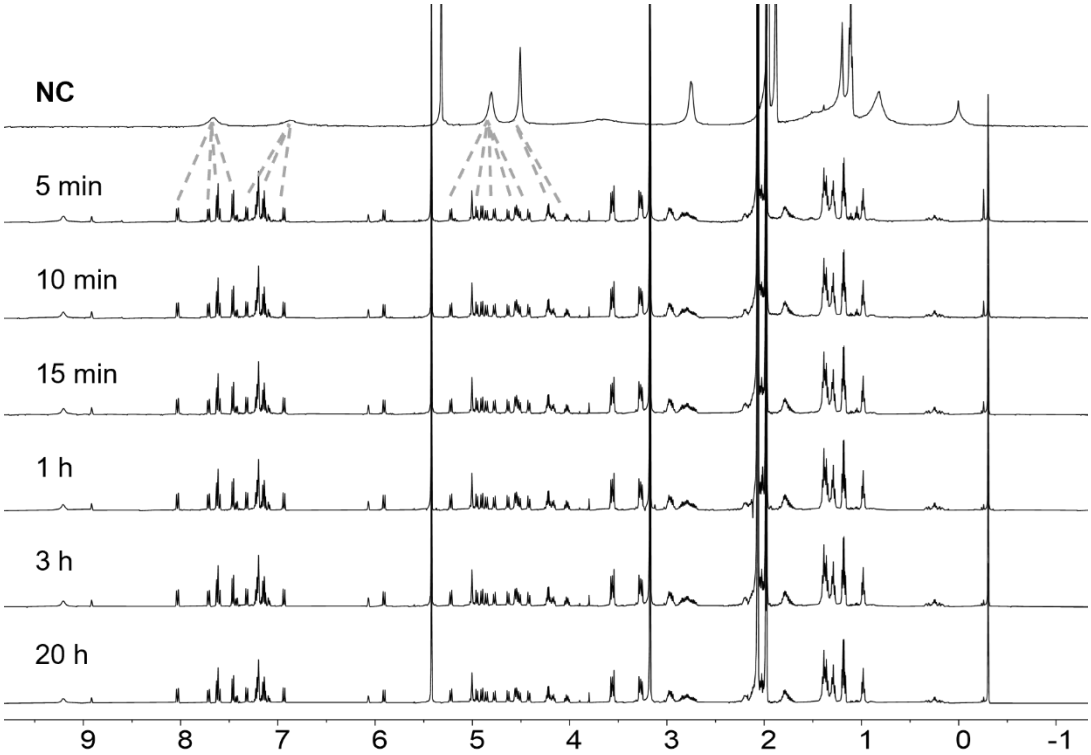

Figure S119. ^{1}H NMR spectra (500 MHz, CD_2Cl_2:CD_3CN (*v*/*v* = 1:1), 1.0 mM, 298 K) of **NC** after addition of **A7** at different time.

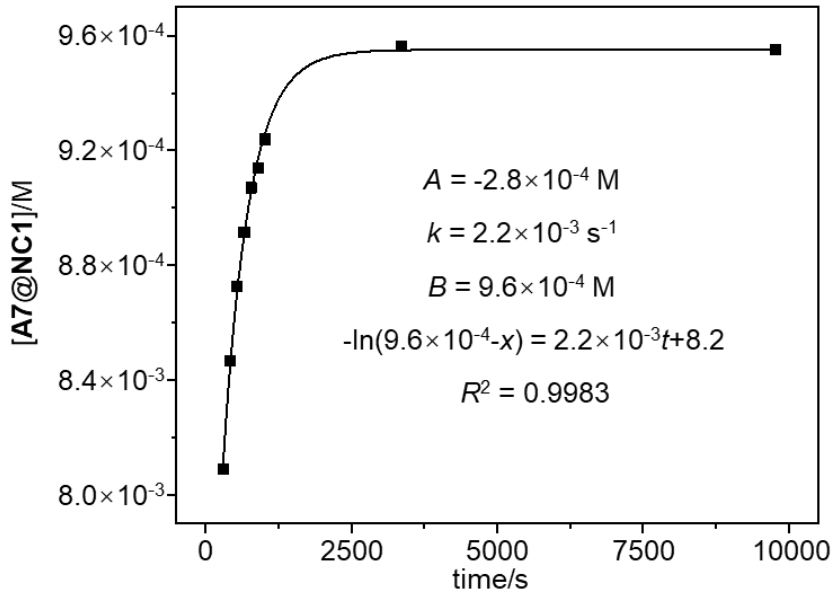

Figure S120. Change in concentration of **A7@NC1** against time and the fitted kinetic data.

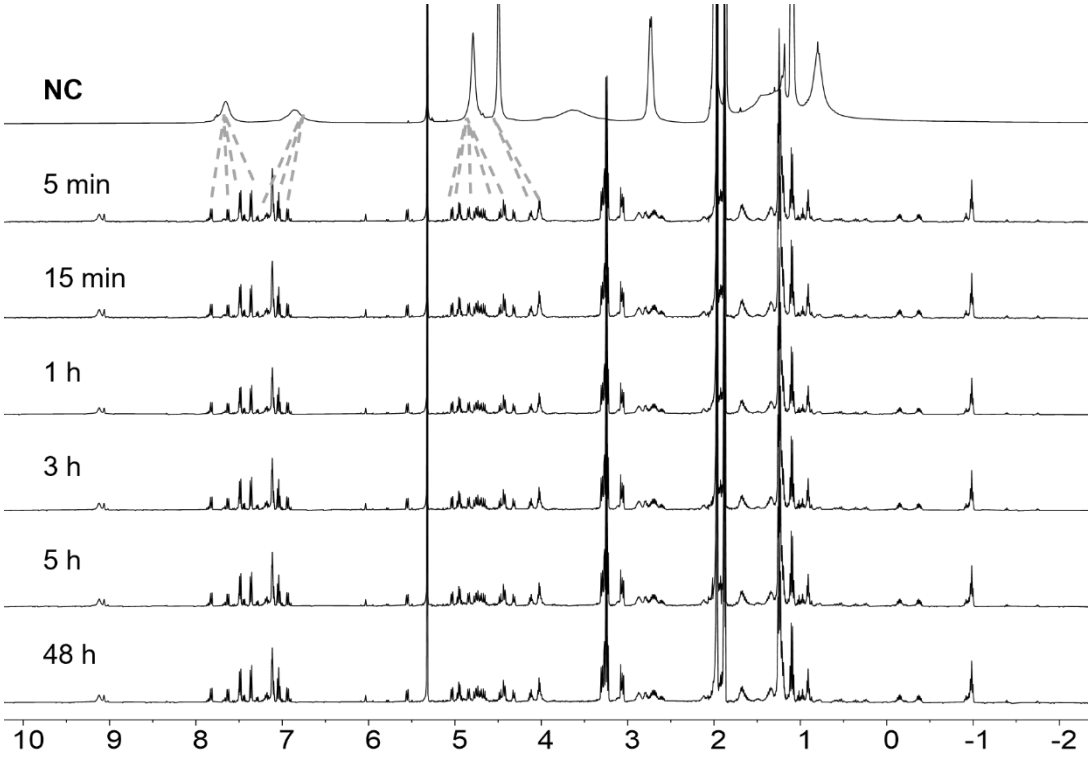

Figure S121. ^{1}H NMR spectra (500 MHz, CD_2Cl_2:CD_3CN (*v*/*v* = 1:1), 1.0 mM, 298 K) of **NC** after addition of **A8** at different time.

Table S4. Summary of kinetic data obtained for **A1** to **A8**.

	k/s^{-1}	k_{-1}/s^{-1}	k_{-2}/s^{-1}	$c_{1,0}$/mM	$c_{2,0}$/mM	$c_{1,e}$/mM
A1	5.5×10^{-5}	2.9×10^{-6}	5.2×10^{-5}	0.36	0.67	0.95
A2	8.2×10^{-5}	6.7×10^{-6}	7.5×10^{-5}	0.31	0.64	0.92
A3	6.5×10^{-5}	1.0×10^{-5}	5.5×10^{-5}	0.34	0.66	0.84
A4	4.2×10^{-3}	5.0×10^{-4}	3.7×10^{-3}	0.21	0.79	0.88
A5	1.1×10^{-4}	1.1×10^{-5}	9.9×10^{-5}	0.50	0.50	0.90
A6	3.4×10^{-4}	2.7×10^{-5}	3.1×10^{-4}	0.31	0.69	0.92
A7	2.2×10^{-3}	1.0×10^{-4}	2.1×10^{-3}	0.33	0.67	0.96
A8	/	/	/	/	/	/

Predicting kinetic data for complexes of A1 to A8

From Figure 5, correlation between the dissociation rate constant and thermodynamic stability of the host-guest complexes of **NC** and **G1** to **G24** can be described by equations *S*21 and *S*22.

$$lnk_{-1} = -1.08lnK_{a1} + 3.18 \quad (S24)$$

$$lnk_{-2} = -1.08lnK_{a2} + 2.95 \quad (S25)$$

Dissociation rate constants (k_{-1} and k_{-2}) of complexes of **NC** and **A1** to **A8** can then be predicted using *S*21 and *S*22. The required time for reaching conformational equilibrium can therefore be predicted by equation *S*27 and *S*28 by assuming the equilibrium has been reached with 95% of conversion (for comparison with NMR data with a 5% error in integration).

$$0.95x_e = -x_e e^{-(k_{-1}+k_{-2})t_{95\%}} + x_e \quad (S26)$$

$$t_{95\%} = \frac{\ln\left(\frac{x_e}{x_e - 0.95x_e}\right)}{k_{-1} + k_{-2}} \quad (S27)$$

Table S5. Predicted dissociation rate constants and the equilibration time for **A1** to **A7**.

	ln k_{-1}	ln k_{-2}	$t_{95\%}$/min
A1	-12.86	-9.98	1567
A2	-11.96	-9.58	1013
A3	-11.45	-9.89	1253
A4	-7.91	-5.98	26.5
A5	-10.58	-8.17	249
A6	-11.32	-9.14	644
A7	-9.48	-6.41	44.7

References

1 L. P. Cao, M. Sekutor, P. Y. Zavalij, K. M. Majerski, R. Claser, L. Isaacs, *Angew. Chem. Int. Ed.* 2014, **53**, 988.

2 F. Jia, H. V. Schröder, L. P. Yang, C. V. Essen, S. Sobottka, B. Sarkar, K. Rissanen, W. Jiang, C. A. Schalley, *J. Am. Chem. Soc.* 2020, **142**, 3306.